

https://dspace.org/

A palaeoecological and taphonomic analysis of microfossils from MIS 5 layers in Cave1, Klasies River main site, South Africa.

Faul, Inèz

2021
https://hdl.handle.net/10539/33052

Downloaded from a DSpace repository. https://dspace.org/

A palaeoecological and taphonomic analysis of microfossils from MIS 5 layers in Cave 1, Klasies River main site, South Africa.

Inèz Faul

2005431

Supervisors:

Prof Sarah Wurz

Res Prof Carin Andersson Dahl

Dr Karen van Niekerk

Masters project submitted in fulfilment of the requirements of the Degree of Masters in Archaeology of University of the Witwatersrand in 2021.

DIVISION OF ARCHAEOLOGY SCHOOL OF GEOGRAPHY, ARCHAEOLOGY AND ENVIRONMENTAL STUDIES.

Declaration

I declare that this dissertation is my own, unaided work. It is being submitted for the Degree of Master of Science in the University of the Witwatersrand, Johannesburg. It has not been submitted before for any degree or examination in any other University.

Name: Inèz Faul

Date: 20 August 2021

Signature:



Abstract

Research conducted at Klasies River main site (KRM) has contributed to interpretations regarding early modern human behaviour during the Middle Stone Age in South Africa between Marine Isotope Stage (MIS) 5c-d (110–93 ka). The current interpretations of the climatic and environmental background against which early human groups developed at KRM could be described in finer detail. The new excavations conducted at the main site create new opportunities for researching the paleoenvironmental context of early modern humans from perspectives not previously considered. Microfossils such as ostracods and foraminifera have been useful indicators of past environmental conditions during the Holocene in South Africa. Recent microscopic investigations revealed that ostracods and foraminifera are preserved in the KRM MIS 5 sediments from four layers dating between 100 - 110 ka. The layers investigated here are layer SMONE (MIS 5c), BOS-One (MIS 5d), BOS-Two (MIS 5d), and BOS-Three (MIS 5d). The abundance of the ostracods is higher during times when the site was used as primarily a knapping site with relatively less intensive occupation (in the BOS-Three layer) and is less prevalent during times of intense human occupation (in the SMONE layer). The most abundant ostracod taxon in all the layers, *Gomphocythere obtusata*, can be found in freshwater to slightly saline conditions, which suggests the presence of a fresh- to brackish water source nearby. The lesser abundance of ostracods in the upper layer, SMONE perhaps imply more dry conditions during the deposition of SMONE and more moist conditions during the formation of the BOS-layers. The foraminifera occur in lesser quantities and have likely been transported from outside of the KRM site.

Keywords: MSA, paleoenvironment, ostracods, foraminifera, MIS 5 c-d.

Acknowledgements

Firstly, and most importantly, I would like to acknowledge and thank my dream team of supervisors, Prof. Sarah Wurz, Prof. Carin Andersson, and Dr Karen van Niekerk. This project has been an incredible journey and I could not have asked for better supervisors. Thank you for every draft that you have read and for every comment that you took the time to make. I will forever be grateful for every opportunity and learning curve that I have had the privilege to engage with under your supervision. I would also like to thank Prof. Christopher Henshilwood (NRF SARChi) who kindly funded this project, along with the University of the Witwatersrand and the SapienCE project.

To Prof. P Frenzel, Prof. J Holmes, Prof. K Martens and Prof. D Horne, thank you for always being willing to assist me with all of my ostracod-related questions. Your contributions to this project have been invaluable. I would also like to thank Dr. E Bergh from Iziko Museums for assisting with the identification of benthic foraminifera.

To my family, friends, and Peter Boxall, thank you for supporting me in my Masters journey and for tolerating my deadline (and often caffeine) induced panics. I love and appreciate you all.

Table of Contents

Declaration i

Abstract ii

Acknowledgements iii

Table of Contents iv

List of Figures viii

List of Tables xi

Chapter 1: Introduction 1

1.1 Research problem 6

1.2 Research question 7

1.3 Hypothesis 7

1.4 Aims 7

1.5 Objectives 7

1.6 Rationale 8

1.7 Structure of thesis 9

Chapter 2: Literature Review- Environmental conditions on the southern Cape coast 10

2.1 Introduction 10

2.1.1 Present-day climatic conditions on the southern Cape Coast 10

2.1.2 The paleoenvironment in the southern Cape during MIS 5c-d 11

i) Palaeoenvironmental data from Blombos Cave 12

ii) Palaeoenvironmental data from Pinnacle Point 14

iii) Palaeoenvironmental data from Vankervelsvlei 16

2.1.3 Palaeoenvironmental data from KRM 17

i) Shellfish data from KRM 17

ii) Microfauna and large mammal fauna from KRM 18

2.2 Conclusion 19

Chapter 3: Literature review- Ostracods and foraminifera 20

3.1 Introduction 20

3.2 Ostracods 21

3.2.1 General description of ostracods 21

i) Morphology and life cycle 21
ii) Habitat 22
iii) Dispersal 23
iv) Approaches used for paleoenvironmental inferences using ostracods 24
a) Shell chemistry 24
b) Morphological Observations 25
3.2.2 Ostracod studies from Pleistocene archaeological deposits 25
3.2.3 Ostracod case studies from South Africa 26
i) Verlorenvlei 26
ii) The West coast of South Africa 28
iii) Summary of South African case studies 31
3.2.4 Theoretical approaches 32
i) Uniformitarianism (the present is the key to the past) and Indicator Taxa 32
ii) Thanatocoenosis and Taphocoenosis 33
3.2.5 Conclusion 34
3.3 Foraminifera 35
3.3.1 General description of foraminifera 35
3.3.2 Foraminifera and the paleoenvironment 37
i) Determining Holocene sea level changes 37
ii) Distinguishing between natural and cultural deposits 38
3.3.3 Conclusion 39
Chapter 4: Material and methods 40
4.1 Material 40
4.2 Methods 42
4.2.1 Sample preparation 42
i) Preliminary analysis 42
ii) Expanding the sample size 43
iii) Splitting samples 43
4.2.2 Sample picking and identification 45
i) Microscopy 46
ii) Comparative database 47
iii) Scanning Electron Microscopy 48

4.2.3 Quantitative analysis 49
i) Census counts 49
ii) Abundance data 49
iii) Confidence intervals 50
iv) Analysing the assemblage composition 51
4.2.4 Geochemical analysis of ostracod valves 51
Chapter 5: Results 53
5.1 Introduction 53
5.2 Ostracods 53
5.2.1 Ostracods: Taxonomy 53
5.2.2 Ostracod abundances 63
i) Absolute abundance (number specimens/gram washed sediment >150µm) 63
ii) Relative abundance (% of total number of ostracods within the sample) 65
iii) Comparing the relative abundance and absolute abundance data of ostracods 69
iv) Confidence intervals 69
5.2.3 Average ostracod sizes 72
5.2.4 Adult: juvenile ratio of ostracods 72
Geochemical analysis of ostracod valves (pilot study) 73
5.3 Conclusion 76
5.4 Foraminifera 77
5.4.1 Foraminifera: Taxonomy 77
5.4.2 Foraminifera abundances 78
i) Absolute abundance (number specimens/gram sediment >150µm) of foraminifera 78
ii) Relative abundance (% of total number of foraminifera within the sample) 81
iii) Comparing the relative abundance and absolute abundance data of foraminifera 83
iv) Confidence Intervals 83
5.4.3 Geochemical analysis of foraminiferal tests 83
Chapter 6: Discussion and conclusion 86
6.1 Introduction 86
6.2 Ostracods from KRM: Taxonomy and ecology in wider context 86

6.3 Ostracods and site formation at KRM 89
6.4 Change through time in the ostracod assemblage at KRM 91
i) Absolute abundances 91
ii) Relative abundances 92
6.5 Adult:juvenile ratios and assemblage composition 93
6.6 An isotopic perspective on ostracod calcification and the environment 93
6.7 Foraminifera from KRM: taxonomy and ecology in wider context 96
6.8 Foraminifera and site formation at KRM 98
6.9 The palaeoenvironment during MIS 5c-d at KRM 100
6.10 Limitations to study and future analysis 101
6.11 Conclusion 102
References 104
Appendices 121
Appendix A 121
Section A.1 121
General description of ostracods 121
General description of foraminifera 122
Appendix B 123
Section B.1 123
Appendix C 125
Section C.1 Raw data 125
Section C.2 SEM images 130
Section C.3 Systematics 142
Appendix D 145
Section D.1 Isotope data 145

List of Figures

Figure 1.1 The locations of the archaeological sites Klasies River (KRM) (34°6′29.17″S, 24°23′24.50″E), Blombos Cave (BBC) (34°24′52″S, 21°13′21″E) and Pinnacle Point (PP) (34° 12' 11.88 1

Figure 1.2 Layout of Klasies River main site (adapted from Deacon & Geleijnse (1988) by Wurz *et al*. 2018) 2

Figure 1.3 Klasies River main site with caves 1, 1A, 1B and 2 (image from KRM excavation archives, unknown photographer) 3

Figure 1.4 The stratigraphic context of the KRM main site (adapted from Deacon & Geleijnse (1988) and Grine *et al.* (2017) by Wurz *et al*. 2018) 4

Figure 1.5 The location of the Witness Baulk in Cave 1 (highlighted) (Wurz *et al*. 2018) 5

Figure 2.1 The southern Cape coast with the locations of KRM, BBC, PP, and Vankervelsvlei. 12

Figure 3.1 The location of the Keiskamma Estuary, Kariega Estuary, Langebaan Lagoon, Verlorenvlei, and Knysna Estuary in relation to KRM 20

Figure 3.2 The west coast of South Africa analysed by Fürstenberg *et al*. (2017) 29

Figure 3.3 The various salinity ranges of an estuary - based on information and figures by Ohrel & Register (2006) and www.e-education.psu.edu/earth107/node/1026 30

Figure 4.1 The MIS 5c-d layers (SMONE; BOS-One; BOS-Two; BOS-Three) from the Witness Baulk in cave 1 where the samples were collected (Brenner *et al*. 2020) 41

Figure 4.2 Fixed Splitter (Tetard & Marchant 2020) 45

Figure 4.3 Black picking tray with grids. 46

Figure 4.4 Micropaleontological storage cell 47

Figure 4.5 Equation to determine the absolute abundance of microfossils 50

Figure 4.6 Equation to determine the relative abundance of microfossils 50

Figure 5.1 A) External view of ostracod taxon *Gomphocythere obtusata* with visible articulation and depression in the surface. B) Internal view of *Gomphocythere obtusata* with visible muscle scars and inner lamella 56

Figure 5.2 SEM images of *Gomphocythere obtusata*. A) External view of valve with visible reticulation and dark stains B) Internal view of valve with visible muscle scars and lamella. 57

Figure 5.3 A) External view of *Sarscypridopsis aculeata* valve with pitted surface and the remains of stout spines. B) Internal view of Sarscypridopsis *aculeata* valve with visible muscle scars and inner lamella 58

Figure 5.4 SEM images of *Sarscypridopsis aculeata* A) External view of valve with pitted surface and dark stains B) Internal view of valve with inner lamella. 58

Figure 5.5 A) External view of *Physocypria cf. castanea* valve with post-depositional ornamentation. B) Internal view of *Physocypria cf. castanea* valve visible lamella..... 60

Figure 5.6 SEM images of Physocypria cf. castanea A) External view of valve B) Internal view of valve with visible lamella and hinge..... 61

Figure 5.7 SEM image of inner view of *Ilyodromus* sp. valve..... 62

Figure 5.8 Absolute abundance of ostracods (number specimens/gram sediment >150µm) with indication of stratigraphic zones 64

Figure 5.9 Relative abundance (%) per layer of the four ostracod taxa from KRM (juveniles included) 67

Figure 5.10 Relative abundance of ostracods with indication of stratigraphic zones (juveniles excluded) 68

Figure 5.11 Confidence Intervals for ostracod abundances..... 71

Figure 5.12 Stable oxygen isotope ($\delta^{18}O$) results from the KRM layers 74

Figure 5.13 Stable carbon isotope ($\delta^{13}C$) results from the KRM layers. 75

Figure 5.14 Absolute abundance of foraminifera with indication of stratigraphic zones..... 80

Figure 5.15 Relative abundance of foraminifera with indication of stratigraphic zones..... 82

Figure 5.16 Confidence Intervals for foraminifera relative abundance 85

Figure 6.1 Stable isotope values with indication of stratigraphic zones..... 94

Figure A.1 Diagram of the comparative anatomy of ostracod specimens (Olempska *et al*. 2012: 568; Figure 3)..... 121

Figure A.2 The basic morphological features of a benthic foraminifera (after Murray 1979) (from Strachan 2013: 7) 122

Figure C.2 SEM image of *Ammonia japonica* 131

Figure C.3 SEM image of *Ammonia* sp. 132

Figure C.4 SEM image of *Cassidulina* cf. *laevigata* 133

Figure C.5 SEM image of *Cribroelphidium articulatum* 134

Figure C.6 SEM image of *Elphidium* sp 135

Figure C.7 SEM image of *Globigerinoides* sp. 136

Figure C.8 SEM image of *Lagena* sp. 137

Figure C.9 SEM image of *Nonion boueanum* 138

Figure C.10 SEM image of *Spirillina vivipara* 139

Figure C.11 SEM image of unidentifiable foraminifera specimen 140

Figure C.12 *G. obtusata* with dark stains on the valve exterior 141

List of Tables

Table 1.1 The context of the KRM samples according to sub-unit, stratigraphic layer, and MIS stage. 6

Table 2.1 Sea level changes during MIS 5d-c in the Mossel Bay area (after Cawthra *et al.* 2018) 11

Table 5.1 Ostracod census count per layer from KRM 54

Table 5.2 Ostracod absolute abundances per layer from KRM (decimals are rounded up)..... 63

Table 5.3 Ostracod relative abundances per layer from KRM (decimals are rounded up)..... 66

Table 5.4 Measurements of ostracods recorded at Verlorenvlei by Martens *et al*. (1996) compared to ostracod measurements from Klasies River Cave 1..... 72

Table 5.5 Adult: juvenile ratios 73

Table 5.6 Foraminifera census count per layer from KRM..... 78

Table 5.7 Foraminiferal absolute abundances per layer from KRM (decimals are rounded up). 79

Table 5.8 Foraminiferal relative abundances per layer from KRM (decimals are rounded up) ... 81

Table B.1 MIS ages with their approximate start ages relevant to this study as defined by Wadley (2015:168)..... 123

Table B.2 Characteristics of ostracod growth stages (instars) as proposed by Kesling (1951:94-100). 124

Table C.1 Sediment sample context from KRM..... 125

Table C.2 The census data from the 29 sediment samples (Ostracods)..... 126

Table C.3 The census data from the 29 sediment samples (Foraminifera) 128

Table D.1 Summary of stable carbon ($\delta\,^{13}C$) and oxygen ($\delta\,^{18}O$) isotope results..... 145

Table D.2 Summary of stable carbon ($\delta\,^{13}C$) and oxygen ($\delta\,^{18}O$) isotope samples that did not weigh enough for the results to be interpreted accurately..... 147

Chapter 1: Introduction

The Klasies River Main site (KRM) (Figure 1.1) is a sequence of caves located in the Eastern Cape province of South Africa. The site is on the Tsitsikamma coast between the mouth of the Klasies River, roughly 500 meters to the west, and Druipkelder Point approximately 1 km to the east (Deacon & Geleijnse 1988). The site was one of the most intensely occupied sites in this region between 120 000 and 55 000 years ago (Wurz *et al*. 2018). The remains of anatomically modern humans and early evidence for the utilisation of marine and terrestrial resources have been uncovered at KRM (Grine *et al*. 2017; Wurz *et al*. 2018). An example of the archaeological evidence for coastal adaptation that KRM has yielded includes a 21m deep shell midden (Deacon & Geleijnse 1988; Wurz 2012; Nel *et al.* 2018). The midden formed as a result of the occupation of hunter-gatherer-fishers.

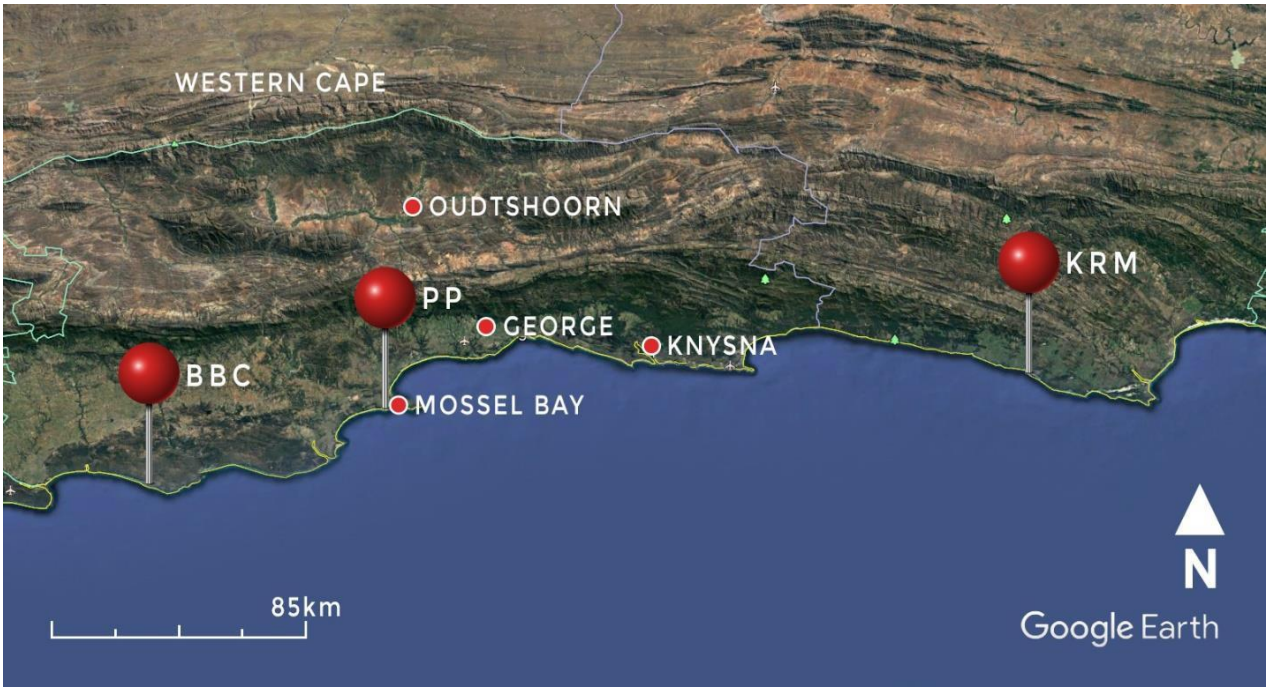


Figure 1.1 The locations of the archaeological sites Klasies River (KRM) (34°6′29.17″S, 24°23′24.50″E), Blombos Cave (BBC) (34°24′52″S, 21°13′21″E) and Pinnacle Point (PP) (34° 12' 11.88"S, 22° 5' 11.04"E).

Two caves, namely Cave 1 and Cave 2 (Figure 1.2; Figure 1.3), and two associated overhangs, namely Cave 1A and Cave 1B (Figure 1.2; Figure 1.3) make up the Klasies River main site (Wurz *et al*. 2018). Caves 1 and 1A (Figure 1.2; Figure 1.3) are 6 meters

above sea level (asl), and cave 2 (Figure 1.2; Figure 1.3) is 18 metres asl, but sea level changes during the Pleistocene likely resulted in distances from the coast varying and new areas opening or other areas becoming flooded as the sea retreated or rose (Wurz *et al.* 2018).

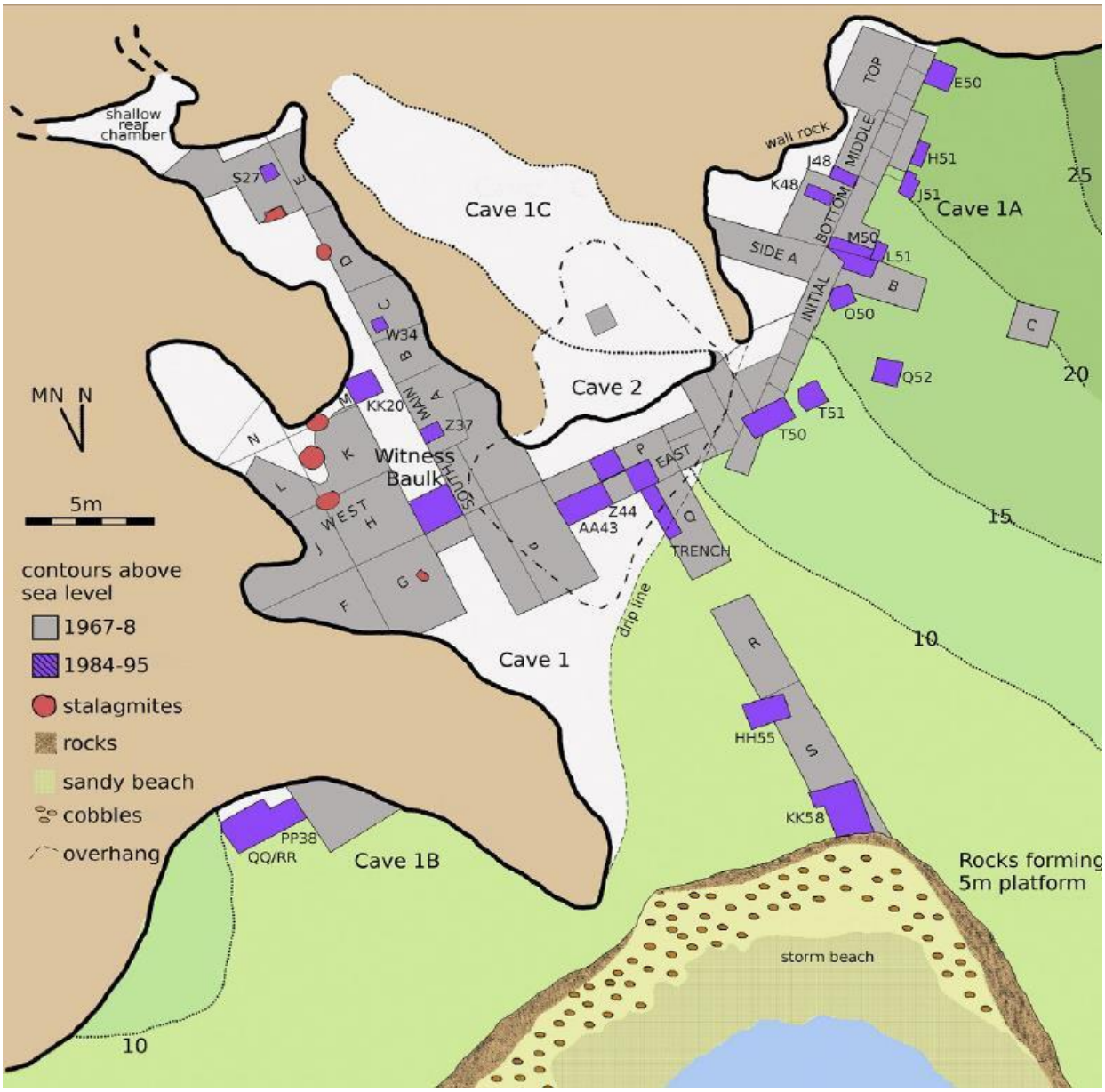


Figure 1.2 Layout of the Klasies River main site (adapted from Deacon & Geleijnse (1988) by Wurz *et al*. 2018).



Figure 1.3 Klasies River main site with caves 1, 1A, 1B and 2 (image from KRM excavation archives, unknown photographer).

A relatively level continental shelf borders the southern Cape coast (where KRM is situated) and formed a large coastal plain when the sea levels were at their lowest during the last glacial period (Dingle & Rogers 1972; van Andel 1989; Compton 2011). This coastal plain is known as the Agulhas bank and is, at present, a submerged extension of the continent (Compton 2016). In addition to adding land to the continent, the coastal plain also added various resources, such as plants and animals, for early modern humans to exploit (van Andel 1989; Compton 2011). The expansion of the land meant that some sites that used to be close to the ocean were further away during glacial periods, which might have hindered the exploitation of the marine resources (van Andel 1989).

John Wymer was the first to excavate at the main site in 1967 and 1968 (Singer & Wymer 1982) followed by Hilary Deacon (1984-1995) and thereafter by Sarah Wurz (SW, 2015 to present). Excavations undertaken by Wymer identified several layers (layers 40-1) (Singer & Wymer 1982). The MSA deposits at the main site were classified according to different lithological members by Deacon (Wurz *et al.* 2018), corresponding to Singer & Wymer's layers. The Deacon classification system is also followed by Wurz. In Cave 1

the lowest member is classified as the Light Brown Sand member (LBS, by Singer & Wymer, SW Layer 38), followed by the Rubble Brown Sand (RBS, SW Layer 37), Shell and Sand (SAS, SW layers 16-14), as well as the White Sand (WS, SW layer 13) members (Wurz *et al.* 2018) (Figure 1.4). The SAS member (SW Layer 36-23), Rock Fall (RF, SW layer 22) and Upper member (SW Layers 21-1 in Cave 1A and 1-5 in Cave 2) occur in Cave 1A (Wurz *et al.* 2018). The SAS member is the thickest unit (Wurz *et al.* 2018), comprising more than 10 metres of deposit. In Cave 1, the SAS member is further divided into sub-members, from top to bottom: SAS Rubble (SASR, SW Layer 14), SAS Wedge (SAS-W, SW Layer 15), the SAS Upper (SASU, SW Layer 16 in Cave 1) and SAS Lower (SASL, SW Layer 17 in Cave 1) sub-members.

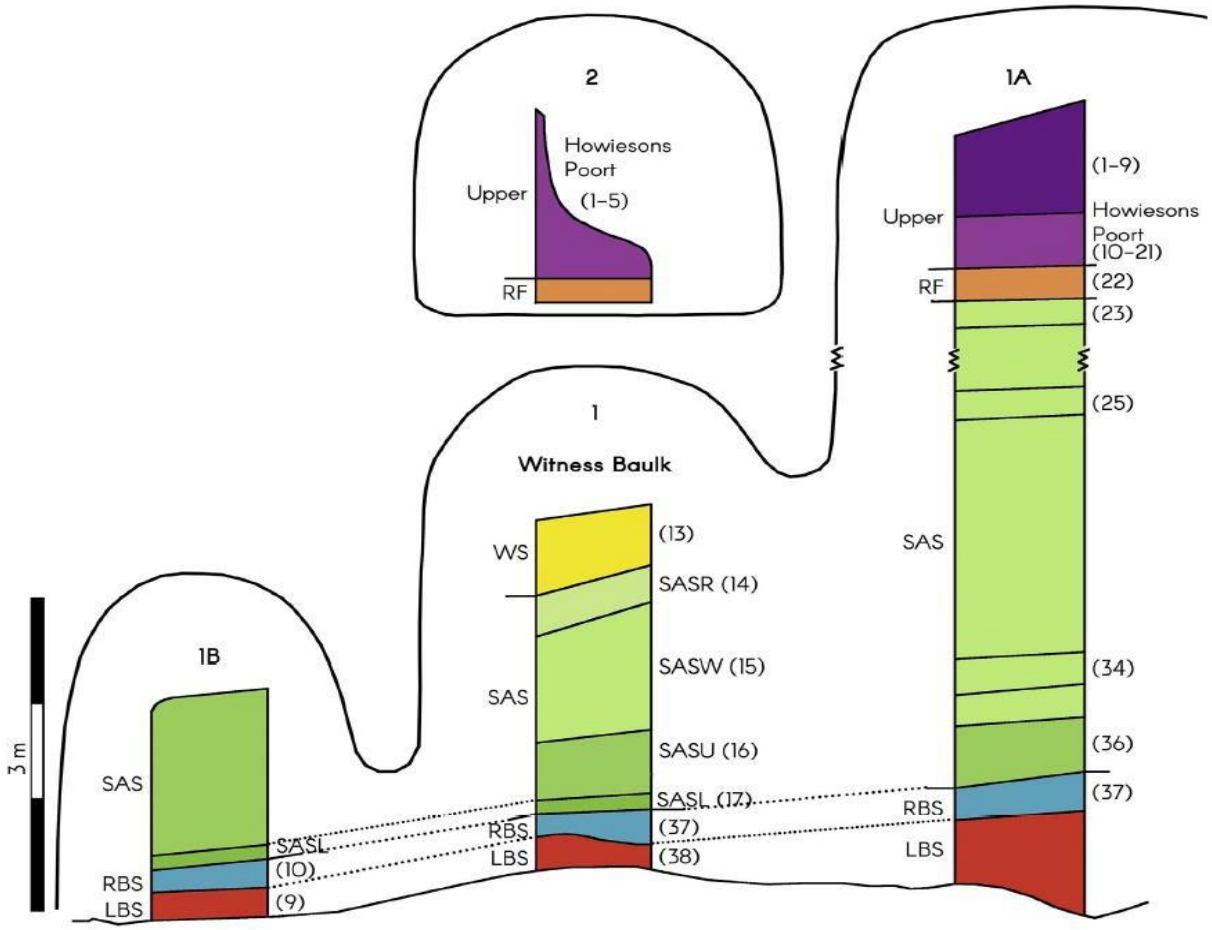


Figure 1.4 The stratigraphic context of the KRM main site (adapted from Deacon & Geleijnse (1988) and Grine *et al.* (2017) by Wurz *et al*. 2018).

This study focuses on deposits from Cave 1, in the Witness Baulk (Figure 1.5), excavated between 2015 and 2018 by Wurz. The Witness Baulk is a baulk of sediment approximately 12m in length that is situated in the middle section of cave 1 (Wurz *et al.* 2018). The sediments analysed here are from squares A1-C3 in the witness baulk excavated by Wurz between 2015 and 2018 (Figure 1.5).



Figure 1.5 The location of the Witness Baulk in Cave 1 (highlighted) (Wurz *et al*. 2018).

Four layers are discussed in this project, namely Shell Midden ONE (SMONE), Black Occupational Soils ONE (BOS-One), Black Occupational Soils TWO (BOS-Two) and Black Occupational Soils THREE (BOS-Three) (Table 1.1). These layers belong to the MSA ll lower techno-complex. Age estimates place the SMONE deposits in MIS 5c (Wurz *et al*. 2018), and BOS-Three in MIS 5d, at around 110 ka (Brenner & Wurz 2019).

Table 1.1 The context of the KRM samples according to sub-unit, stratigraphic layer, and MIS stage.

Sub-member	Layer	Singer & Wymer (1982) equivalent layer	Date	Techno-complex	MIS Stage
SASL	SMONE	17 a	101 ± 12 ka (Eggins *et al*. 2005)	MSA ll lower (also referred to as the "Mossel Bay")	MIS 5c
SASL	BOS-One	17 b	*ca.*110 (Brenner & Wurz 2019; Brenner *et al*. 2020)	MSA ll lower (also referred to as the "Mossel Bay")	MIS 5d
SASL	BOS-Two	17 b	*ca.*110 (Brenner & Wurz 2019; Brenner *et al*. 2020)	MSA ll lower (also referred to as the "Mossel Bay")	MIS 5d
SASL	BOS-Three	17 b	*ca.*110 (Brenner & Wurz 2019; Brenner *et al*. 2020)	MSA ll lower (also referred to as the "Mossel Bay")	MIS 5d

1.1 Research problem

Studies that focus on palaeoenvironmental conditions during MIS 5 have been conducted at KRM using proxies such as micromammals (for example, Avery 1987; Nel *et al*. 2018), shellfish remains (for example, Langejans *et al*. 2012, 2017) and faunal remains (for example, Klein 1976). Although these studies do infer environmental changes within MIS

5 at KRM, most of the data have been clustered into large temporal units. In addition to this, changes in human occupational patterns and post-depositional processes have yet to receive detailed research attention. A higher resolution palaeoenvironmental and site formation record is needed to comprehend the conditions that influenced the occupational patterns related to early modern humans at KRM. This study is the first archaeological study in a Pleistocene context in South Africa to investigate palaeoenvironmental and site formation conditions using ostracods and foraminifera.

1.2 Research question

What can be learnt about the site formation processes and the palaeoenvironment during MIS 5c-d at Klasies River through the analyses of microfossils such as ostracods and foraminifera?

1.3 Hypothesis

i. There are differences in the ostracod and foraminifera fauna in the sediment of layers SMONE (MIS 5c) and BOS-One, Two and Three (MIS 5d) from Cave 1 at KRM, indicating fluctuations in the environment and depositional processes.

1.4 Aims

i. To improve the understanding of palaeoenvironmental conditions during MIS 5c-d at KRM through the analysis of ostracods and foraminifera and contribute to a higher resolution palaeoenvironmental record.
ii. To gain insight on the relationship between microfossil abundances and depositional processes inside the cave during MIS 5c-d.

1.5 Objectives

i. Extract the ostracods and foraminifera from sediment samples collected during previous excavations at KRM.
ii. Identify different taxa of ostracods and foraminifera through a microscopic study.
iii. Compare these taxa to taxa found during other studies conducted in South Africa (for example, Martens *et al*. 1996; Fürstenberg *et al*. 2017).

iv. Determine the palaeoenvironmental correlates of the identified species.
v. Determine the relationship between depositional processes and the abundance of the identified species.
vi. Conduct a stable oxygen and carbon isotope analysis on the ostracods to shed light on past water temperatures, as well as precipitation and evaporation ratios.
vii. Interpret this knowledge in the context of other palaeoenvironmental research at KRM and contemporaneous sites on the southern Cape coast.

1.6 Rationale

Early MIS 5 is associated with early expressions of typically modern human behaviours (for example, Henshilwood *et al*. 2009; Henshilwood *et al*. 2011; Wadley 2015; Wurz 2019). At Klasies River evidence for "innovative" cultural practices such as the use of ochre and bone tools have been found in the lower MIS 5 levels in Cave 1 (Wurz 2000, 2019; Deacon & Wurz 2005; d'Errico & Henshilwood 2007). Large mammal faunal (Klein 1976; Van Pletzen 2000, Van Pletzen-Vos *et al*. 2019; Reynard & Wurz 2020), microfaunal (Nel *et al*. 2018) and shellfish (Langejans *et al*. 2012, 2017) evidence broadly indicate environmental changes within MIS 5 but the data have been lumped in large temporal units. Both MIS 5c and 5d deposits are grouped within these discussions but it is likely that palaeoenvironmental and depositional conditions differed during the relatively warmer period MIS 5c versus the relatively colder period MIS 5d (Wadley 2015). Some studies suggest that different rainfall patterns would have occurred during these phases (for example, Braun *et al*. 2019).

Ostracods are small bivalved crustaceans with low-magnesium calcite carapaces (Holmes 1992; Boomer *et al*. 2003). Ostracods can live in a wide range of aquatic environments (for example lakes and estuaries) and are useful proxies for inferring paleoenvironmental conditions as they secrete their shells using ions from ambient water (Boomer *et al*. 2003; Caporaletti 2011; Börner *et al*. 2013). Foraminifera are single-celled organisms that have species-specific environmental preferences, thus making them useful for the reconstruction of past environmental conditions (Jones 2013; Strachan 2013; Strachan 2016; Strachan *et al*. 2014, 2015, 2016, 2017).

New excavations at KRM of deposits that date to between MIS 5c-d provide the opportunity to investigate palaeoenvironmental and site formation conditions from a more detailed perspective within these different MIS 5 layers. This type of evidence has not yet been investigated in the context of Middle Stone Age studies. As previously mentioned, the broadly contemporaneous layers from previous excavations have yielded skeletal remains from early modern humans (SASL sub-Member, Cave 1) (for example, Grine *et al*. 2017) and abundant shellfish remains (for example Thackeray 1988; Langejans *et al.* 2012, 2017) that also point to human occupation of the site. This study can, therefore, contribute to understanding the depositional milieu of these early modern humans. Palaeoenvironmental research by analysing ostracods can contribute to the current understanding of the environmental context in which early MIS 5 subsistence strategies, site choices and technological innovations of *Homo sapiens* occurred.

1.7 Structure of thesis

This thesis is divided into six chapters. Chapter 1 focuses on the background to the site and the various research problems, statements, and hypotheses that are investigated. Chapter 2 and Chapter 3 are both literature reviews, where Chapter 2 investigates the palaeoenvironmental data available from various sites on the southern Cape coast, and Chapter 3 reviews the literature available on ostracods and foraminifera. Chapter 4 discusses the material and methods that were used in the microfossil analysis. In Chapter 5 the results of the analysis are presented, and Chapter 6 discusses and interprets these results. Chapter 6 also serves as a conclusion chapter.

Chapter 2: Literature review

Environmental conditions on the southern Cape coast

2.1 Introduction

This literature review discusses the modern-day environmental conditions of the southern Cape coast of South Africa (section 2.1.1) to create a comparison for later palaeoenvironmental inferences. A general description on sea level changes during MIS 5 is given in section 2.1.2 and literature on the paleoenvironment during the MIS 5 period from other nearby archaeological southern Cape sites such as Pinnacle Point (PP; cave PP13B; PP29; Crevice Cave), Blombos Cave (BBC) and the peatland Vankervelsvlei is also examined. The palaeoenvironmental conditions in which the MIS 5c-d deposits from KRM were formed are reviewed in section 2.1.3.

2.1.1 Current climatic conditions on the southern Cape Coast

Present-day climatic conditions in the south-west of South Africa consists of Mediterranean-type winter rainfall (May-September) in contrast to the east and northeast that mainly experience rainfall during the summer (Braun *et al*. 2019). The southern Cape is a transitional region between winter and summer rainfall where rain falls year-round. Today, temperatures in the southern Cape coast can be described as moderate with a yearly average temperature of ~18 ºC (Esteban *et al*. 2020). The south coast of South Africa is near the confluence of the Atlantic and Indian Oceans, as well as two oceanic systems, namely the cold Benguela Upwelling on the west coast and the warm Agulhas Current on the east coast (Lutjeharms *et al.* 2001; Bar-Matthews *et al*. 2010). The waters of the warm Agulhas Current that seep into the South Atlantic is an important component of the global thermohaline system (Lutjeharms *et al*. 2001; Bar-Matthews *et al*. 2010). The diverse marine ecosystem found in these waters is largely due to the confluence of cold and warm waters at the south coast (Bar-Matthews *et al*. 2010).

Today, the shoreline at KRM is about 30 metres from the main site. There is a cobble beach in the cove beneath the main site which was one of the main sources of raw stone material (Deacon & Geleijnse 1988). The site is on the easternmost extent of the Palaeo-Agulhas plain and faces the Indian ocean (van Andel 1989).

2.1.2 The paleoenvironment in the southern Cape during MIS 5c-d

The samples analysed in this study are from the KRM layers dating to Marine Isotope Stage (MIS) 5c-d using time frames suggested by Wadley (2015) (see Appendix B; Section B.1; Table B.1). Interstadial MIS 5c was relatively warmer, whereas MIS 5d was a relatively cooler period (Wadley 2015). Regressive sea level conditions (when submerged areas are exposed due to lower sea levels) generally characterised MIS 5d in the Groot Brak area (231 km west of KRM) in the southern Cape (Table 2.1). Relatively less information is available for MIS 5c, but it seems to have been characterized by relatively higher sea levels (Cawthra *et al*. 2018) (Table 2.1).

Table 2.1 Sea level changes during MIS 5d-c in the Mossel Bay area (after Cawthra *et al.* 2018).

Depth or orthometric height (m to Mean sea level)	OSL age (ka) or relative age	Outcrop	Sea level movement
- 25 meters	115.4 ± 7 (MIS 5d)	Submerged deposit	Regressive/Still stand
- 36 meters	110.7 ± 7 (MIS 5d)	Submerged deposit	Regressive
- 34 meters	108.5 ± 6 (MIS 5d)	Submerged deposit	Regressive
- 31 meters	109.8 ± 7 (MIS 5d)	Submerged deposit	Transgressive
- 29 meters	109.3 ± 8 (MIS 5d)	Submerged deposit	Transgressive
- 24 meters	93.9 ± 5 (MIS 5c)	Submerged deposit	Stillstand to regressive

Due to the location of KRM at the easternmost section of the continental shelf on a coast with a steep bathymetric profile (Van Andel 1989: 143) the effects of sea level changes were not as prominent as the changes further west in the region of the Agulhas Bank (such as at BBC; Figure 2.1). The average distance between the site and the shoreline was between 2.02-2.32 km away (roughly -49 m RSL) during the MSA II (Langejans *et al*. 2012). A study by Dor (2017) found that the coast was between 3.2 km (at 110 ka) and 1.29 km (at 101 ka) away from the site.

Various proxies have been used to examine palaeoenvironmental conditions during MIS 5 at sites on the southern Cape coast. At Pinnacle Point (Figure 2.1), Blombos Cave, and KRM shellfish remains have been analysed (for example Marean 2010; Langejans *et al.*

2012, 2017; Brenner *et al*. 2020). At the latter two sites faunal analyses have also been undertaken (for example Klein 1976; Badenhorst *et al*. 2016; Van Pletzen-Vos *et al*. 2019; Reynard & Wurz 2020) and microfaunal data for MIS 5 are available from PP (Rector & Reed 2010) and KRM (Avery 1987; Nel *et al*. 2018). Stable oxygen and carbon isotope analysis on ostrich eggshells at BBC (Roberts *et al*. 2016) and speleothems at PP (Bar-Matthews *et al.* 2010; Braun *et al*. 2019) have also been undertaken. At Vankervelsvlei (Figure 2.1) fossilised pollen remains (Quick *et al.* 2016) provide information on the palaeoenvironment during MIS 5.



Figure 2.1 The southern Cape coast with the locations of KRM, BBC, PP, and Vankervelsvlei.

i) Palaeoenvironmental data from Blombos Cave

Blombos Cave (Figure 2.1) is located in the Blombosfontein Nature Reserve, about 300 km east of Cape Town and 361 km west of Klasies River, on South Africa's southern Cape coastline (Roberts *et al*. 2016). The BBC is well known for its MSA archaeological remains, such as an ochre-processing workshop that dates to roughly 100 ka (Henshilwood *et al*. 2011), that have improved our knowledge of early modern development of humans during the MSA. At present, BBC is 34.5 meters above sea level and approximately 100 meters away from the ocean (Grine *et al*. 2000; Jacobs *et al*.

2020). The area is dominated by fynbos vegetation (Grine *et al.* 2000; Jacobs *et al.* 2020). This section will focus on the M3 Phase.

There are three MSA levels that have been divided into four phases at BBC, from youngest to oldest, namely M1 (layers CD-CA), M2 upper (layers CFD-CF), M2 lower (layers GCAC-CGAA), and M3 (layers CPA-CH) (Jacobs *et al*. 2020). The MSA sedimentary layers are dated using optically stimulated luminescence (OSL) to between ~100 and 70 ka ago (Jacobs *et al*. 2020). The layer at the top of M3 phase (layer CH) dates to 82 ± 4 ka and the lowermost (CPA) dates to 98 ± 5 ka (Jacobs *et al.* 2020). The M3 phase at BBC is broadly comparable to layers SMONE to BOS-Three from KRM in both age and shellfish densities (Brenner *et al.* 2020), and is further discussed here. The various types of proxy evidence suggest that environmental conditions during the M3 phase were relatively stable, but gradual changes did start to happen towards the end of M3 phase (Jacobs *et al*. 2020) as discussed below.

Jacobs *et al.* (2020) propose that the sea levels were between -49 and -42 meters below sea level during the M3 Phase, based on data from aeolian and palaeosol sequences (also see Roberts *et al*. (2008)). Fisher *et al*. (2010) suggest that the shore was roughly 2 ± 2 km away from BBC at 100 ka when the M3 Phase was deposited. The shellfish assemblage in the M3 Phase is dominated by *Turbo sarmaticus*, *Patella* sp., *Perna perna* and *Dinoplax gigas*, which are all indicative of rocky intertidal conditions (Langejans *et al.* 2012). These taxa would have been available on the widened region of rocky coast during a large portion of this period. The number of *Choromytilus meridionalis* and the presence of *Cymbula granatina* at BBC suggest that the Sea Surface Temperature (SST) during the M3 phase was likely cooler than during the M1 and M2 phases (Langejans *et al.* 2012). The presence of shellfish such as *Turbo sarmaticus*, *Dinoplax gigas*, and *Cymbula oculus* (that also occur in cooler waters) do however indicate that the differences in SST's were not too severe (Langejans *et al.* 2012).

In a faunal study conducted by Badenhorst *et al*. (2016) on the 00 – 80 ka layers from BBC (layers CH to CL and their sub-layers), a wide range of mammalian taxa were found to be present in the M3 phase. The presence of certain mammalian taxa present evidence for an environment that was moist, open at times (layer CJ), rocky with some closed

elements, and had a combination of a sandy substrate and aeolian cliffs (Badenhorst *et al*. 2016).

Roberts *et al*. (2016) used stable oxygen and carbon isotopes from ostrich eggshells and faunal proxies to analyse environmental changes. The surrounding vegetation that was eaten by an ostrich during the breeding season (in which the eggs were laid) is reflected in the stable carbon isotopes of the eggshells, while the stable oxygen isotopes reflect the water that the ostrich consumed (Roberts *et al*. 2016). The data from the stable isotopes were used in combination with previous studies conducted on shellfish (layers CP to CH) and faunal remains (layers CL to CH) (Badenhorst *et al*. 2016; Roberts *et al*. 2016). Roberts *et al*. (2016) notes a substantial enrichment in $\delta^{13}C$ and $\delta^{18}O$ between layers CJ - CI which had likely occurred by the end of the M3 Phase at roughly 90 ka. After the $\delta^{13}C$ enrichment, the warmer water shellfish taxon *Cymbula oculus* becomes more abundant (Roberts *et al*. 2016). This indicates that there was likely less influence of easterlies, thus resulting in increased westerly winds, winter rainfall, and suppressed upwelling (Roberts *et al*. 2016). The equal presence of *Cymbula oculus* (warmer water species) and *Cymbula granatina* (cold water indicator species) in layers CJ and CI/CH implies increased near-shore upwelling, easterly winds, summer rainfall, a rocky coast and increased C4 grasses in the region (Roberts *et al.* 2016; Jacobs *et al.* 2020). An increase in browsers and mixed feeder faunal taxa, perhaps associated with the presence of C^3 grasses (adapted to cool regions and winter rainfall zones), also occurred before the carbon isotope enrichment of the ostrich eggshells at the end of the M3 Phase (Roberts *et al*. 2016).

ii) Palaeoenvironmental data from Pinnacle Point

Pinnacle Point consists of multiple coastal caves (>20) located approximately 10 km west of the Mossel Bay point on South Africa's southern Cape coast and 266 km away from Klasies River (Figure 2.1). Pinnacle Point is located in the transition region between winter and summer rainfall where rain could fall year-round (Braun *et al*. 2019). The earliest evidence for coastal occupation and shellfish collection dates to *ca.* 164 ka from PP13B (Marean 2010). The PP13B cave is currently in proximity to a rocky intertidal zone and faces the Indian ocean (Fisher *et a*l. 2010). This section will focus on the records from

PP13B, PP29, and Crevice Cave and units that are broadly contemporaneous to the MIS 5c-d deposits from KRM are highlighted.

The archaeological deposits from PP13B date to between 74 and 91 ka (Fisher *et al*. 2010). The PP13B shoreline is characterised as a rocky shore with sandy beaches during MIS 5c, and a sandy shore during MIS 5d (Fisher *et al*. 2010; Brenner *et al*. 2020). The MIS 5d units are dominated by *Donax serra*, a species that indicates sandy beaches (Jerardino & Marean 2010; Fisher *et al*. 2010) but some *Perna perna* specimens are present (Fisher *et al.* 2010). Shellfish specimens that indicate cold water conditions such as *Cymbula granatina* are absent at PP13B (Jerardino & Marean 2010; Brenner *et al*. 2020). The increased occurrence of *Perna perna* and *Turbo sarmaticus* suggests that the shore became rockier towards the end of MIS 5c, but the presence of white mussel suggests that sandy beaches were also present (Jerardino & Marean 2010; Brenner *et al*. 2020).

Braun *et al*. (2019) use speleothem oxygen and carbon stable isotope ratios from PP29 at Pinnacle Point as proxies for terrestrial climate change. PP29 is an open cave that was wave cut and occasionally closed by coastal dunes (Braun *et al.* 2019). The PP29 speleothem record covers the period between 112 and 43 ka. Braun *et al*. (2019) report that low stable carbon isotope values were recorded for MIS 5, which indicates that C3 plants are the dominant type of vegetation. Mixed vegetation is present at roughly 107 ka (Braun *et al*. 2019). Stratiform rainfall with low values of δ18O occurred during the early part of MIS 5, but there was likely an increase in convective rainfall at 106 ka and 87 ka (Braun *et al*. 2019). Stratiform rainfall is characterized by "…weak vertical air motion and greater horizontal homogeneity" (Hong *et al*. 1999: 1195). Convective rainfall regions are associated "…with heavy precipitation and vertical air motions much larger than the typical fall velocities of ice crystals" (Hong *et al*. 1999: 1195). Summer rainfall occurred at roughly 106 ka and change from afromontane forests likely occurred at 108–96 ka toward forest margin and fynbos vegetation 96 ka –70 ka (Braun *et al*. 2019).

Faunal data from PP13B (98 ka – 91 ka) suggest the presence of more open, mosaic habitats (Rector & Reed 2010; Carr *et al*. 2016), Micromammal remains infer more closed vegetation and fynbos biome in early MIS 5 (Matthews *et al*. 2009, Matthews *et al*. 2011;

Braun *et al*. 2019). Both the micromammal and faunal record suggest that the environment around Pinnacle Point was consistent during MIS 5 (Rector & Reed 2010; Brenner *et al.* 2020). The shore was likely close to PP13B throughout most of MIS 5 (Brenner *et al*. 2020). The density of shellfish remains at PP13B is much lower than KRM and BBC M3 (Brenner *et al*. 2020).

iii) Palaeoenvironmental data from Vankervelsvlei

Vankervelsvlei is located 400 km east of Cape Town and 200 km west from KRM (Figure 2.1) and is situated in the Knysna Afrotemperate Region ecosystem, on the landward edge of the Wilderness embayment (Quick *et al.* 2016). The Knysna Afrotemperate Region is the biggest section of the southern Cape afrotemperate forests. Vankervelsvlei is a type of bog known as a "*schwingmoor"* (Quick *et al.* 2016). A "*schwingmoor"* usually originates from oligotrophic lakes that are overrun by floating vegetation (Quick *et al.* 2016). The vegetation mat thickens over long periods of time and can later become a habitat for some terrestrial plant species (Quick *et al.* 2016). Vankervelsvlei receives all of its water and nutrients from rainwater. Fossilised pollen remains along with charcoal and sedimentological records from cores were used to gain insight into environmental change in the southern Cape since MIS 5 (Quick *et al.* 2016).

High percentages of *Ericaceae* (heaths) were found in the period that covers ~96-70 ka (Quick *et al.* 2016). The record from ~108-96 ka likely had limited rainfall seasonality and drought stress, as suggested by the presence of afrotemperate forest (seen in high levels of *Podocarpus* pollen) (Quick *et al*. 2016). Sporadic stages of transitional scrub forest and thicket on the nearby dunes is implied by the occurrence of coastal thicket elements in the ~108-96 ka period (Quick *et al*. 2016). Furthermore, fynbos elements (represented by *Ericaceae*) are less noticeable during this period than in the period covering ~96-37 ka, which suggests that conditions were warmer during ~108-96 ka (Quick *et al*. 2016). Low rainfall seasonality is suggested by reduced charcoal fragment frequencies, which indicates less frequent fires, during ~108-96 ka (Quick *et al*. 2016). The data gathered from Vankervelsvlei suggests that the period ~96-37 ka was generally associated with mesic conditions (conditions that have a moderate moisture supply) (Quick *et al*. 2016).

There is an increase in Ericaceae pollen and decrease in *Podocarpus,* which implies increased rainfall seasonality and cooler temperatures (Quick *et al*. 2016).

Data from PP (speleothems) and Vankervelsvlei (fossil pollen) roughly cover the same time period (Braun *et al*. 2019). The record from Vankervelsvlei indicates a change from Afromontane forests at 108–96 ka toward forest margin and fynbos vegetation at 96–70 ka (Quick *et al*. 2016). The change in vegetation is possibly attributed to a climatic change year-round rainfall and warm conditions to winter rain-fall (Quick *et al*. 2016).

2.1.3 Palaeoenvironmental data from KRM

At present KRM is located within the broad Fynbos Biome (Mucina & Rutherford 2006; Wurz *et al*. 2018) and the vegetation consists mostly of forest, thicket, grassland and fynbos (van Wijk *et al*. 2017). The majority of the rocks from KRM are quartzite of the Cape Supergroup (Deacon & Geleijnse 1988). The groundwaters at KRM are acidic, which can negatively influence the preservation of archaeological deposits that contain materials such as bones (Deacon & Geleijnse 1988; van Pletzen 2000). Despite the acidic groundwaters, bone is preserved at KRM because of a source of calcium carbonate that is drained from a fossil dune overlying the site (Deacon & Geleijnse 1988; van Pletzen 2000).

i) Shellfish data from KRM

Rocky shores with tidal pools and small rocky islands are some of the components that are present on the coast surrounding KRM today (Langejans *et al*. 2017). Layer SMONE contains high densities of shellfish such as *Turbo sarmaticus* and *Perna perna* (Brenner *et al*. 2020). The layers below SMONE, namely BOS-One & Two, contain the highest shellfish density and are also dominated by brown mussel and alikreukel (Brenner *et al*. 2020). The presence of these shellfish imply that the shoreline was likely rocky during these phases (Brenner *et al*. 2020). Cold-water specimens were absent in the samples, which indicates that temperatures were warmer (Brenner *et al*. 2020). The density of shellfish decreases in BOS-Three, and alikreukel accounts for the majority of the shellfish present (Brenner *et al*. 2020). Unlike the previous layers, BOS-Three has the lowest density of brown mussel, but there is an increase in species diversity (Brenner *et al*.

2020). White mussel occurs more frequently in BOS-Three, which implies a shift towards an environment with sandy shores (Brenner *et al*. 2020).

Langejans *et al*. (2017) taxonomically analysed the mollusc assemblages from the MSA ll lower phase (also referred to as the Mossel Bay Phase, see Table 1.1) to infer environmental conditions. These data suggest that the site was likely surrounded by rocky shores and that sea levels were moderately high during this time (Langejans *et al.* 2017). Pelagic fish (fish that occupy the water column) are less prominent in the MSA II phase, but a greater number of estuarine fish is reported (von den Driesch 2004; Langejans *et al.* 2017). The data support the hypothesis of the formation of an estuary at the mouth of the Klasies River (von den Driesch 2004; Langejans *et al.* 2017).

Archaeological remains of *T. sarmaticus* have been used by Loftus *et al*. (2017) to determine seasonal stable oxygen isotope ratios and sea surface temperatures (SST) on archaeological sites on the southern Cape coast, KRM included. The stable oxygen isotope results from KRM indicate that the SST for between 115-120 ka were at roughly 12.0°C to 16.9°C (Loftus *et al.* 2017). The temperature results for the 90-95 ka period indicate SST's between 11.1°C and 16.0°C, and for the period between 80-85 ka between 10.3°C and 16.2°C (Loftus *et al.* 2017).

ii) Microfauna and large mammal fauna from KRM

The analysis of microfauna (Nel *et al*. 2018; Maringa 2020) and large mammal fauna (Klein 1976; van Pletzen-Vos *et al*. 2019; Lap 2020; Reynard & Wurz 2020) have served as terrestrial paleoenvironmental proxies at KRM. Analysis of a microfaunal sample from BOS-Three (Witness Baulk) (MIS 5d) infers that MIS 5d was a mosaic environment with "vlei-like" water bodies (Maringa 2020). Furthermore, the analysis of micromammal remains show that soil staining and encrustation are the two most common types of post-depositional modifications in these layers, thus indicating that water was present (Maringa 2020).

The Nel *et al*. (2018) study analysed the microfauna in the layers from cave 1A excavated by Deacon at KRM that date from *ca.* 120 ka to *ca*. 85 ka. The presence of the Cape spiny mouse (*Acomys subspinosus*) in the micromammal assemblage, suggest that fynbos elements were constant during MIS 5 (Nel *et al.* 2018). Between 115 and 108 ka,

more seasonal precipitation largely confined to summer months was present, and during the period between 109 and 90 ka the rainfall was likely more aseasonal (Nel *et al.* 2018).

The most abundant large mammal fauna in the MSA II at KRM include the Cape fur seal, eland, Cape grysbok, Cape buffalo and bushbuck (Van Pletzen-Vos *et al.* 2019). In the material that Deacon excavated large fauna that are indicative of open habitats, such as equids and alcelaphines, are relatively less frequent in the MSA ll SAS Member and the browsers and mixed feeders are more abundant. Klein (1976) also reports a decrease in fauna that are indicative of an open environment, which likely suggests that the vegetation was more closed during MSA II in the Singer & Wymer sample. The abundance of frog remains in the MSA II is high, which indicates that there was likely enough water to support a similar range of frog abundances as in the present day (van Dijk 2006).

2.2 Conclusion

There is evidence for different palaeoenvironmental conditions during MIS 5d and MIS 5c in the southern Cape with rocky shores more prevalent in MIS 5c. Somewhat drier conditions at PP, Vankersvelsvlei and Blombos Cave are also indicated during MIS 5c. The lack of precise dating of the various trends prevents a more detailed comparison of conditions. At KRM, the conditions during MIS 5d, at 110ka as reflected in layer BOS-Three were likely moist and evidence suggests that water affected the condition of microfauna post depositionally. The environment at the time when SMONE (MIS 5c) was deposited in less moist conditions than the BOS-layers.

Chapter 3: Literature review

Ostracods and foraminifera

3.1 Introduction

In this chapter a general background on ostracod and foraminifera morphology, habitat preferences, and dispersal methods will be discussed. The palaeoenvironmental context of these microfossils and case studies from locations in South Africa (Figure 3.1) and abroad will also be reviewed. Lastly, there is a discussion regarding theoretical approaches associated with the occurrence of the microfossils in sediments. Ostracods and foraminifera readily fossilise in sediments (Frenzel & Boomer 2005).

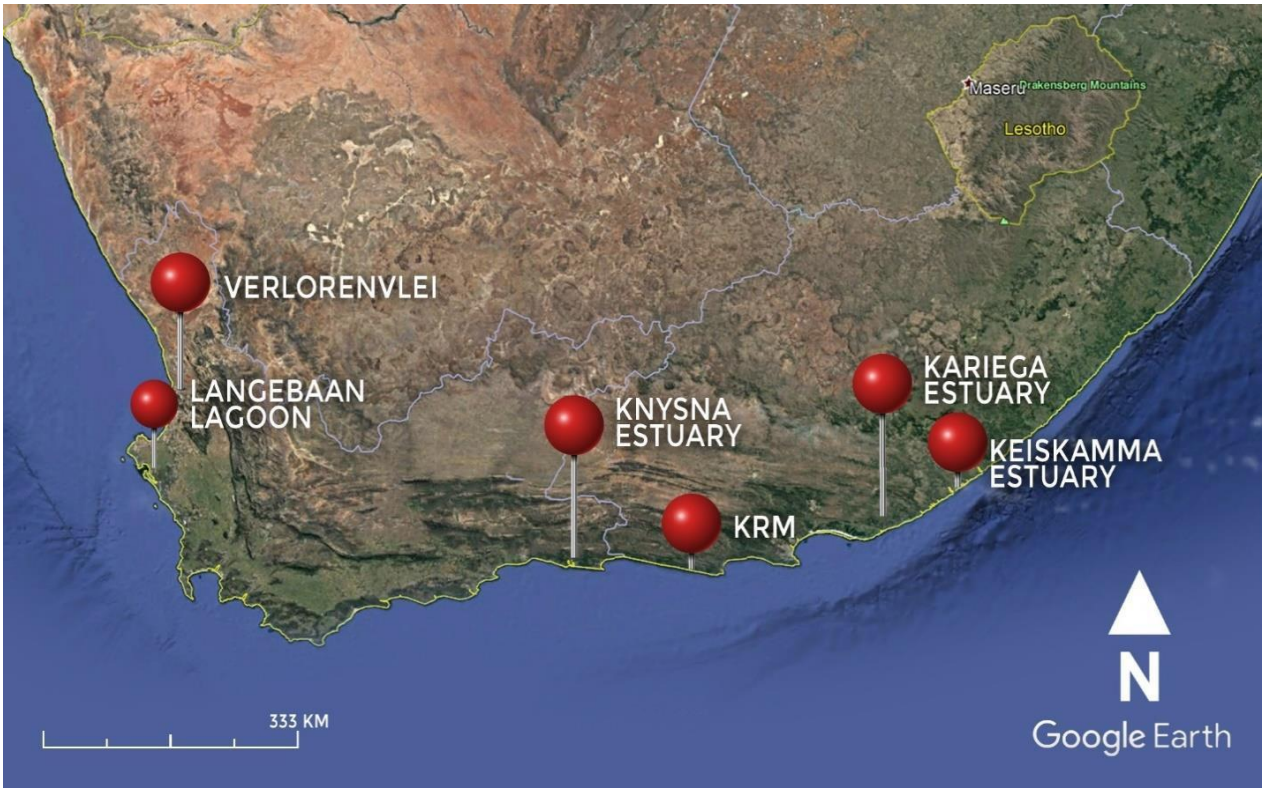


Figure 3.1 The location of the Keiskamma Estuary, Kariega Estuary, Langebaan Lagoon, Verlorenvlei, and Knysna Estuary in relation to KRM.

3.2 Ostracods

Ostracods are effective paleoenvironmental proxies, as they are sensitive to changes in environmental conditions of their aquatic habitats (Griffiths & Holmes 2000). Ostracods have specific ecological preferences (Martens *et al*. 1996) and the stable isotope composition of their shells mirrors the geochemistry of the water that they live in while they secrete their shells (Turpen & Angell 1971; Griffiths & Holmes 2000). In this section, the general morphology, habitats, dispersal methods, and the palaeoenvironmental significance of ostracod shells is reviewed. Furthermore, literature on ostracods in archaeological deposits and ostracods in South African case studies is discussed. Lastly, the theoretical approaches used to interpret ostracod assemblages is summarised.

3.2.1 General description of ostracods

i) Morphology and life cycle

Ostracods are bi-valved crustaceans (Appendix A, Section A.1; Figure A.1) (Kesling 1951; Martens *et al*. 1996; Griffiths & Holmes 2000; Karanovic 2012) that can be found in virtually all types of aquatic environments, such as lakes, marine habitats, brackish water habitats, and salt marshes (Holmes 1992; Griffiths & Holmes 2000; Börner *et al*. 2013).

Ostracods are made up of two valves that completely cover the body and are together known as the carapace (the hard-upper shell of crustaceans) (Martens 1998; Karanovic 2012). The valve margins where two lamellae (thin layers of organic tissue) are fused contain important structures for taxonomic identification (Martens 1998). The majority of ostracod species are easily identifiable from their carapaces' remains, which includes morphological features such as the carapace size and shape, the ornamentation on the outside of the carapace, muscle scars, and hinge morphology (Holmes 1992).

Ostracod growth phases are sporadic (Kesling 1951). Every time an ostracod completes a growth phase (also known as an instar or moulting stage) the ostracod changes both in size and shape (Kesling 1951). From the fist moulting stage, ostracods are covered inside the carapace (Karanovic 2012). The shell shape of the first instar is similar to the oval or rounded shape of the egg that the ostracod hatches from and is weakly calcified (Kesling 1951). Ostracods moult eight times before reaching adulthood (Kesling 1951; Griffiths &

Holmes 2000). The different juvenile moulting stages can cause various taxonomic problems, as the exact instars before the final adult instar are difficult to determine (Hanai *et al*. 1988). Temperature and salinity can control a wide range of biological variables, some of which are linked to the moulting process (Mezquita *et al*. 1999). Mezquita *et al*. (1999) suggest that high water temperatures (20-24 °C) provide the highest moulting and calcification rates and shortest time between moulting stages. The ostracod secretes a carapace during a moulting stage that consists of low-magnesium calcite using Ca^{+2} (calcium ions) and HCO_3 (bicarbonate ions) from the surrounding water (Börner *et al.* 2013). Within hours or days the ostracod shell calcification will occur in equilibrium with the surrounding water (Turpen & Angell 1971; Börner *et al*. 2013). The components used to form the new shell during a moulting phase is not stored prior to moulting, but is rather acquired after moulting from the host waters (Turpen & Angell 1971; Börner *et al*. 2013).

ii) Habitat

As previously mentioned, ostracods are found in the majority of aquatic ecosystems around the world (for example, freshwater bodies, thermal springs, and rivers) (see Holmes 1992; Karanovic 2012; Börner *et al*. 2013). Ostracods also occur in temporary habitats in small water bodies, such as rock pools that only receive water from rain (Jocque *et al*. 2006; Karanovic 2012). There are certain ostracods that are adapted to live in semi-terrestrial habitats, such as fen soil and leaf litter (Danielopol & Vespremeanu 1964; Griffiths & Holmes 2000; Karanovic 2012).

Ostracods are mainly deposit feeders (Karanovic 2012). The diet of ostracods consists of sources such as biofilms (Lawrence *et al*. 2002), invertebrate faeces, algae, dead and living plant material, and organic detritus (Karanovic 2012).

If changes occur in the temperature, salinity, or pH of the water, for example, then it will affect ostracod communities as they are sensitive to these factors (Griffiths & Holmes 2000; Ruiz *et al*. 2013). If the temperature of the waters changes with increasing or decreasing depth, or seasonal change, then it can be a catalyst for changes in the density and diversity of ostracod communities (Ruiz *et al*. 2013). Salinity is a key component in regulating ostracod communities, as certain ostracods can only live within specific salinity ranges (Ruiz *et al*. 2013). The pH of the host waters is an important factor that influences

ostracod communities, as most ostracod species cannot be found in waters with a pH of < 5 because more acidic waters make it difficult for ostracods to receive sufficient calcium uptake for carapace calcification (Boomer *et al*. 2003; Ruiz *et al*. 2013).

Changes in the environment can cause phenotypic variations in ostracod assemblages (Frenzel & Boomer 2005). The genotype stays the same despite environmental changes (Frenzel & Boomer 2005). This is known as environmentally cued polymorphism (see Peypouquet *et al*. 1988; Frenzel & Boomer 2005). Thus, if moulting occurs at different times and under different environmental circumstances, individuals from a single population can be morphologically different (Frenzel & Boomer 2005). The most significant variations in correlation with depth, temperature, salinity, and nutrient availability include ornamentation, noding, and pore shape (Frenzel & Boomer 2005). Ostracods are also sensitive to variables in their habitat, such as the energy levels, depth, size, permanence, and substrate type of the waterbody they live in (Griffiths & Holmes 2000).

"The adaptation of each species to the environment in which it lives results in a more or less well-defined set of habitat conditions favourable for the growth and maintenance of populations, that is, the niche of the species" (Mesquita-Joanes *et al*. 2012: 24). The ostracods niches will vary depending on how tolerant they are to desiccation, pH, and salinity (Mesquita-Joanes *et al*. 2012). In addition, their ability to swim, crawl or dig into the interstitial environment, energy and oxygen requirements, and rate of development will also determine their niches (Mesquita-Joanes *et al*. 2012).

iii) Dispersal

Live ostracods are not very mobile and are not known to travel over long distances by themselves (Karanovic 2012). The main way for ostracods to disperse themselves over long distances is through passive dispersal (Karanovic 2012). Methods of passive dispersal include adhering to birds (usually waterfowl), amphibians (see Lopez *et al*. 2005) humans, fish (see Vinyard 1979), insects, plants, or amphibians (Karanovic 2012). Ostracod eggs can also be transported by the wind, drifting algae, or storm events (Frenzel & Boomer 2005) and can survive extremely low temperatures or high altitudes (see Karanovic 2012). Some ostracods families are more successful in dispersal than

others, as they can produce eggs that are resilient despite long-term desiccation and freezing (Karanovic 2012). Ostracod eggs that are dry-resistant can remain viable for roughly 50 to 100 years and can thus still be dispersed passively (Martens 1994; Karanovic 2012). Parthenogenetic reproduction is another dispersal strategy for ostracods, especially the three freshwater lineages (Cytheroidea, Darwinuloidea, Cypridoidea) (Karanovic 2012). Parthenogenetic reproduction infers that the species can reproduce and start a new population with a single fertile female (Karanovic 2012).

iv) Approaches used for paleoenvironmental inferences using ostracods

a) Shell chemistry

The most commonly used approach for the geochemical analysis of ostracod shells includes trace element analysis and stable isotope analysis (Holmes & de Deckker 2012). An arrangement of low-magnesium calcite crystals and fibrils that include protein and chitin make up the mineralogical structure of ostracod shells (Bate & East 1972; Holmes & de Deckker 2012). Due to the fact that low-Mg calcite is relatively stable, ostracod shells are effective to use for both oxygen and carbon isotope analysis (Holmes & de Deckker 2012). The geochemistry of the host waters that ostracods are in at the time of valve secretion is therefore reflected in the trace element chemistry and stable isotope composition of the ostracod shells (Griffiths & Holmes 2000; Caporaletti 2011).

A stable isotope refers to an atom with an equal number of protons, but a different number of neutrons (see Caporaletti 2011). These atoms do not decay, and therefore a single element and its isotopes produce identical electric change, however, the anatomic weight and physical attributes will differ (see Caporaletti 2011 and references therein). Isotopic fractionation is caused by these differences (see Caporaletti 2011). Stable carbon and oxygen isotopes are both regularly used for palaeoenvironmental studies in both marine and non-marine settings (for example, Holmes 1996; Griffiths & Holmes 2000; Caporaletti 2011). Information regarding the temperature of water, precipitation/evaporation ratio and chemical composition of the host water can be gathered through the stable oxygen isotope analysis of ostracod shells (see Leng & Marshall 2004; Caporaletti 2011). The ratios of stable oxygen isotopes are influenced by factors such as the $\delta^{18}O$ of the water mass, vital effects, and temperature (Caporaletti 2011; Börner *et al.* 2013). Stable carbon

isotopes are also controlled by salinity and temperature, but seasonal productivity and the exchanges that take place between the atmosphere and water also have an influence (Caporaletti 2011). The biogenic (product produced by biological lifeforms) part is managed by factors such as the growth rate of the ostracod shells and their diets (see Leng & Marshall 2004; Caporaletti 2011).

b) Morphological Observations

Ostracod valves are often found in Quaternary sediments. These valves are usually less than 3mm in length if the individual had reached the final adult instar (Griffiths & Holmes 2000). As discussed in section 3.2.1 i), morphological observations (such as the size and shape of the valves) may indicate environmental changes between different habitats and different stratigraphic intervals (Lord *et al*. 2012). The shape and size of the ostracod species can provide information on some palaeoenvironmental conditions (Ruiz *et al*. 2013). If the environment was stable, for example, larger and more geometric ostracod carapaces may be present in the assemblage (Ruiz *et al*. 2013). Other examples include ostracords with irregular shaped pores can be found in oligohaline to hypersaline waters and carapaces that are the richest in magnesium are usually the most reticulated ones (Ruiz *et al*. 2013).

3.2.2 Ostracod studies from Pleistocene archaeological deposits

The role of ostracod research within the geoarchaeological approach has become more prominent over the years. Ostracods in archaeological contexts are usually used in combination with other geoarchaeological approaches, such as sedimentological and geochemical data, or even in collaboration with other paleoenvironmental proxies such as pollen (Mazzini *et al*. 2015). The fact that multiple ostracod species occur in specific environmental conditions makes them useful proxies for inferring paleoenvironmental conditions (Holmes 1992; Martens *et al*. 1996; Karanovic 2012; Mazzini *et al*. 2015).

Ostracods have for example been used to gain insight on sea level and archaeological history of the Thames River at Swanscombe, England (White *et al*. 2013). Swanscombe, Kent, is a hominin site (dating to MIS 11), located on the south bank of the River Thames, east of London (White *et al*. 2013). The study by White *et al*. (2013) analysed and described ostracod and mollusc sequences of Dierden's Pit from MIS 11. Material of

archaeological and palaeontological significance have been uncovered from the exposures of the Swanscombe sequence (White *et al*. 2013). Two stone-tool industries, namely the Clactonian and Acheulian, were uncovered at Barnfield Pit, which forms part of the Swanscombe sequence (White *et al*. 2013). Dierden's Pit was among the few quarries that yielded the Pleistocene gravels as well as underlying Cretaceous Chalk in this area (White *et al*. 2013). The ostracod sequence at Dierden's Pit infers the first clear evidence of the increasing introduction of brackish water at Swanscombe (White *et al*. 2013). The "Rhenish" suite of freshwater molluscs was first recognised in Dierden's Pit (White *et al*. 2013). The "Rhenish" suite is used as evidence of the possible confluence of the Thames and Rhine systems during the Pleistocene (White *et al*. 2013). Further evidence of a possible brackish influence was provided by anadromous fish's remains (White *et al*. 2013). The presence of the ostracod species *Cyprideis torosa* supports previous studies that reported remains of hydrobiid molluscs, Bottle-nosed Dolphin, and anadromous fish implying brackish water conditions from Dierden's Pit (White *et al*. 2013).

No research using ostracods has been done on South African Pleistocene archaeological cave deposits to make paleoenvironmental inferences. Case studies that analyse ostracods in water bodies in South Africa were therefore studied to identify the paleoenvironmental conditions associated with various South African ostracod species.

3.2.3 Ostracod case studies from South Africa

i) Verlorenvlei

Verlorenvlei is approximately 180 km north of Cape Town and 700 km west from KRM (Figure 3.1), on the west coast of South Africa, near Eland's Bay (Martens *et al*. 1996; Meadows *et al*. 1996). Verlorenvlei is a semi-estuarine coastal lake, river and reed-swamp that is one of the few permanent lentic waters with a paleontological record in southern Africa (Martens *et al*. 1996; Meadows *et al*. 1996; Fürstenberg *et al.* 2017). Verlorenvlei is situated close to the Middle Stone Age site Diepkloof Rock Shelter. The summer months are typically hot and dry, while most of the rain occurs during the winter months (Martens *et al*. 1996). During the warmer summer months, high temperatures contribute to mass evaporation from Verlorenvlei (Meadows *et al.* 1996). The Verlorenvlei river is allogenic (has an external source) and also intermittent (Meadows *et al*. 1996).

The river only feeds the swamp and lake system during the winter and early summer rainfall season (Meadows *et al*. 1996). The open water lake is linked to the ocean by a hydraulically-inactive estuary channel (Meadows *et al*. 1996). An exchange between the ocean and the lower lake system occurs when flooding happens in winter or when high spring tides transgress past the sandbar that overlies the rock barrier at the mouth (Meadows *et al.* 1996).

Martens *et al*. (1996) analysed the extant ostracod communities of Verlorenvlei to investigate their relationship and tolerance to salinity as well as their preferences for certain habitats (Martens *et al*. 1996). This study provides information on extant ostracods recorded at Verlorenvlei to contribute to the interpretation of ecological preferences of older ostracod assemblages (Martens *et al*. 1996). This case study is an example of a "uniformitarian" approach, as discussed in Chapter 4. Fifteen ostracod species were identified by Martens *et al*. (1996) at Verlorenvlei (Martens *et al*. 1996). The ostracods were sampled during the dry season (April 1993) and wet season (October 1994). Samples were taken from seven stations during the dry season, and two additional stations were sampled on the same gradient during wet season (both of which become inundated during the wet season) (Martens *et al*. 1996). The salinity was reported to fluctuate substantially during different seasons at the sampling stations that were located closer to the mouth (Martens *et al*. 1996). The pH levels recorded by Martens *et al*. (1996) did range between 6.9 and 8.8 (a pH of 7 is neutral). The variation in pH can likely be attributed to photosynthesis of some plants (Martens *et al*. 1996). Surface temperatures of roughly 20°C and higher were also reported (Martens *et al.* 1996).

The most extensive part of the lake was reported to have low salinity (Martens *et al*.1996). The salinity does however get more variable as proximity to the sea increases and the water can become hypersaline (Martens *et al*. 1996). The majority of the species recorded by Martens *et al*. (1996) at Verlorenvlei are, to a certain degree, indicative of saline or alkaline conditions. This is illustrated by the presence of ostracod species such as *Sarscypridopsis aculeata*, *Gomphocythere capensis*, and *Sarscypridopsis glabrata* (Martens *et al*. 1996). Some species, such as *Physocypria capensis*, *Cypridopsis vidua* and *Limnocythere inopinata* can also occur in freshwater (Martens *et al*. 1996). No marine

ostracod species were reported in the highly hypersaline parts of the lake, which suggests that these areas are likely not permanent (i.e., they dry out during certain months) (Martens *et al*.1996).

A previous analysis of the ostracod fauna at Verlorenvlei conducted by Sinclair *et al*. (1986) reported five freshwater ostracod species. Only one species, namely *Zonocypris tuberosa*, was also recorded by Martens *et al*. (1996). However, Martens *et al*. (1996) explore the possibility that some of the identifications made by Sinclair *et al*. (1986) were incorrect. This includes the misidentification of *Sarscypridopsis aculeata* as *S. gregaria* and *Paracypretta acanthifera* as *P. rubra* (Martens *et al.* 1996). *Sarscypridopsis aculeata* and *Paracypretta acanthifera* are indicators of more saline conditions and were identified by Martens *et al.* (1996). A comparison of Martens *et al*. (1996) and Sinclair *et al.* (1986) might suggest that conditions were possibly less saline during the Sinclair *et al*. (1986) survey; however, Martens *et al*. (1996) could not create a direct comparison as the time of year in which Sinclair *et al*. (1986) conducted their survey remains ambiguous.

The analysis of ostracods from Verlorenvlei is used to establish environmental preferences and habitats. The Verlorenvlei case study creates the foundation for the ostracod identification in this project. The Verlorenvlei study from Martens *et al*. (1996) is one of the few that analyse specifically fresh- and brackish water ostracods in South Africa.

ii) The West coast of South Africa

Fürstenberg *et al*. (2017) conducted a faunistic survey of 25 coastal lakes, estuaries, and ponds along the west coast of South Africa (between the Cape of Good Hope and the Olifantsrivier) (Figure 3.2) in May 2014 to create a dataset containing ecological and distribution data of ostracods and foraminifera for paleoenvironmental reconstructions. Little work has been done to investigate the ecology of brackish water ostracods in South Africa and most identifications rely on only a few publications (such as Martens *et al*. 1996). Fürstenberg *et al*.'s study (2017) contributes further to understanding the biodiversity of brackish water foraminifera and ostracods in South Africa. This study suggests that habitat structure was the main component that influenced the distribution of 19 benthic foraminifera specimens and 32 ostracod specimens (Fürstenberg *et al*.

2017). However, the study also highlights the usefulness of ostracods and benthic foraminifera for salinity reconstructions (Fürstenberg *et al.* 2017).

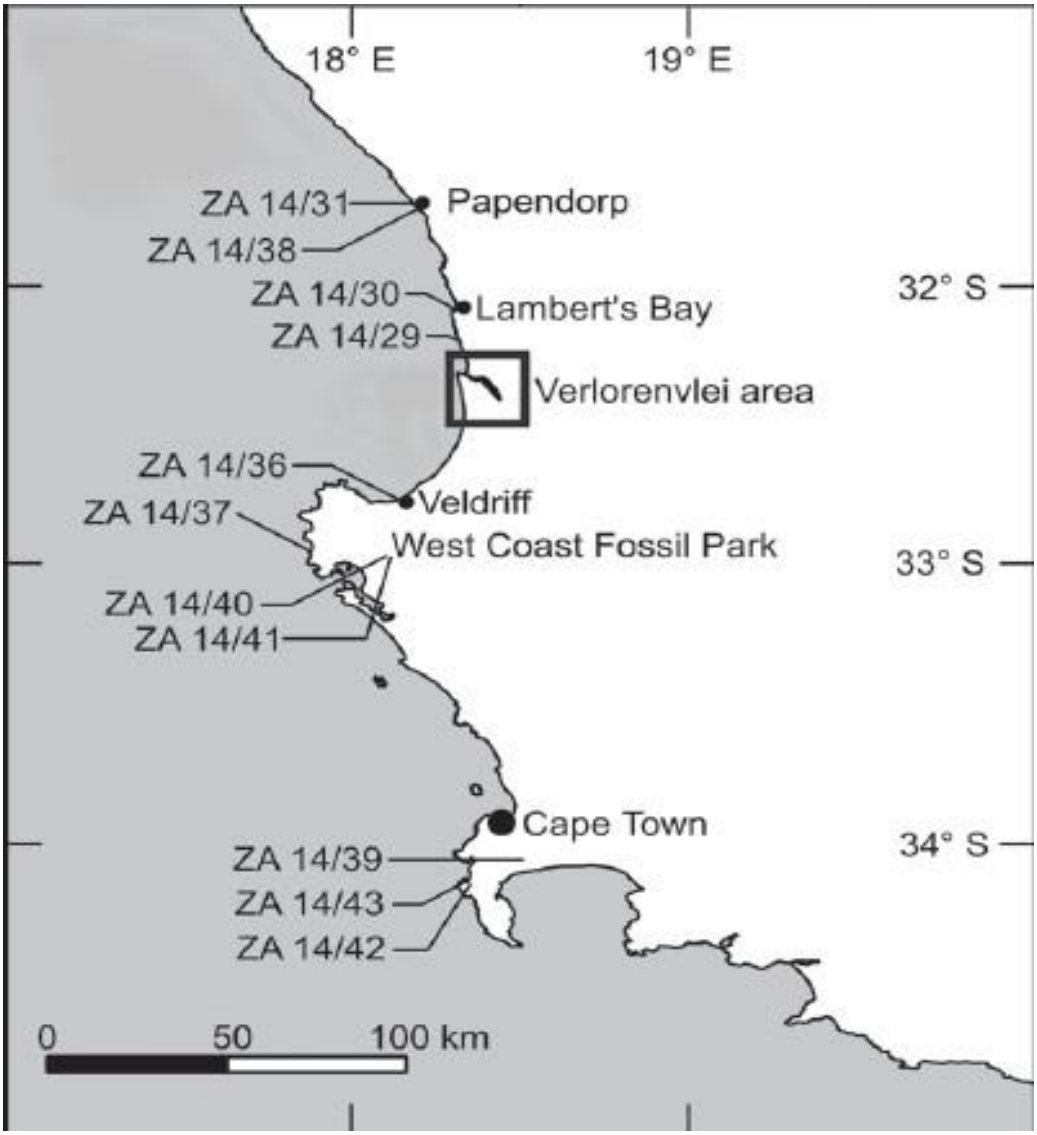


Figure 3.2 The west coast of South Africa analysed by Fürstenberg *et al*. (2017) (Figure by Fürstenberg *et al*. 2017: 330).

All the areas that were sampled are located in the winter rainfall zone, which is characteristically climatically semi-arid (Fürstenberg *et al*. 2017). The areas of Verlorenvlei that were sampled include the estuary channel (which is hydraulically inactive for a large portion of the year), as well as the marshlands at the rivers (Fürstenberg *et al*. 2017). The majority of salinity classes (measured as parts per thousand, also known as ppt) did show specific correlations with certain ostracod species,

for example *Macrocypris* sp. was present in the limnetic range (open area of a freshwater body) whereas live specimens of *Ilyocypris bradyi* was the only ostracod taxon present in the oligohaline range (< 5.0 ppt) (Figure 3.3).

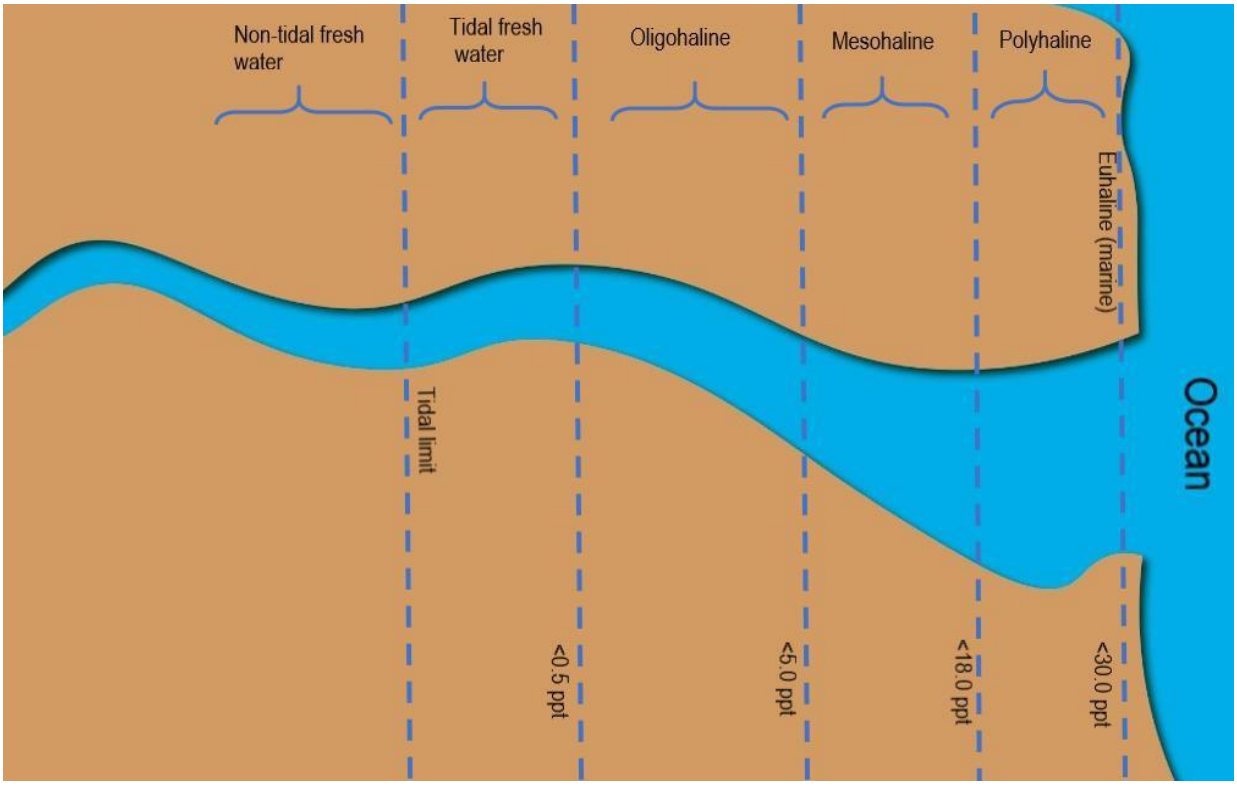


Figure 3.3 The various salinity ranges of an estuary – inspired by information and figures by Ohrel & Register (2006) and www.e-education.psu.edu/earth107/node/1026.

Living *Gomphocythere capensis* and *Physocypria capensis* were present in the limnetic to mesohaline range (freshwater to waters of < 18.0 ppt) (Figure 3.3) (Fürstenberg *et al*. 2017). The ostracod taxon *Leptocythere hartmanni* (both living and fossil) was restricted to the polyhaline range (<30 ppt) (Figure 3.3) (Fürstenberg *et al*. 2017). The highest diversity of taxa occurred in the euhaline range (waters with similar salinity to the ocean, roughly 30 to 35 ppt) (Fürstenberg *et al*. 2017). The only living species of ostracod found in hypersaline conditions was *Sarscypridopsis glabrata* (Fürstenberg *et al*. 2017). However, empty valves of *Physocypria capensis* (common in South Africa, occurs in saline and freshwater conditions), *Cytheromorpha milleri*, *Gomphocythere obtusata* (usually occurs in freshwater, but has been reported in slightly saline conditions), *Sarscypridopsis aculeata* (occurs in more saline conditions), *Xestoleberis sp*. and

Cyprideis sp. were also found in the hypersaline conditions (Fürstenberg *et al*. 2017). Fürstenberg *et al*. (2017) reported empty valves of *S. aculeata* at salinities of >90 ppt on the west coast of South Africa. As with the previous taxon, this does not necessarily equate to the ecological tolerance of *Sarscypridopsis aculeata* (Fürstenberg *et al.* 2017). Some species of ostracod were not present in the study conducted by Fürstenberg *et al*. (2017), but were described in the Martens *et al*. (1996) study of Verlorenvlei. This can be attributed to the fact that Fürstenberg *et al*. (2017) only sampled during the dry season, whereas Martens *et al*. (1996) sampled in the dry and wet seasons. During the dry season, some areas of Verlorenvlei dry up completely, while the same area can be inundated during the wet season, for example stations eight and nine, as described by Martens *et al*. (1996). The sampling season is therefore important as ostracods cannot survive in an environment that has completely dried up.

The research conducted by Fürstenberg *et al*. (2017) provides data on how ostracod communities in South Africa reflect habitat type, structure, and salinity ranges. Thus, making for an effective case study to place the ostracod assemblage from KRM into a broader context.

iii) Summary of South African case studies

In the Verlorenvlei study, Martens *et al*. (1996) identified fifteen species of ostracod from two surveys. This study analysed extant ostracod communities in relation to their salinity and habitat preferences and tolerances. Due to ambiguity caused by a previous study conducted at Verlorenvlei, this study was unable to conclude whether there were significant changes in salinity in the main lake at Verlorenvlei (Martens *et al*. 1996).

The West coast study conducted by Fürstenberg *et al.* (2017) analysed the distribution of foraminifera and ostracods from twenty-five sites in South Africa. This study concludes that one can differentiate between three main types of habitats for future palaeoenvironmental reconstructions, namely hyperhaline conditions (high abundances of the ostracod *Sarscypridopsis glabrata*), still water areas of lakes with limnetic to oligohaline conditions, and ponds or semi-enclosed parts of lakes with low salinity and the presence of *Sarscypridopsis aculeata* (Fürstenberg *et al*. 2017).

3.2.4 Theoretical approaches

i) Uniformitarianism (the present is the key to the past) and Indicator Taxa

By assuming that the environmental requirements of organisms in the past were similar to those of their most closely related living representatives is one of the most basic methods of interpreting past environments (Dodd & Stanton 1990). The principle of uniformitarianism first became known in 1795 when James Hutton published his “Theory of the Earth” (Neale 1983). In this publication, Hutton theorizes that the natural processes observed today could explain certain geological changes that occurred in the past (Hutton 1795; Neale 1983). In the early 1800’s, Charles Lyell edited and distributed Hutton’s approach (Neale 1983). Lyell’s uniformitarianism approach suggests that the ecological response of species does not change through their histories (Scott 1963). In addition to geology, many researchers have also been applying the principle of uniformitarianism to ecology (Scott 1963; Dodd & Stanton 1990) and micropaleontology, in this case ostracods (Neale 1983; Boomer *et al*. 2003) and foraminifera (Haunold *et al*. 1997).

The environmental characteristics of the life habitat of an ostracod assemblage and the environment of deposition can be inferred by using uniformitarian and palaeobiological approaches in addition to suprageneric, generic and species composition information (Boomer *et al*. 2003). Uniformitarian approaches are relevant when applied to Quaternary and late Neogene assemblages, as they may include large numbers of extant or closely related taxa (Boomer *et al*. 2003).

The fact that ostracods can be ascribed to various environmental ranges, makes them effective to use as indicator taxa when analysed as a part of a fossil or “dead” assemblage (Lord *et al*. 2012). When used as “indicator taxa”, the ostracods are used to suggest that the past environmental range could have been similar to the range of modern assemblages (uniformitarian approach) (Lord *et al*. 2012). The various ostracod species in an assemblage will have a “survival range”, which refers to an environment in which certain species might be present, but will not necessarily thrive (Lord *et al.* 2012). In addition to this, the ostracods will also have a “total climatic range”, which refers to an environment in which they can live and reproduce (Lord *et al*. 2012). The main focus

should, however, be placed on the “optimum range”, which refers to a set of climatic conditions that the ostracods prefer above most others (Lord *et al*. 2012).

Modern analogue approach is also used in a more modernised context as a means of comparing fossil assemblages with modern (Simpson 2012).

ii) Thanatocoenosis and Taphocoenosis

A key part of analysing ostracods is distinguishing the original living association (biocoenosis) and the *in situ* “fossil life assemblage” (thanatocoenosis) from the dead assemblages that have been subjected to transport and sorting (taphocoenosis) (Boomer *et al.* 2003; Frenzel & Boomer 2005; Lord *et al*. 2012). The biocoenosis becomes a thanatocoenosis after death (Boomer *et al*. 2003). The ostracod assemblage is influenced by components such as the dissolution of weakly calcified instars or different mortality rates (Boomer *et al*. 2003). In this case the assemblage is not a ”real” biocoenosis, but rather an autochthonous thanatocoenosis (Boomer *et al*. 2003). Boomer *et al*. (2003) suggest that an *in situ* life assemblage is defined as an autochthonous thanatocoenosis and a death assemblage that has been subjected to *post-mortem* transport is an allochthonous taphocoenosis. This definition will be used in context of the KRM project.

In marginal marine environments it is particularly important to distinguish between an autochthonous thanatocoenosis and an allochthonous taphocoenosis, as *post-mortem* transportation and redeposition of valves are common occurrences (Frenzel & Boomer 2005). Allochthonous (originating from a different area to where the organism was deposited) assemblages can occur when inflowing freshwater, storms, or waves of tidal currents, deposit foreign ostracod assemblages to different environments (Frenzel & Boomer 2005). The sorting (according to weight, shape and size) of the various instars of ostracod valves may occur after the assemblage has been deposited (post-depositional) and can therefore cause analytical biases (Frenzel & Boomer 2005).

The following types of population structures may indicate the level of sorting an assemblage has been subjected to (according to Whatley 1983; Frenzel & Boomer 2005). The first type of population structure, known as a “low energy environment”, is typical of secluded parts of estuaries at the tidal coast (Whatley 1983; Frenzel & Boomer 2005).

This type of population structure contains all juvenile stages as well as male and female specimens (Whatley 1983; Frenzel & Boomer 2005). The second type of population structure is known as “high energy life or death assemblages”, and exclusively contains adults and larger juveniles, which indicates more exposed sand flats or tidal channels (Whatley 1983; Frenzel & Boomer 2005). The third type of population structure is known as a “low energy death assemblage,” which exclusively contains small juveniles and is also observed on more exposed sand flats, similar to the second population type (Whatley 1983; Frenzel & Boomer 2005).

If a sub-fossil ostracod assemblage is completely unaltered, then the assemblage should (in principle) be dominated by juveniles (Frenzel & Boomer 2005). However, in reality, the majority of these recent and fossil ostracod assemblages contain mostly larger individuals from later instars (Frenzel & Boomer 2005: 72). This serves as evidence of taphonomic influence in the preservation of a sample as smaller shells are more fragile (Frenzel & Boomer 2005). The majority of fossil taphocoenoses ostracod assemblages will likely contain both allochthonous and autochthonous components (Lord *et al*. 2012). It is important to note that the taphonomic processes start before the final burial (Boomer *et al*. 2003). Therefore, one must take into account that even if a sub-fossil ostracod assemblage has been collected from an enclosed and seemingly unaltered environment, the assemblage is still unlikely to completely reflect the living population (Boomer *et al*. 2003).

3.2.5 Conclusion

Ostracods are bivalved crustaceans that are abundant in nearly every aquatic habitat on earth. They are effectively used to determine palaeoenvironments and have been applied to archaeological studies. Research papers regarding the analysis of ostracods in South Africa are rare, but two main studies, namely Martens *et al.* (1996) and Fürstenberg *et al*. (2017) will be used for comparison in the present study at KRM. Regarding theoretical approaches to interpret ostracod assemblages, uniformitarian and indicator taxa approach can be effective for determining the environmental characteristics of a dead or fossil ostracod assemblage, as they assume that one taxon will exhibit the same environmental characteristics in the present day and in the past. In addition to this, the

fossil or dead ostracod assemblages are able to reconstruct the biocoenosis of the original assemblage to a certain extent if the population structure is determined, which is an essential component for understanding the depositional environment (Boomer *et al*. 2003; Frenzel & Boomer 2005; Lord *et al*. 2012).

3.3 Foraminifera

Foraminifera are single-celled organisms (Appendix A, Section A.1; Figure A.2) (Jones 2013). The protoplasm of foraminifera is enclosed within a hard shell called a “test” (Sen Gupta 1999; Jones 2013; Murray 2013) and the organisms are generally small (<1 mm) although some species may exceed 1 cm (Murray 2013). Foraminifera that are living, dead, or fossilised can occur in various environments, for example brackish to marine waters (BouDagher-Fadel 2018). The type of foraminifera in question (planktic or benthic) will reveal more about their environmental preferences. Foraminifera are not common in terrestrial habitats, but they have previously been identified in the KRM sediments micromorphological slides by Susan Mentzer (Mentzer *et al*. 2015).

The samples from KRM contain some foraminifera so it is pertinent to know which dispersal methods are responsible for their occurrence in the deposits, and how foraminifera have been used in studies regarding archaeological deposits. Foraminifera used in South African case studies to determine sea level change in the Holocene is also discussed.

3.3.1 General description of foraminifera

There are two main types of foraminifera, benthic (bottom-dwelling) and planktic (occurring in the water column) (Jones 2013). Benthic foraminifera can occur as both agglutinated and calcareous forms and they can be found in various types of habitats ranging from shallow to deep waters, including the ocean and estuarine systems (Jones 2013). Agglutinated foraminifera refer to foraminifera that create their tests by sticking detrital (organic) material together and can survive in environments with no carbonate (Hemleben & Kaminski 1990; Strachan 2013). A calcareous test is secreted by the organism and the calcite is usually either low or high magnesium (Jones 2013). Planktic foraminifera have tests that are made of globular chambers that keep the organisms afloat

(BouDagher-Fadel 2015). The shells of planktic foraminifera are composed of secreted calcite or aragonite (BouDagher-Fadel 2015). Foraminifera growth is continuous and achieved through increasing a single chamber, or by adding new chambers (Jones 2013). Unlike the ostracods, the foraminifera do not moult their tests.

Benthic foraminifera can move around in two ways, namely in an active dispersal scenario or a passive dispersal scenario (Alve 1999). The only way for foraminifera to conduct active dispersal is through self-locomotion or within sediment that is in suspension (Alve 1999). Both of these methods will only result in travel over short distances (Alve 1999). Active dispersal through self-locomotion is however unlikely due to the slow speed of movement and the lack of direction of the organism (Murray 2013). Passive dispersal of foraminifera entails the release and transport of juveniles in embryonic stages and passive suspension of various growth stages (Alve 1999). Foraminifera can be transported by sticking to larger marine animals and also by sticking to the feet of certain bird species (Resig 1974; Murray 2013). Sediment reworking caused by storms can result in shelf foraminifera being transported from the ocean to and from other parts of estauries (Mills *et al.* 2013; Strachan 2016). Multiple environmental variables, such as temperature and salinity, influence the distribution patterns of foraminifera (Murray 2013).

Rosendahl *et al*. (2007) report on archaeological finds from Mort Creek in Australia and suggest that cultural activities by Aboriginal communities (for example, the consumption of marine animals) may have led to foraminifera being displaced into terrestrial sites. Some taxa (such as *Elphidium crispum*) can attach themselves to seagrass and can be eaten by seagrass grazers such as turtles (Rosendahl *et al*. 2007). Turtle remains have been excavated at Mort Creek and it is likely that the foraminifera found in the same layers originate from the turtle stomach contents (Rosendahl *et al.* 2007). Foraminifera can also be introduced into terrestrial sites by natural processes such as tidal action (Rosendahl *et al*. 2007).

It is important to note that some species of foraminifera preserve better than others, potentially causing a taphonomic bias even in relatively recent sedimentary records (Sen Gupta 1999).

3.3.2 Foraminifera and the paleoenvironment

i) Determining Holocene sea level changes

Benthic foraminifera from salt marshes and estuaries in the southern, western and eastern Cape have been studied as indicators of sea level change and changes in paleoenvironment (for example, Franceschini *et al.* 2005; Strachan *et al*. 2014, 2015, 2016, 2017). The surface assemblages of salt-marsh foraminifera differ in relation to their position in the tidal frame, thus making them effective sea level proxies (Strachan *et al.* 2015). The studies were conducted at Knysna (Strachan 2016; Strachan *et al*. 2016, 2017), Kariega (Strachan 2013; Strachan *et al*. 2014, 2015), and Keiskamma estuaries (Strachan 2016; Strachan *et al*. 2016, 2017) (Figure 3.1).

Assemblages of foraminifera are vertically zoned along the surface elevational gradients, which are linked to the tidal elevations and inundation rates (Strachan 2013; Strachan *et al.* 2014). Strachan *et al*. (2014) analysed core samples from the salt marshes and constructed a late Holocene sea level model. Modern assemblages of foraminifera were also examined and they did display a vertical zonation across the surface of the marsh (Strachan *et al.* 2014). Strachan *et al*. (2014) found that there was a significant increase of agglutinated foraminifera towards the upper parts of the core and decrease further down the core. The base of the core contained calcareous foraminifera that infer shallow subtidal conditions (Strachan *et al.* 2014).

Galpins salt-marsh is an intertidal salt-marsh system at Kariega (Strachan *et al.* 2014). Strachan *et al*. (2015) use modern assemblages of foraminifera as reference for analysing the vertical zones in salt-marshes. The modern assemblage is used in a “modern analogue method” to compare the fossil assemblage to (Strachan *et al.* 2015). The past salt-marsh surface elevations and relative sea levels are reconstructed by indicating the contexts of specific foraminifera assemblages and applying these to the fossil foraminifera assemblages that are in the salt-marsh core (Strachan *et al.* 2015). Strachan *et al.* (2015) found that agglutinated taxa (such as *Jadammina macrescens*) were mainly found in the high mash areas and the middle marsh area had an abundance of taxa such as *Miliammina fusca* and *Trochammina inflata.* The calcareous taxa (such as *Haynesina germanica* and *Ammonia batava*) were found in the mud flats (Strachan *et al.* 2015).

The study conducted by Strachan *et al.* (2016, 2017) showed that approximate Holocene sea level reconstructions are reliant on the accurate characterisation of the relationship between modern benthic foraminifera assemblages and their relationship with the given environment representative of a study site. This is known as the modern analogue approach. The two sites that were used for the Strachan *et al.* (2016, 2017) analysis are Keiskamma and Knysna estuaries (Figure 3.1). Elevation is understood to be the key environmental variable that controlled the distribution of salt-marsh foraminifera at the estuaries, although other environmental variables such as pH and salinity also play a role in the distribution of microfossils (Strachan 2013; Strachan *et al*. 2014, 2015,2016, 2017). The environmental conditions in the low-marsh zone (where most calcareous forms were found) are more stable and subaerial exposure is limited (Strachan *et al.* 2017). The environmental conditions in the high-marsh zones, that tend to reach the survival threshold, contained more agglutinated forms (Strachan *et al.* 2017). Studies on sea level change need *in situ* foraminifera assemblages, unlikely to be found in cultural deposits such as those from KRM.

The analysis conducted by Strachan (2013) and Strachan *et al*. (2014, 2015, 2016, 2017) confirm the preliminary study of Franceschini *et al*. (2005) that found that foraminiferal assemblages exhibit a vertical zonation related to elevation and the abundance and type of vegetation.

b) Distinguishing between natural and cultural deposits

Foraminifera from the Mort Creek site complex, Australia

The Mort Creek Site Complex is located on the west bank of Mort Creek, on the west coast of Rodds Peninsula (Queensland, Australia) (Rosendahl *et al*. 2007). The site consists of both natural and cultural shell deposits. Rosendahl *et al*. (2007) analysed foraminifera to ascertain whether deposits are of natural or cultural origin, as sediments that display characteristics of mixing (for example bioturbation) can often make it difficult to identify cultural layers. The Mort Creek study suggests that cultural shell deposits will display certain characteristics that will not be observed in natural deposits and uses the density of foraminifera to establish the difference (Rosendahl *et al*. 2007). Foraminifera are abundant in ocean waters, and natural deposits are often created by marine

processes such as higher tide levels (Rosendahl *et al*. 2007). If the sediment was deposited by marine action, then the deposit should have an abundance of foraminifera (Rosendahl *et al*. 2007). However, foraminifera will be either rare or absent if the deposit was formed by cultural actions (Rosendahl *et al*. 2007). The foraminifera may still occur in cultural deposits, as some processes (like certain types of foraging activities) can result in the redeposition of foraminifera (Rosendahl *et al*. 2007).

Rosendahl *et al*. (2007) analysed 14 sediment samples from four excavation squares. Morphological elements were identified, the foraminiferal samples were quantified and photos were taken. Ten foraminiferal taxa were identified, and density analyses enabled the distinction between natural and cultural deposits. The natural deposits contained >1000 foraminifera per 100 g of sediment, whereas cultural deposits contained <50 foraminifera per 100 g of sediment. The study by Rosendahl *et al.* (2007) concludes that foraminifera can be introduced to terrestrial deposits through various cultural and natural deposits.

3.3.3 Conclusion

Foraminifera are single celled protists that are often used in palaeoenvironmental reconstructions and have been applied to archaeological sediments, for example at Mort Creek in Australia (Rosendahl *et al*. 2007) to gain perspective on the origin of the deposit (natural or cultural). However, in South Africa they have mostly been used in sea level reconstructions from the Holocene, for example Strachan (2013) and Strachan *et al*. (2014, 2015, 2016, 2017) and not in an archaeological context.

Chapter 4: Material and methods

This chapter discusses the materials and methods used to analyse the microfossils from KRM. Four layers that date to MIS 5c-d were selected for analysis (as discussed in Chapter 1). The material used for microfossil analysis will be discussed first, followed by the various methods used to process, count, and quantify the various samples. The final section will discuss the methodology used for the stable isotope analysis.

4.1 Material

Deposits from layers Shell Midden One (SMONE), Black Occupational Soils ONE (BOS-One), Black Occupational Soils TWO (BOS-Two) and Black Occupational Soils THREE (BOS-Three) (Figure 4.1) that form part the SASL sub-member were examined for the presence of microfossils. The lowermost part of the SASU sub-member (which is above the SASL sub-member) has been dated to around 100 000 years old (Eggins *et al*. 2005; Wurz *et al*. 2018) and speleothem material from the BOS-Three layer date to 110 000 years ago (Brenner & Wurz 2019; Brenner *et al*. 2020).

All sediment samples were collected during field seasons at KRM between 2015 and 2017. Sediment samples for each layer and square were collected in the field as excavations progressed. A sample was collected daily from each excavated square's bucket prior to wet or dry sieving (Prof S Wurz, personal communication, Feb. 2020). Samples for this project were selected from boxes of available samples from Prof Sarah Wurz' laboratory in the Origins Centre at the University of the Witwatersrand. Care was taken to select samples with similar amounts of sediment in them. Various sediment samples from layers SMONE (MIS 5c), BOS-One, BOS-Two, BOS-Three (MIS 5d) from the Witness Baulk (Cave 1) were analysed.

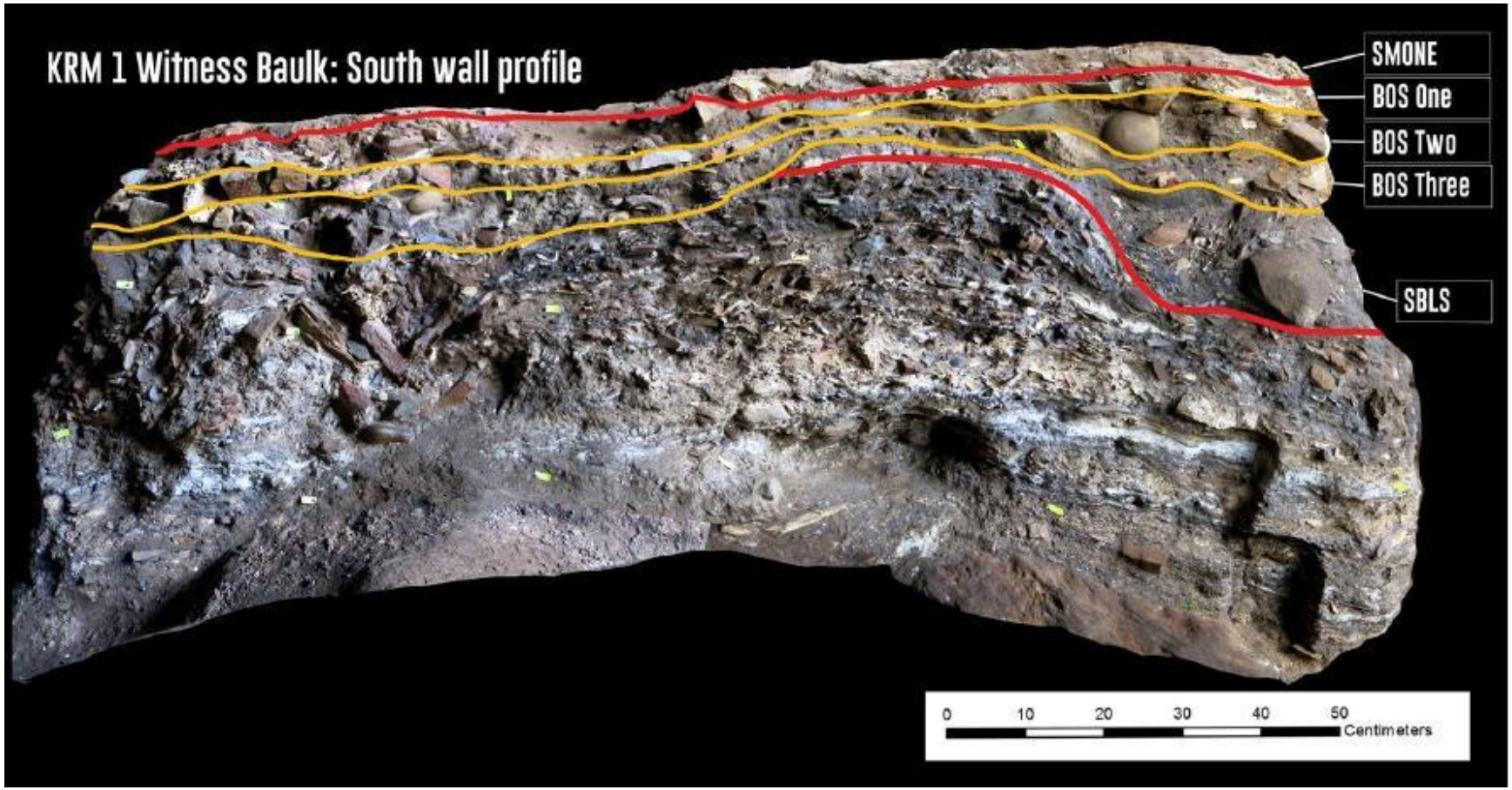


Figure 4.1 The MIS 5c-d layers (SMONE; BOS-One; BOS-Two; BOS-Three) from the Witness Baulk in cave 1 where the samples were collected (Brenner *et al*. 2020).

4.2 Methods

The primary analysis of sediment samples from the KRM layers took place at the University of the Witwatersrand between February 2019 and September 2020. Two research stays were conducted in Europe to further assist with the processing and analysis of the microfossils. The first was from May 2019 to June 2019 at the University in Bergen, and at NORCE, Norway facilitated by Research Prof. Carin Andersson. The second took place in March 2020 at the Friedrich-Schiller University in Jena, Germany, facilitated by Prof. Peter Frenzel.

4.2.1 Sample preparation

i) Preliminary analysis

Preliminary analysis of 17 samples from KRM (Appendix C; Section C.1; Table C.1) and microfossil identification training took place from May to June 2019 at the NORCE Climate Sediment laboratory in Bergen, Norway. The sediment samples were disaggregated in water for roughly eight hours using the Infors HT Orbitron shaker platform. Samples were washed with water through 1mm (coarse fraction), 150 µm and 63 µm sieves to remove clay and silt. The >150 µm fraction was examined for microfossils, as this fraction is likely to have a good number of easily identifiable adult specimens (after Bé 1959: 84). When processing foraminiferal samples, it is important to bear in mind that processing methods are not standardised, which creates complications when one project is compared to another (Jones 2013). The suggestion to analyse the >150 µm fraction was initially introduced to be used in planktonic foraminiferal studies by Bé (1959). The Bé (1959) study suggests that specimens less than 150 µm in size can cause difficulties for identification, as a smaller fraction will contain more juveniles. The conventional sieve size used for the recovery of ostracods is 125 µm (Horne & Siveter 2016). However, some ostracod specimens range from 0.2mm (200 µm) in juvenile stages up to 1mm in length (Martens *et al*. 1996) in adult stages, which one can argue, still allows for a sufficient number of microfossils to be collected from the >150 µm fraction. Strachan (2013), for example, wet sieved their subsamples through 500 µm and 63 µm mesh size sieves. Thus, a 150µm sieve is therefore a good compromise as this removes an excess of juveniles that would complicate this pilot study and will still retain planktic foraminifera.

The <63 µm fraction was not used for quantitative analysis, as it may contain a high number of juvenile microfossils that can be difficult to accurately identify due to the lack of adult features (Schönfeld 2012; Horne & Siveter 2016).

Sieves were washed between uses, as a sieve that is not properly washed can potentially contaminate other samples and create inaccurate results (Rosendahl *et al*. 2007; Murray 2006). The washed samples were transferred into labelled beakers, and placed into the drying oven at a low temperature, roughly 60ºC (Horne & Siveter 2016), for a few hours to create the residue used for analysis. The time spent in the drying oven varied according to the amount of moisture that needed to evaporate from the sample after washing.

ii) Expanding the sample size

To enlarge the sample after the first exploratory stage of analysis, an additional fifteen sediment samples from KRM (Appendix C; Table C.1; Table C.1) were washed in January 2020 at the Environmental Laboratory located in the Bernard Price Building at the University of the Witwatersrand, Johannesburg. The methods for processing the samples remained the same as those undertaken in Norway, with the exception of disaggregating the samples using the Infors HT Orbitron shaker platform. To compensate for the absence of the shaker platform, samples were placed in a beaker filled with water for a few hours (the time was dependent on the clast size that needed to dissolve). The weight (measured on Ohaus Scout scale, located in the second-floor lab at the Origins Centre, University of the Witwatersrand) of the sediment samples for the various fractions, the microfossils, and the excavation square and layer from Cave 1 was recorded (Appendix C; Section C.1; Table C.1; Table C.2; Table C.3).

iii) Splitting samples

The standard procedure for counting microfossils involves repeatedly splitting a sample in half until an aliquot containing ≥300 microfossil specimens is obtained (Tetard & Marchant 2020). Adhering to standards initially set by Dryden (1931), a minimum count of 300 individual microfossil specimens were counted for this project (Dryden 1931: 237; Sen Gupta 1999: 74; Tetard & Marchant 2020: 1). If there is a high abundance of microfossils in the sediment sample, splitting the sample can be time-consuming, as the

sample needs to be divided multiple times to obtain the desired aliquot size (Tetard & Marchant 2020). A 3D printed fixed dry sediment splitter (Figure 4.2) designed for micropaleontological analysis by Tetard & Marchant (2020) was used to split the samples for this project. The fixed 3D printed dry splitter works as follows: First the sediment sample is poured into the funnel, which has a small hole at the bottom; the particles then fall through the hole and hit the conical section below, evenly dispersing the sample in all angles (Tetard & Marchant 2020: 2). The samples used were split into $\frac{1}{2}$; $\frac{1}{4}$; $\frac{1}{8}$; $\frac{1}{16}$ and $\frac{1}{32}$ fractions. The smallest fraction was analysed first to determine which fractions would be best to analyse in order to reach a ≥300 count for the microfossils. An entire split should be counted regardless whether the count exceeds 300 specimens, as the species distribution poured out onto the picking tray is uneven and unlikely to be homogeneous (Schönfeld 2012). An inaccurate species composition is more likely if parts of the split are not taken into account (Schönfeld 2012). Within each KRM layer, multiple samples from different excavation squares in the Witness Baulk were analysed and each sample was divided into a split that was analysed. The data from the multiple excavation square samples were then added together to gather information on the differences between layers. An attempt was made to count a minimum of 300 specimens from every sample.

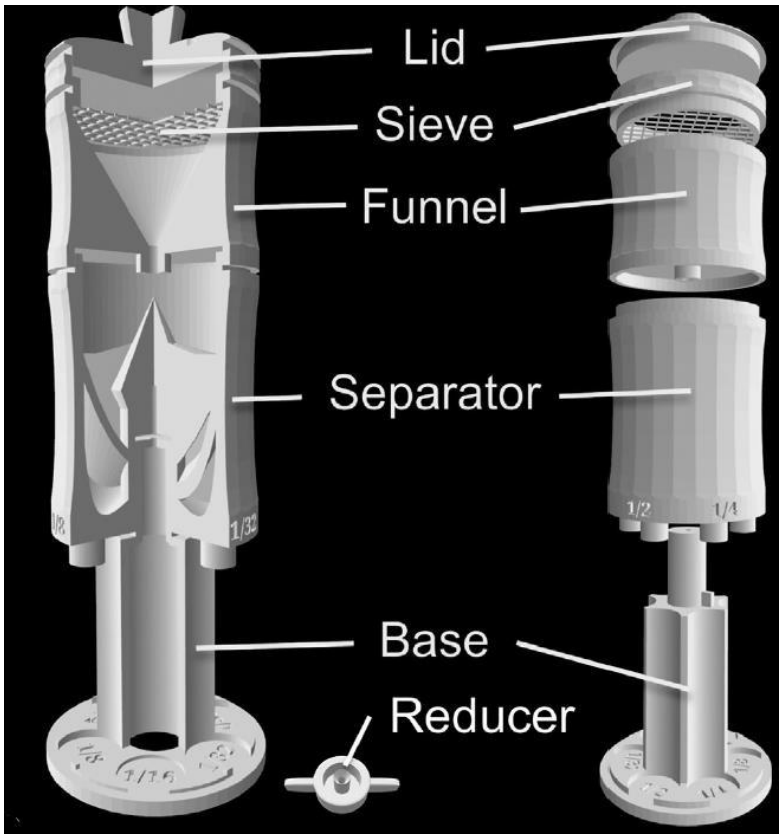


Figure 4.2 Fixed Splitter (Tetard & Marchant 2020).

4.2.2 Sample picking and identification

Both microfossil groups were picked out from the samples under a binocular microscope (Olympus SZ51) using a slightly dampened size 00-000 artist brush. The brush was dampened with water to make sure that the microfossils easily adhere to the brush. The fractioned sample is poured onto a black picking tray with grids (Figure 4.3) and then systematically examined under the microscope. A black picking tray is preferable, as the foraminifera and ostracods usually appear light in colour when viewed under a light microscope (Horne & Siveter 2016).

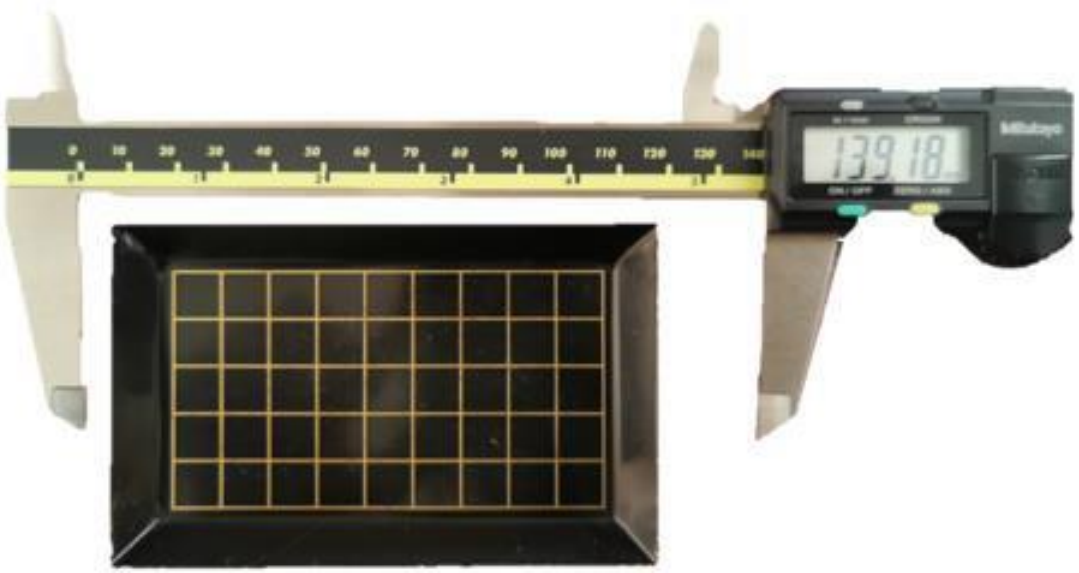


Figure 4.3 Black picking tray with grids.

i) Microscopy

The microfossils were studied under 60x-100x magnification (as used by Strachan 2013). Ostracods in later moulting stages with distinctive morphological features were placed into a taxon category. Ostracod valves that were early instars with little morphological features were placed into a juvenile category and if ostracods were too broken (no morphological features visible) then they were not added to the census counts or abundance data. Adding pieces of broken ostracod shells to the abundance data will increase the statistical margin of error, as one cannot be certain of how many pieces one valve had broken into. Adult foraminifera were also placed into a taxon category where possible, but if the specimens were too eroded or juvenile then they were placed into an “unidentifiable” category.

Thereafter they were placed into labelled micropaleontological storage cells (Figure 4.4) with glass covers. Microfossils were sorted according to cave number, excavation square, layer, date, and taxon (as seen in Figure 4.4). Microfossils can become static, so glass covers were used instead of plastic ones (Horne & Siveter 2016). Conventional light microscope photos were taken using the Keyence digital microscope located at the Geosciences Institute at the Friedrich-Schiller University of Jena, and the Olympus

microscope in the Origins Centre at the University of the Witwatersrand. Samples that best represented the microfossils in question (such as valve reticulation in ostracods and external ornamentation for foraminifera) were selected from the micropaleontological storage cells and light microscope and SEM photographs were taken.



Figure 4.4 Micropaleontological storage cell.

ii) Comparative database

A comparative database for the ostracod and foraminiferal fauna was compiled using literature from Martens *et al*. (1996), and Fürstenberg *et al*. (2017) for the ostracods and Strachan *et al*. (2015, 2016, 2017) and Fürstenberg *et al*. (2017) for the foraminifera. Little information regarding freshwater ostracods is available for South Africa, therefore Martens *et al*. (1996) and Fürstenberg *et al*. (2017) were used as the primary sources. The morphological features and ecological preferences of each taxon was noted in the database.

iii) Scanning Electron Microscopy

Scanning Electron Microscope (SEM) images were taken using the Phenom desktop SEM located in the Evolutionary Sciences building at the University of the Witwatersrand.

The SEM was used to further establish key morphological features that were not visible under a light microscope. The selected microfossils were picked from the micropaleontological slides with a thin artist brush and transferred to a prepared stub. The stub is prepared by placing a black carbonate tape sticker using a tweezer on the flat top-side of the stub. One must be mindful not to touch the carbonate tape with anything other than a tweezer, as this can create obstructions in the image and influence the SEM results. Gloves are also used to assist the user to not contaminate samples, as this will be visible on the SEM photos. The microfossil sample sticks to the carbon tape and the stub is placed on a platform that is inserted into the SEM. The details (sample name and genus/species) of each microfossil was noted for reference purposes by taking a normal light microscope picture before SEM photos were taken.

The SEM photos of ostracods were taken from various angles (after Martens *et al*. 1996) to ensure that morphological features, such the outer-and inner lamella, and valve reticulation, are visible. Detailed images of the inside of the ostracod valves and muscle scars were examined, as these may contain species specific attributes (Karanovic 2012). The classification of foraminiferal specimens is reliant on the analysis and identification of general morphological and microstructural features (for example, Dreher & Flocks 2011). When SEM photos of the foraminiferal specimens were taken, the arrangement of foraminiferal chambers, wall structures, apertures, and external ornamentation was taken into account, as these form part of the important morphological features (Dreher & Flocks 2011).

Results from the SEM were sent to Prof. Koen Martens (Royal Belgian Institute of Natural Sciences) and Prof. Peter Frenzel to confirm the identification of ostracods. The SEM photos of the benthic foraminifera were sent to Dr Eugene Bergh (Iziko Museums of South Africa), and the planktonic foraminifera SEM photos to Prof. Carin Andersson to confirm classifications.

4.2.3 Quantitative analysis

After the microfossils were identified (assigned to a taxon) and counted under a binocular microscope, the data was captured in the census count sheet.

i) Census counts

A census count sheet is designed to record and quantify microfossils from sediment samples. Census count data can be used in various types of analysis for researching biodiversity and for providing the ecological context of microfossils in palaeoecology and micropaleontology (Vermeij & Herbert 2004; Yasuhara *et al*. 2017). The raw data provided by the census counts are used for analysis, such as determining relative abundance data (as is the case for this project) as well as cluster and detrended canonical correspondence analysis (for example, in Morley & Hayward (2012)). The microfossils from each KRM sample were identified to genus and species level (where possible) and documented in a census count sheet. The split, weight, excavation square, and layer were also recorded on the sheet. The data from the census count was used in determining relative abundance and adult: juvenile ratios. While calculating abundance data, it was taken into account that a valve= 1 and carapace = 2 specimens (as stated by Boomer *et al*. 2003).

ii) Abundance data

Analysing species abundance is an important aspect in describing the ecological context of fossil species or death assemblages and for evaluating preservation and sampling biases (Vermeij & Herbert 2004). The relative abundance percentage is based on the total specimens that were counted in the census count per sample (Suchéras-Marx *et al*. 2019). Relative abundances do have limitations when used by themselves, as the relative abundance of one taxon will be dependent on the abundance of all other taxa, as relative abundance data is always a sum of 100 (Finnegan & Droser 2005). The errors of relative abundance are displayed as 95% Confidence Intervals (CI's) (according to Clopper & Pearson 1934) and are discussed in the next section. There are two possible explanations for changes in the relative abundance of a species: an "active" scenario and a "passive" scenario. An "active" scenario is when a trend reflects a change in the population density of the group, whereas a "passive" scenario is when the change is driven by population changes in other taxa (Finnegan & Droser 2005). However, Lord *et al*. (2012) states that

differences in fauna are often noted in changes in the relative abundance of key species rather than the presence or absence of another taxon. In this context, one can assume that species that find certain environmental conditions more favourable will have a higher relative abundance as the environment shifts towards their preferred tolerances.

Absolute abundance (Figure 4.5) is measured as the total number of individuals per gram of sediment (Martinez *et al*. 2018). The relative abundance was used to examine the dominance or rarity of individual taxa (Boomer *et al*. 2003). Both absolute and relative abundances were used in this project as it is difficult to interpret the ecological meaning of abundance trends just by using relative abundance data (Finnegan & Droser 2005). A change in the absolute abundance of a taxon will have a corresponding change in the relative abundance data (Finnegan & Droser 2005). This change might be driven as a result of the absolute abundance of other taxa shifting, but where the absolute abundance of a specific taxon does not change (Finnegan & Droser 2005). In this case, the change might be reflected in the relative abundance data (Finnegan & Droser 2005). The splits used in the equation for each sample is given in Appendix C; Section C.1; Table C.1.

$$\text{Absolute abundance} = \frac{\text{split analysed x number of individuals counted}}{\text{weight (of washed} > 150\ \mu\text{m sample)}}$$

Figure 4.5 Equation to determine the absolute abundance of microfossils (by Boomer *et al.* 2003 as well as personal communication by Prof. Carin Andersson).

$$Relative\ abundance\ \% = \frac{Number\ of\ specimens\ counted\ from\ a\ taxon}{Total\ number\ of\ ostracods\ or\ foraminifera\ counted}\ x\ 100$$

Figure 4.6 Equation to determine the relative abundance of microfossils (according to methods described by Boomer *et al*. 2003).

iii) Confidence intervals

Relative abundance data is often considered as the foundation of population analysis and is expressed as either a proportion or percentage, but there is a degree of counting uncertainty that needs to be taken into consideration (Suchéras-Marx *et al*. 2019). Furthermore, it is important to acknowledge the margin of error, as this adds credibility to statistical reliability of interpretations and conclusions (Suchéras-Marx *et al*. 2019). In this

study, the Clopper–Pearson 95% confidence interval method for relative abundance was calculated using PAST 3.23 statistical software as suggested by Suchéras-Marx *et al.* (2019) (introduced by Hammer *et al*. 2001). The Clopper–Pearson 95% CI for each taxon was calculated by selecting the column containing data of taxon of interest and the column containing the total number of individuals in the counted sample (Suchéras-Marx *et al*. 2019). The "Multiple Proportion CIs" function was then selected from the "Univariate" menu (Suchéras-Marx *et al*. 2019). The size of the sample will also influence the CI's, as smaller sample sizes will have larger margins or error (Patterson & Fishbein 1989).

iv) Analysing the assemblage composition

Analysing adult: juvenile ratios provide insight on the type of population structure and the amount of post-depositional transport endured by the assemblage (Boomer *et al*. 2003; Frenzel & Boomer 2005). The population structure of the ostracod assemblages was analysed to determine whether the assemblage is allochthonous or autochthonous, a taphocoenosis or thanatocoenosis (Boomer *et al.* 2003; Frenzel & Boomer 2005). Boomer *et al*. (2003: 157) provide a questionnaire that was used to determine whether the ostracod assemblage from KRM represents a thanatocoenosis or taphocoenosis, and whether the assemblage is autochthonous or allochthonous.

4.2.4 Geochemical analysis of ostracod valves

Traditional stable oxygen isotopes are often used as a salinity and temperature proxy while carbon isotope analysis is used as a productivity proxy (Boomer *et al*. 2003). By analysing ostracod shells for stable oxygen isotopes, information about water temperature and the chemical composition of the host water can be gathered (Holmes 1996; Caporaletti 2011). Training for cleaning ostracod samples for stable oxygen isotope analysis was conducted at the University of Bergen's Facility for Advanced Isotopic Research and Monitoring of Weather, Climate and Biogeochemical Cycling (FARLAB) with Dr Sevasti Modestou. The valves were picked out under a microscope and placed into plastic vials.

Although the samples were already washed (see 4.2.1), the samples that were used for geochemical analysis were cleaned again to remove any remaining detrital material stuck

to the valves. Methanol was used to soak and clean the valves in vials (see Jin *et al*. 2006; Caporaletti 2011). The samples that were taken to Norway were used for the isotope analysis (See Appendix D; Section D.1). The sample was further cleaned using a fine paintbrush (same one used for picking specimens) to lightly remove detrital material from inside the valves. The vials were placed into an ultrasonic bath (filled with deionised water) to clean the valves for a few seconds (see Caporaletti 2011 for examples). The time spent in the ultrasonic bath was dependent on how much detrital material had to be removed. The methanol was then drained from the sample using a pipette and the entire process was repeated until the valves were clean and had no detrital material sticking to the valves. The samples were then checked through a microscope to make sure that no other obstructions were present. The samples were weighed to make sure that there was enough material to work with, as one needs at least 30 µg of ostracod shells to achieve the necessary quantity of material for stable isotope analysis (Caporaletti 2011 and references therein). The samples were then moved to the isotope lab at FARLAB to be analysed for stable isotopes.

The analytical data ($\delta^{18}O$ and $\delta^{13}C$) are reported referenced to the Vienna Peedee belemnite (VPDB) standard via NBS -19 (Caporaletti 2011 and references therein) and an in-house (FARLAB) laboratory standard. The $\delta^{18}O$ value of NBS-19 in relation to VPDB is -2.20 ‰ (Coplen 1994; Caporaletti 2011). For stable carbon isotope ratio ($\delta^{13}C$) VPDB is used along with NBS-19 (Caporaletti 2011). The VPDB standard has a value of 0 ‰. The $\delta^{13}C$ value of NBS-19 in relation to VPDB is +1.95‰ (Caporaletti 2011). The results are reported per mil.

Only the ostracod valves were subjected to stable isotope analysis as they were the most widely distributed microfossils in the samples. When analysing the stable isotope composition of ostracod valves, one must take vital offsets into account, as this is relevant to certain ostracod taxa. Vital offsets are taxon-specific offsets from the predicted isotopic equilibrium (for examples, see von Grafenstein *et al.* 1999; Börner *et al.* 2013). It is therefore important to not mix different taxa when analysing stable isotopes (see Caporaletti 2011; Börner *et al.* 2013). The foraminifera tests were not used for stable isotope analysis. This is further discussed in chapters 5 and 6.

Chapter 5: Results

5.1 Introduction

This chapter presents the results of the taxonomic (microscopy and SEM), quantitative, and stable isotope analysis of the microfossils from the stratigraphic layers SMONE (MIS 5c), BOS-One, BOS-Two, and BOS-Three (MIS 5d) from the Witness Baulk at KRM (Cave 1). The data from the census counts used to determine the absolute abundance (number specimens/gram sediment >150µm) and relative abundance (the proportion or percentage of a certain taxon per sample >150µm) of the ostracods and foraminifera in each sample are discussed in section 5.2.2. A total of 29 sediment samples from KRM were analysed. The following quantities were analysed from the various layers (note: the weight of the sample is the accumulative weight of the entire >150µm washed sample, not the weight after splitting the sample): BOS-One (n=7, total weight of 74 grams), BOS-Two (n=7, total weight of 81 grams), and BOS-Three (n=7, total weight of 147 grams) and SMONE (n=8, total weight of 89.35 grams) (Appendix C; section C.1; Table C.1; Table C.2; Table C.3). The splits that were analysed for the various samples along with the exact context of the sample (square, layer, and excavation date) are given in Appendix C, Section C1, Table C.2.

5.2 Ostracods

5.2.1 Ostracods: Taxonomy

It was noted in the census counts that four ostracod taxa are present in the KRM samples (Table 5.1), namely *Gomphocythere obtusata* (Figure 5.1; Figure 5.2)*, Sarscypridopsis aculeata* (Figure 5.3; Figure 5.4)*, Physocypria* cf. *castanea* (Figure 5.5; Figure 5.6) and *Ilyodromus sp.* (Figure 5.7) (see Systematics in Appendix C; Section C.3).

Table 5.1 Ostracod census count per layer from KRM.

Census Count							
Layer	Total weight (g) of washed >150µm sample (before splitting)	*G. obtusata*	*Physocypria* cf. *castanea*	*S. aculeata*	*Ilyodromus* sp.	Juveniles	Total counted
SMONE	89.4	1241	5	192	1	1134	2573
BOS-One	73.6	1774	32	372	4	1351	3533
BOS-Two	80.5	1678	24	164	15	1004	2885
BOS-Three	146.99	2480	94	356	7	1675	4612

Overall, the preservation quality of the ostracod valves (excluding those from *Ilyodromus* sp.) is adequate for identification to species level. *Ilyodromus* sp. could not be identified to species level as the valves were weakly preserved and the majority of the specimens broke when touched lightly with a thin paintbrush during census counts (valves were mostly broken during washing and sieving).

The most common ostracod taxon in the KRM sequence is *G. obtusata* (Table 5.1; Figure 5.1; Figure 5.2) according to the census counts. Juveniles do make up the second largest number of valves after *G. obtusata*, but are not identifiable (not assigned to genus or species). The second most common identifiable ostracod taxon in the KRM samples is *S. aculeata* (Table 5.1; Figure 5.3; Figure 5.4). The third ostracod taxon, *Physocypria.* cf. *castanea* (Table 5.1; Figure 5.5; Figure 5.6), is less common in the KRM samples than the previous two taxa. Finally, the least taxon in the KRM assemblage is *Ilyodromus* sp. (Figure 5.7).

Gomphocythere obtusata shows clear valve reticulation (also noted by Martens *et al*. 1996) on the outer view of the valve in the light microscope images (Figure 5.1 A) that are not as visible in the SEM images (Figure 5.2). Muscle scars can be seen in the SEM

(Figure 5.1) and light microscope images (Figure 5.2). The calcified inner lamella is also visible in the SEM images (Figure 5.2).

The SEM images of *S. aculeata* (Figure 5.4) show a more detailed picture of the inner and outer lamella on the inside of the valve and the pitted surface on the outer view of the valve than the light microscope images (Figure 5.3). However, the light microscope pictures of *S. aculeata* (Figure 5.3) show the presence of stout spines and the muscle scars better than the SEM images.

Physocypria cf. *castanea* is smooth on the outside of the valve, as seen on the SEM (Figure 5.6) and light microscope images (Figure 5.5). There is slight reticulation on the valves as seen on both Figure 5.5 and Figure 5.6, but this is likely post-depositional and is not a characteristic of the taxon. The valves can occasionally be covered in long setae (Karanovic 2011), but this is not clearly visible on the specimens from KRM. The SEM images (Figure 5.6) clearly show the inner lamella.

The SEM image of *Ilyodromus* sp. (Figure 5.7) shows that there are dark spots present on the valve that could relate to manganese staining. These interpretations are further discussed in the next chapter. Other SEM images of foraminifera (for example, Appendix C; section C.2; Figure C.8) and ostracods (Appendix C; section C.2) show similar dark spots. A calcified inner lamella is also present on the SEM image of *Ilyodromus* sp. (Figure 5.7). As remarked above, the valves from this taxon were very fragile and broke before they could be mounted and positioned and therefore only one SEM picture was successfully taken (this was the only specimen that did not break). It is also one of the first specimens to be identified as *Ilyodromus* sp. The carapace of females from the genus *Ilyodromus* are often slightly larger than that of the male (Shearn *et al*. 2014).

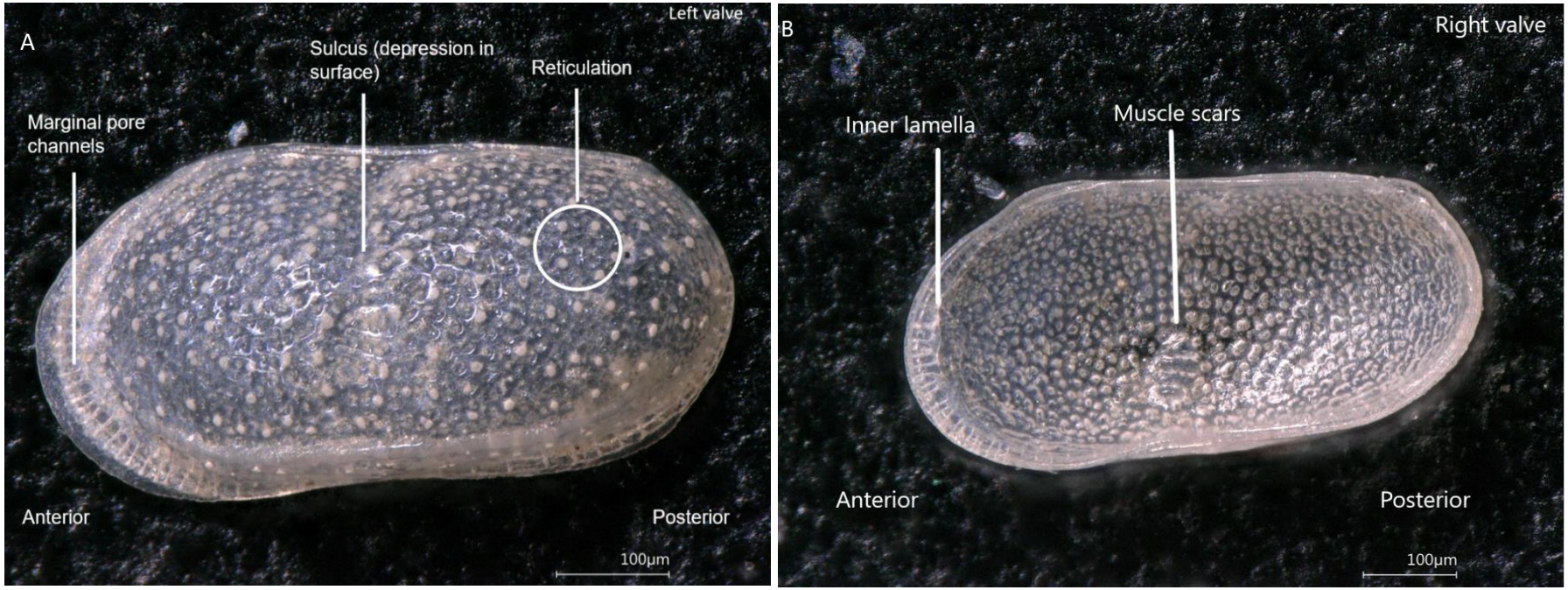


Figure 5.1 A) External view of ostracod taxon *Gomphocythere obtusata* with visible articulation and depression in the surface. B) Internal view of *Gomphocythere obtusata* with visible muscle scars and inner lamella.

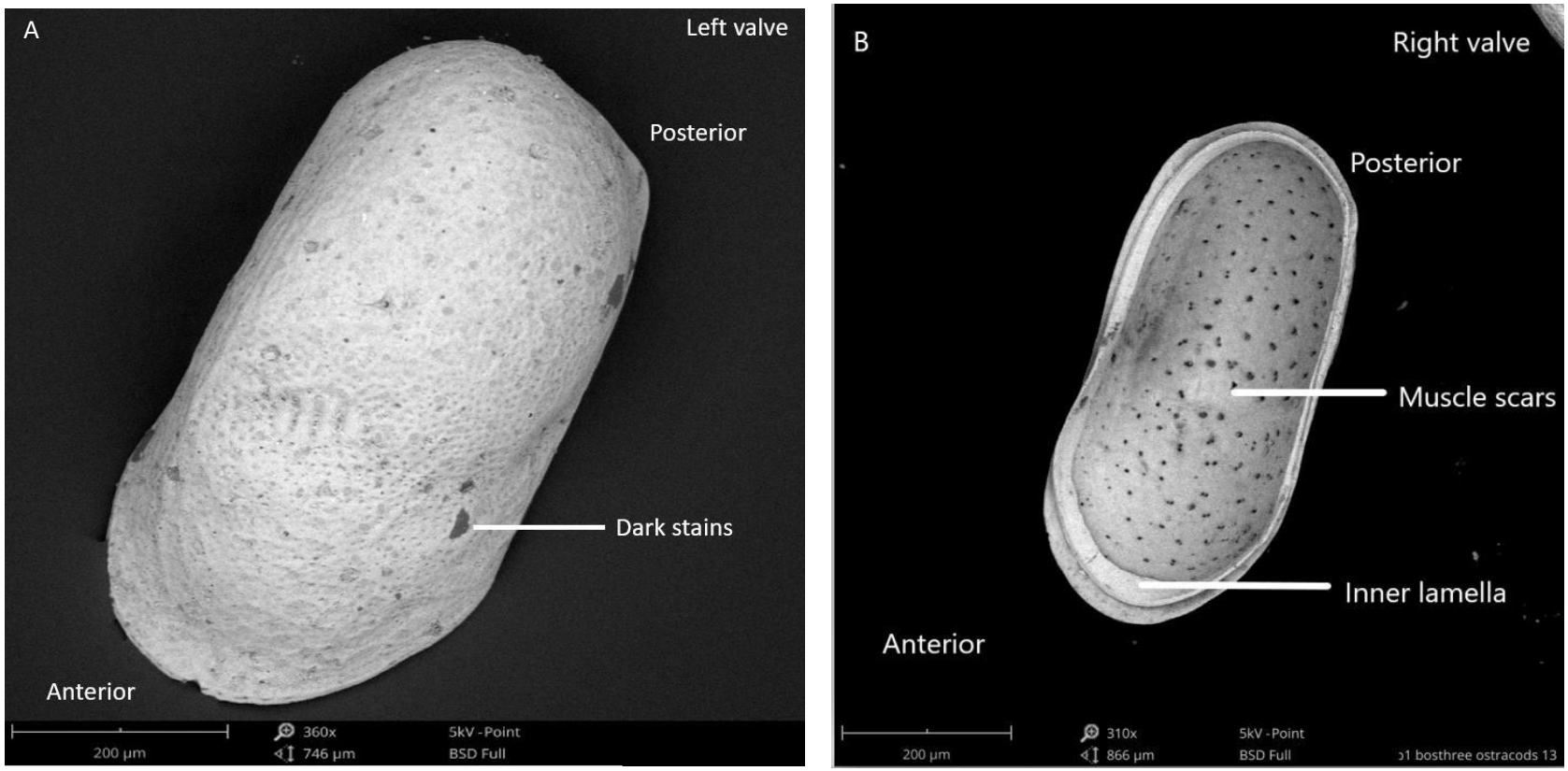


Figure 5.2 SEM images of *Gomphocythere obtusata*. A) External view of valve with visible reticulation and dark stains B) Internal view of valve with visible muscle scars and lamella.

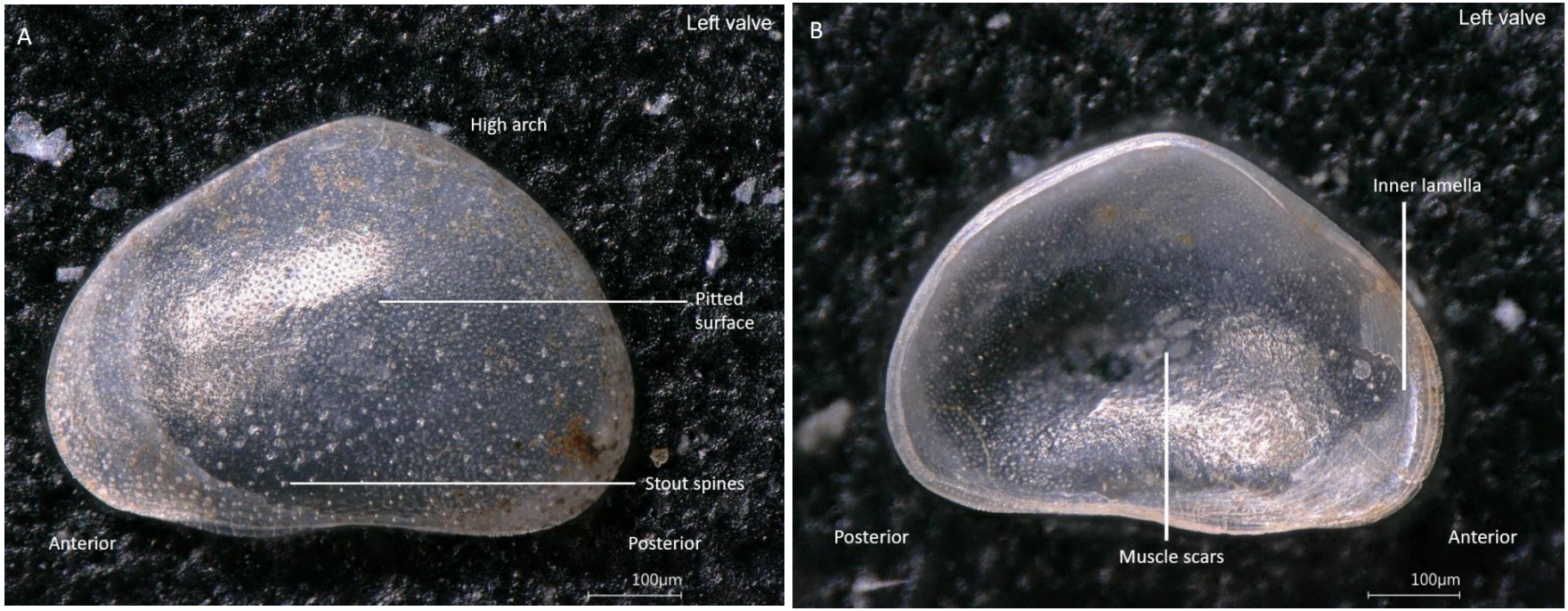


Figure 5.3 A) External view of *Sarscypridopsis aculeata* valve with pitted surface and the remains of stout spines. B) Internal view of Sarscypridopsis *aculeata* valve with visible muscle scars and inner lamella.

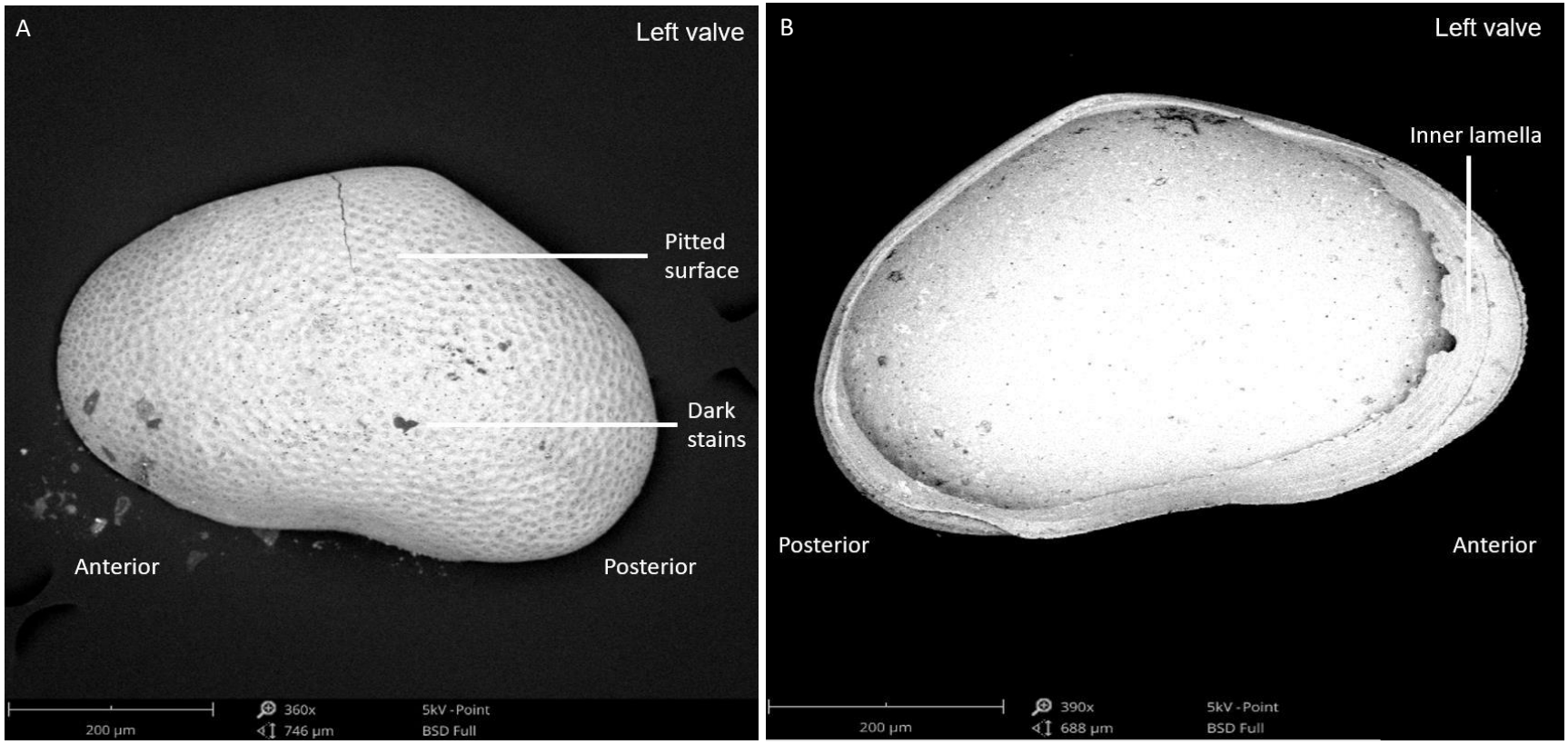


Figure 5.4 SEM images of *Sarscypridopsis aculeata* A) External view of valve with pitted surface and dark stains B) Internal view of valve with inner lamella.

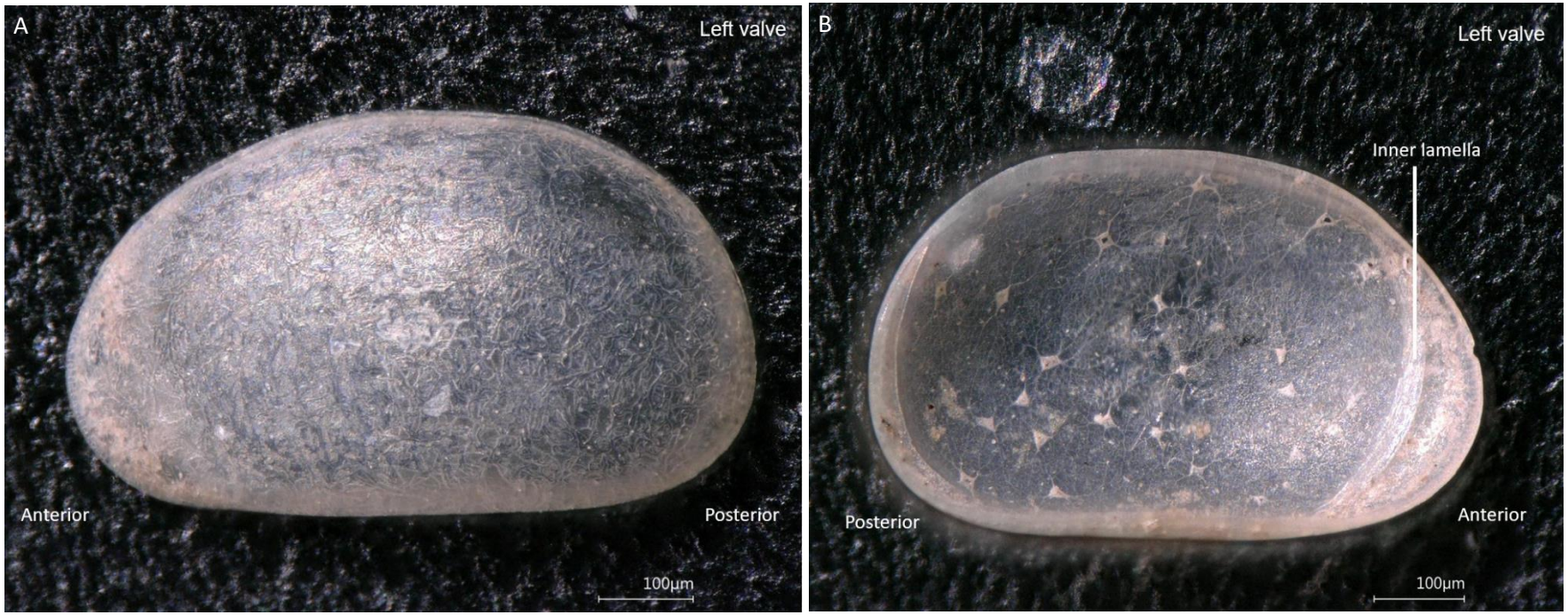


Figure 5.5 A) External view of *Physocypria cf. castanea* valve with post-depositional ornamentation. B) Internal view of *Physocypria cf. castanea* valve visible lamella.

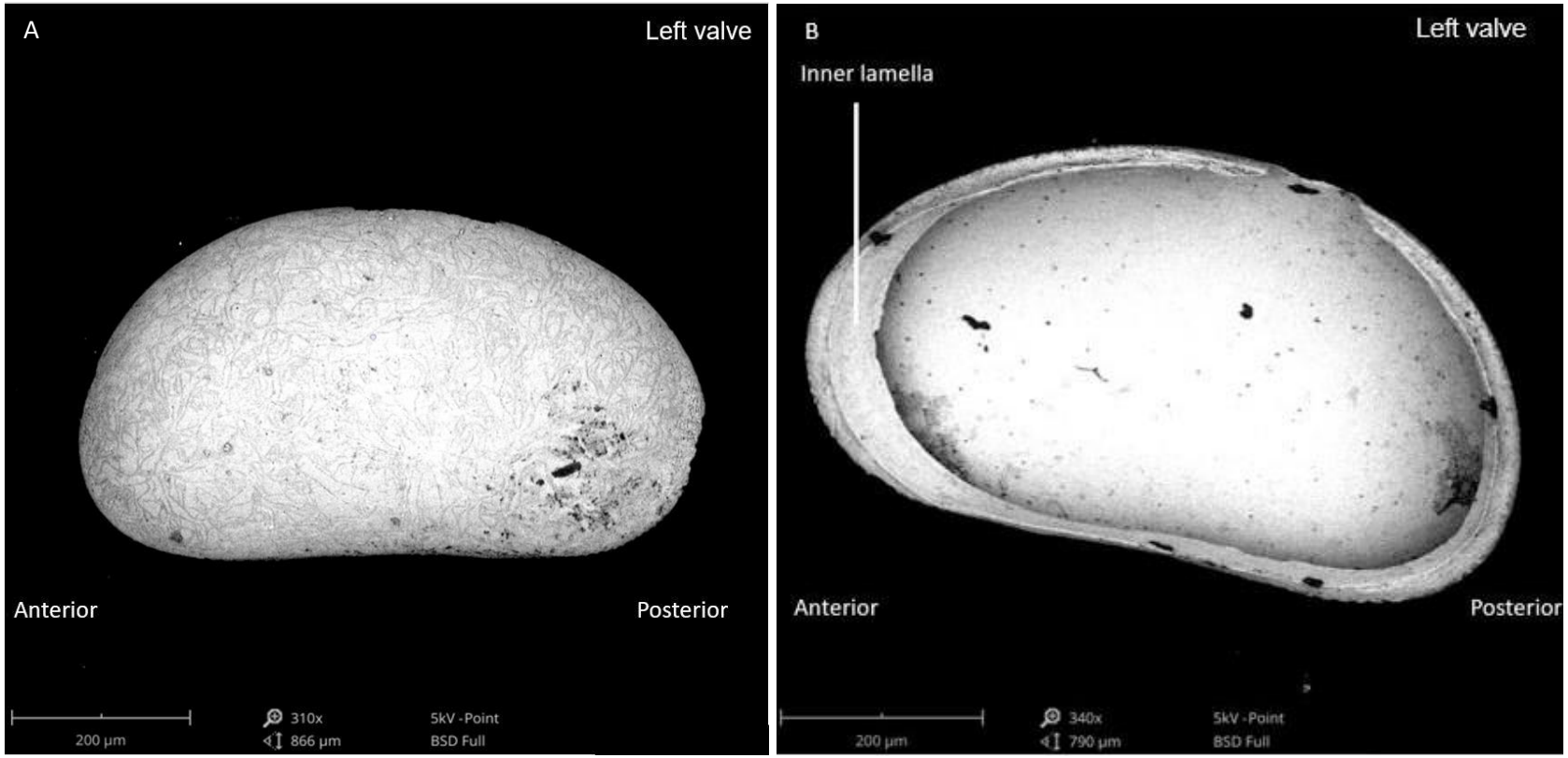


Figure 5.6 SEM images of *Physocypria* cf. *castanea* A) External view of valve B) Internal view of valve with visible lamella and hinge.

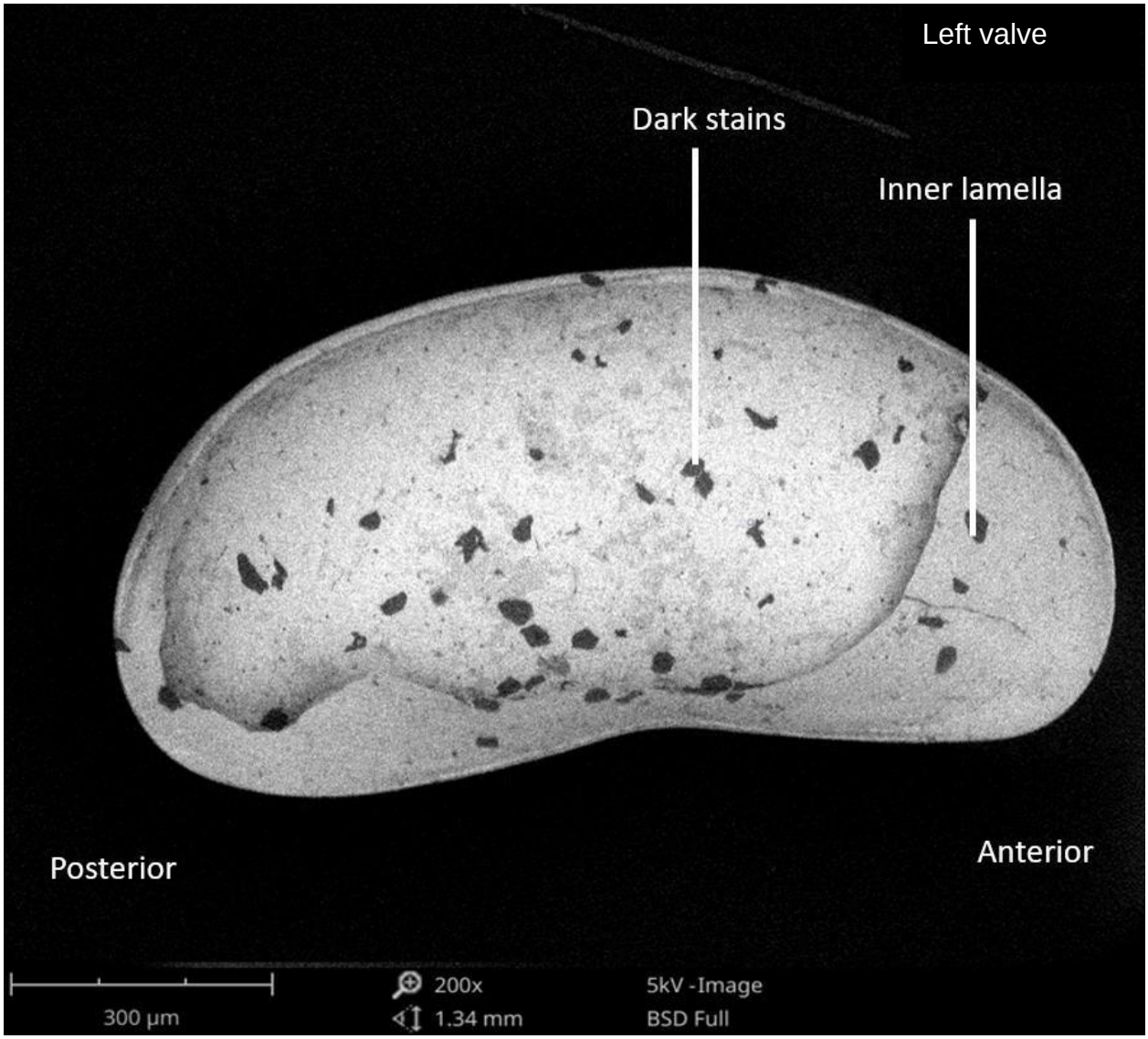


Figure 5.7 SEM image of inner view of *Ilyodromus* sp. valve.

5.2.2 Ostracod abundances:

i) Absolute abundance (number specimens/gram washed sediment >150µm)

Gomphocythere obtusata has the highest absolute abundance out of all the ostracod taxa present, but their abundances differ between the layers (Table 5.2; Figure 5.8). Juvenile ostracod valves have the second greatest absolute abundance in the KRM layers, followed by *Sarscypridopsis aculeata, Physocypria* cf. *castanea,* and *Ilyodromus* sp. in descending order (Table 5.2; Figure 5.8). The absolute abundance of *G. obtusata* is lowest in SMONE, increases in BOS-One, and decreases again in BOS-Two. The greatest absolute abundance of *G. obtusata* is recorded in BOS-Three (Table 5.2; Figure 5.8). Out of all the layers that were analysed, SMONE has the overall lowest ostracod absolute abundance values for all the taxa (Table 5.2; Figure 5.8). There is an increase in the absolute abundance of all ostracod taxa from SMONE to BOS-One (Table 5.2; Figure 5.8). The greatest absolute abundance of *S. aculeata* also occurs in BOS-One (Figure 5.8). However, all ostracod taxa (excluding *Ilyodromus* sp.) decline in absolute abundance from BOS-One to BOS-Two. The greatest absolute abundance of the rarest taxon, *Ilyodromus* sp., is in BOS-Two (Table 5.2; Figure 5.8).

Table 5.2 Ostracod absolute abundances per layer from KRM (decimals are rounded up).

Absolute abundance							
	G. obtusata	*Physocypria* cf. *castanea*	*S. aculeata*	*Ilyodromus* sp.	Total adults	Juveniles	Total absolute abundance
SMONE	489	1	87	0	577	456	1033
BOS-One	3344	78	827	11	4260	2268	6528
BOS-Two	2797	47	310	29	3183	1590	4773
BOS-Three	3642	104	423	7	4176	2419	6595

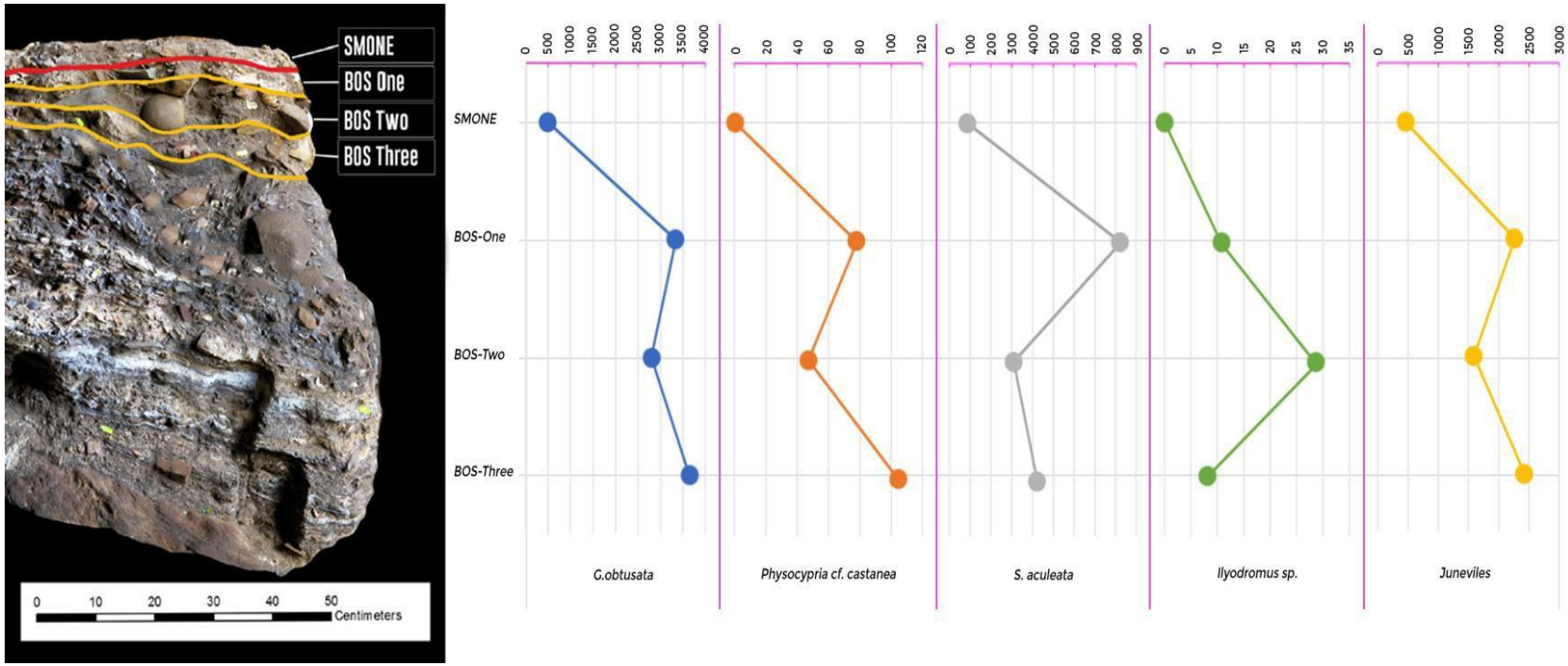


Figure 5.8 Absolute abundance of ostracods (number specimens/gram sediment >150µm) with indication of stratigraphic zones.

The absolute abundances of *G. obtusata*, *S. aculeata*, *Physocypria* cf. *castanea,* and juveniles decrease from BOS-One to BOS-Two, but increase again in BOS-Three (Table 5.2; Figure 5.8). The greatest absolute abundance of the second rarest taxon, *Physocypria* cf. *castanea*, is in BOS-Three*. Physocypria* cf. *castanea,* and *Ilyodromus* sp. both remain rare throughout the sample (Table 5.2; Figure 5.8).

ii) Relative abundance (% of total number of ostracods within the sample)

The relative abundance (%) data suggests that *G. obtusata* is the dominant taxon (81-89%) in the KRM MIS 5c-d samples (Table 5.3; Figure 5.9). The taxon *S. aculeata* (9-17%) accounts for the second most abundant adult ostracod in the assemblage (Table 5.3; Figure 5.9).

Layer SMONE has the highest value of juvenile relative abundance out of all the layers, but has lower values for *G. obtusata* and *Physocypria* cf. *castanea* (Table 5.3; Figure 5.9). There is a decrease in juvenile abundances from SMONE to BOS-One, but the abundances of most of the adult ostracods (excluding *Ilyodromus* sp.) increase from SMONE to BOS-One (Table 5.3; Figure 5.9). In BOS-Two, the highest relative abundance of *G. obtusata* is documented (Table 5.3; Figure 5.9). There is a decrease in *G*. *obtusata* abundance from BOS-Two to BOS-Three, but an increase in *S. aculeata*, *Physocypria* cf. *castanea,* and juveniles (Table 5.3; Figure 5.9)*. Ilyodromus* sp. has the lowest relative abundance out of all the ostracods present in the layers, followed by *Physocypria* cf. *castanea* (Table 5.3; Figure 5.9). The greatest abundance of *Ilyodromus* sp. is seen in BOS-Two and the greatest abundance of *Physocypria* cf. *castanea* is in BOS-Three (Table 5.3; Figure 5.9). There seems to be a possible relationship between the increase of adult ostracods and the decrease of juveniles. For the purpose of making ecological as well as taphonomic inferences, a graph with juveniles (Figure 5.9) and without juveniles (Figure 5.10) is included.

Table 5.3 Ostracod relative abundances per layer from KRM (decimals are rounded up).

Relative abundance (%)				
	G. obtusata	*Physocypria* cf. *castanea*	*S. aculeata*	*Ilyodromus* sp.
SMONE	86	0	13	0
BOS-One	81	1	17	0
BOS-Two	89	1	9	1
BOS-Three	84	3	12	0

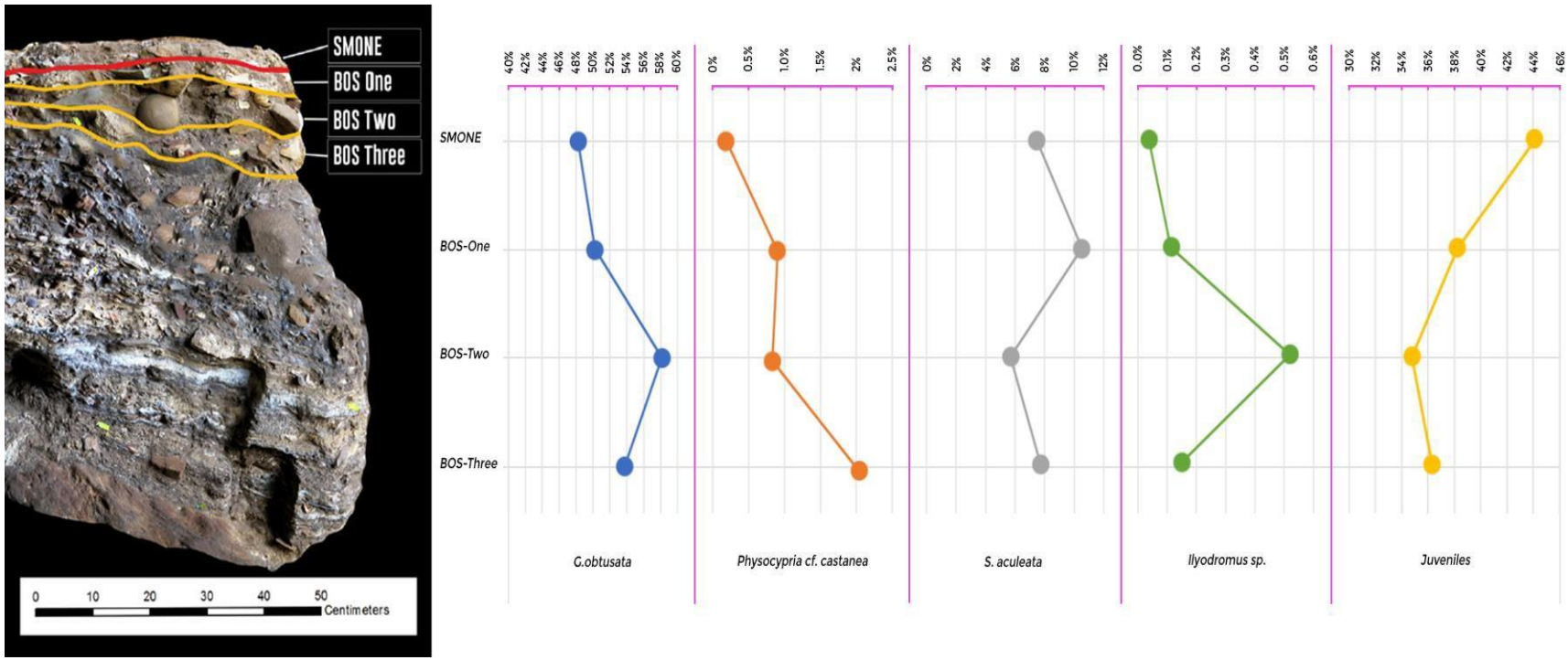


Figure 5.9 Relative abundance (%) per layer of the four ostracod taxa from KRM (juveniles included).

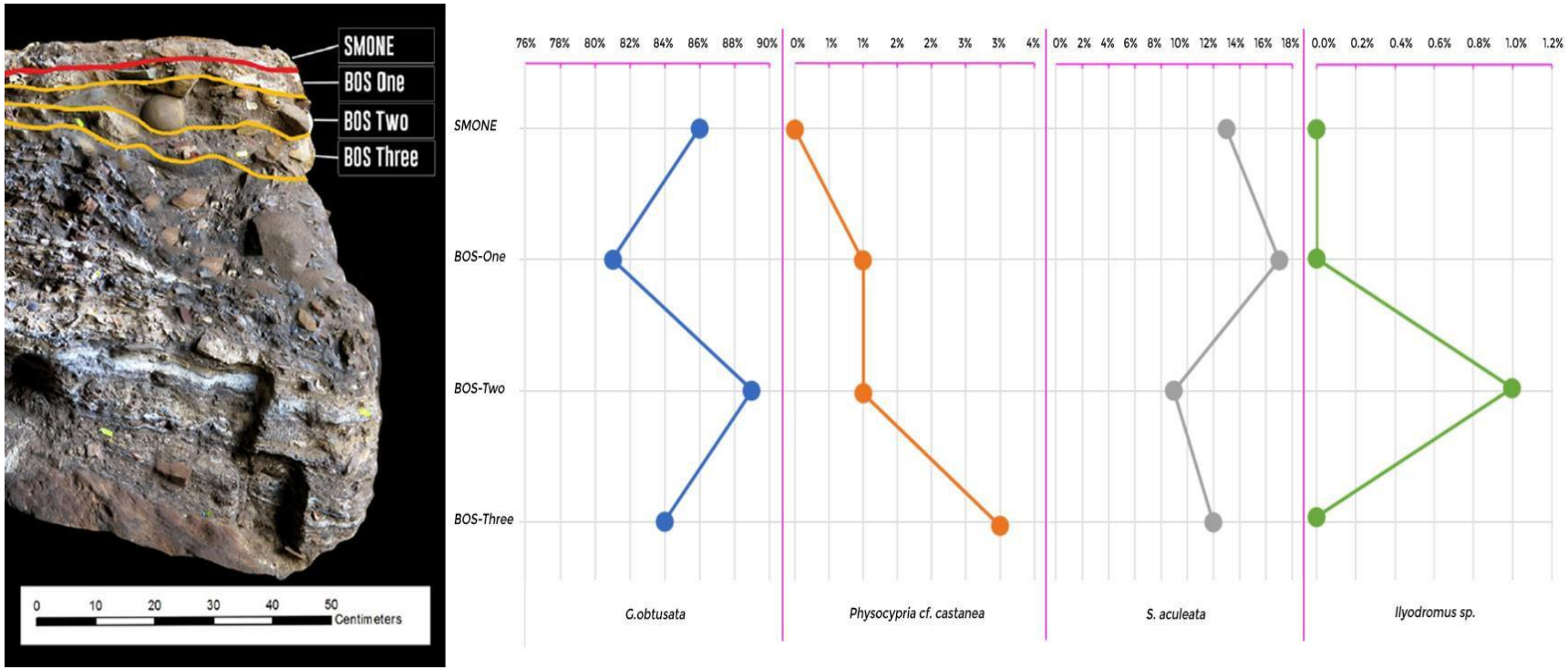


Figure 5.10 Relative abundance of ostracods with indication of stratigraphic zones (juveniles excluded).

iii) Comparing the relative abundance and absolute abundance data of ostracods.

Only four ostracod taxa are present at KRM. The results from the absolute abundance and relative abundance suggest that there is a high abundance of individuals and that there is one taxon that dominates the assemblage. All abundance data indicate that the ostracod taxon *Gomphocythere obtusata* is the dominant ostracod taxon at KRM (Figure 5.8; Figure 5.9) however, both absolute and relative abundance values do differ from layer to layer.

Although SMONE has the highest relative abundance of the juvenile ostracods, the lowest value of absolute abundance for juvenile ostracods can also be observed here (Figure 5.8; Figure 5.10). Juveniles decrease in relative abundance from SMONE to BOS-One, but increase in absolute abundance (Figure 5.8; Figure 5.10). The absolute abundances of all the ostracod taxa increase from SMONE to BOS-One (Table 5.3; Figure 5.9). The relative abundance of *G. obtusata* decreases in BOS-Three, but this layer has the highest absolute abundance value of the taxon (Figure 5.8; Figure 5.9).

iv) Confidence intervals

Statistical confidence limits of abundances are influenced by the number of individual specimens that were analysed per sample (Danielopol *et al*. 2002). This in turn influences the interpretation of temporal trends (Danielopol *et al*. 2002). Smaller sample sizes will therefore lead to larger uncertainties. In Figure 5.11 the dots represent the empirical proportions (the sampled proportion) and their associated 95% Confidence Intervals (CIs) are represented by whiskers (see Suchéras-Marx *et al.* 2019).

The parameter in SMONE (smallest sample size) for *G. obtusata* (dominant ostracod) falls between 0.46 (95% CI lower) and 0.50 (95% CI upper) (Figure 5.11 A). In BOS-One (larger sample size), the width of the CI decreases, and the CIs for *G. obtusata* are between 0.48 (95% CI lower) and 0.52 (95% CI upper). The width of the CI increases again in BOS-Two (smaller sample size) and the CI for *G. obtusata* is between 0.56 (95% CI lower) and 0.60 (95% CI upper) (Figure 5.11 A). The CI for the larrgest sample size (BOS-Three) has a decrease in the width for *G. obtusata* and is between 0.53 (95% CI

lower) and 0.55 (95% CI upper) (Figure 5.10 A). The two rarest taxa, namely *Physocypria* cf. *castanea* (Figure 5.10 C) and *Ilyodromus* sp. (Figure 5.11 D) have a larger CI width compared to specimens that are more abundant, for example, *G. obtusata* (Figure 5.11 A).

Compared to the other layers from KRM, SMONE and BOS-Two (smallest sample sizes) have the largest levels of uncertainty, while there is a decrease in the CI width in BOS-One and BOS-Three (largest sample sizes) (Figure 5.11). The CIs (Figure 5.11) show that as a sample size increases, the width of the CIs decrease.

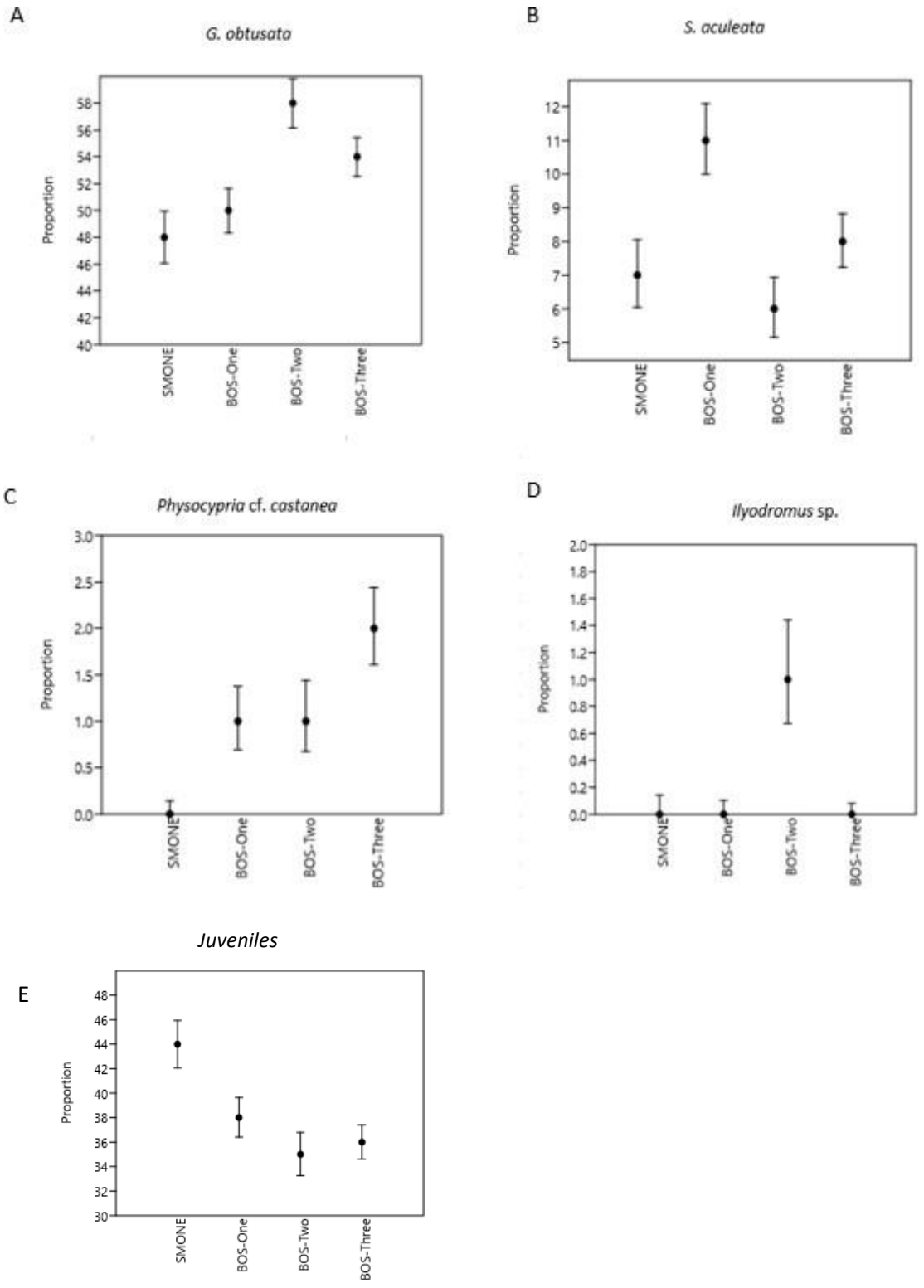


Figure 5.11 Confidence Intervals for ostracod abundances.

5.2.3 Average ostracod sizes

Ostracod sizes from KRM (Table 5.4) are very similar to those reported by Martens *et al*. (1996) from Verlorenvlei. However, the valves from *Gomphocythere obtusata* are closer to the size of the male valves reported at Verlorenvlei. This can be indicative of varying calcification rates in different temperatures. This is discussed further in Chapter 6.

Table 5.4 Measurements of ostracods recorded at Verlorenvlei by Martens *et al*. (1996) compared to ostracod measurements from Klasies River Cave 1.

	Size recorded by Martens *et al*. (1996) (mm)	**Average size in KRM assemblage (mm)**
Gomphocythere obtusata	Between *ca*. 0.75 mm (female) and *ca*. 0.6 mm (male)	*ca.* 0.61 mm
Sarscypridopsis aculeata	*ca*. 0.65 mm	*ca.* 0.63 mm
***Physocypria* cf. *castanea* (*Physocypria* cf. *capensis*)**	*ca.* 0.6-0.7 mm	*ca.* 0.7 mm
***Ilyodromus* sp.**	*ca*. 1 mm (for *I. viridulus*)	*ca*. 1.2 mm

5.2.4 Adult: juvenile ratio of ostracods

The adult: juvenile ratio that is most proportionate is in SMONE, where the ratio is 56% adults to 44% juveniles in the sample (Table 5.5). BOS-Two had the highest variation between adults (65%) and juveniles (35%) in the sample (Table 5.5). BOS-Two had the highest variation between adults (65%) and juveniles (35%) in the sample (Table 5.5).

Table 5.5 Adult: juvenile ratios.

	Adult: juvenile ratio
SMONE	1439: 1134 (56%: 44%)
BOS-One	2182: 1351 (62%: 38%)
BOS-Two	1881:1004 (65%: 35%)
BOS-Three	2937: 1675 (64%: 36%)

The majority of ostracod valves present in the KRM assemblage are disarticulated (single valves only) and belong either to the taxon *Gomphocythere obtusata* or to juvenile instars. As discussed in Chapter 4, the questionnaire presented by Boomer *et al*. (2003: 157) was used to determine whether the ostracod assemblage from KRM represents a thanatocoenosis or taphocoenosis, and whether the assemblage is autochthonous or allochthonous. The KRM assemblage closely matches a low energy thanatocoenosis.

5.2.5 Geochemical analysis of ostracod valves (pilot study)

The results of the $\delta^{18}O$ and $\delta^{13}C$ stable isotopes are presented in Figure 5.12 and Figure 5.13. The samples that were analysed and their isotopic values are presented in Appendix D; Section E.1. The $\delta^{18}O$ stable isotope results show negative values and have a range between -2.6‰ in B1- SMONE (20/02/2015) to -2.3‰ in B3- SMONE (19/02/2015). The $\delta^{18}O$ results have a deviation of 0.1 between layers (see Appendix D, Table D.1). The $\delta^{13}C$ stable isotope values from the sample analysed show negative values for all the samples (Figure 5.13). One sample from BOSONE (see Figure 5.13) is notably different compared to the rest of the isotopic results with a value of -8.32 ‰, and can be considered an outlier. The highest value for the $\delta^{13}C$ stable isotopes is -10.4‰ (A3 - SMONE 20/02/2015) and the lowest value is -8.32‰. The standard deviation for the $\delta^{13}C$ stable isotope ratio is 0.6 (see Appendix D; Section D.1; Table D.1). More samples from the BOS-layers and layer SMONE than reported here were analysed for stable isotopes, but the samples were too small to get accurate results (See Appendix D; Table D.2). The sample size will be increased in future to create a more extensive isotopic record.

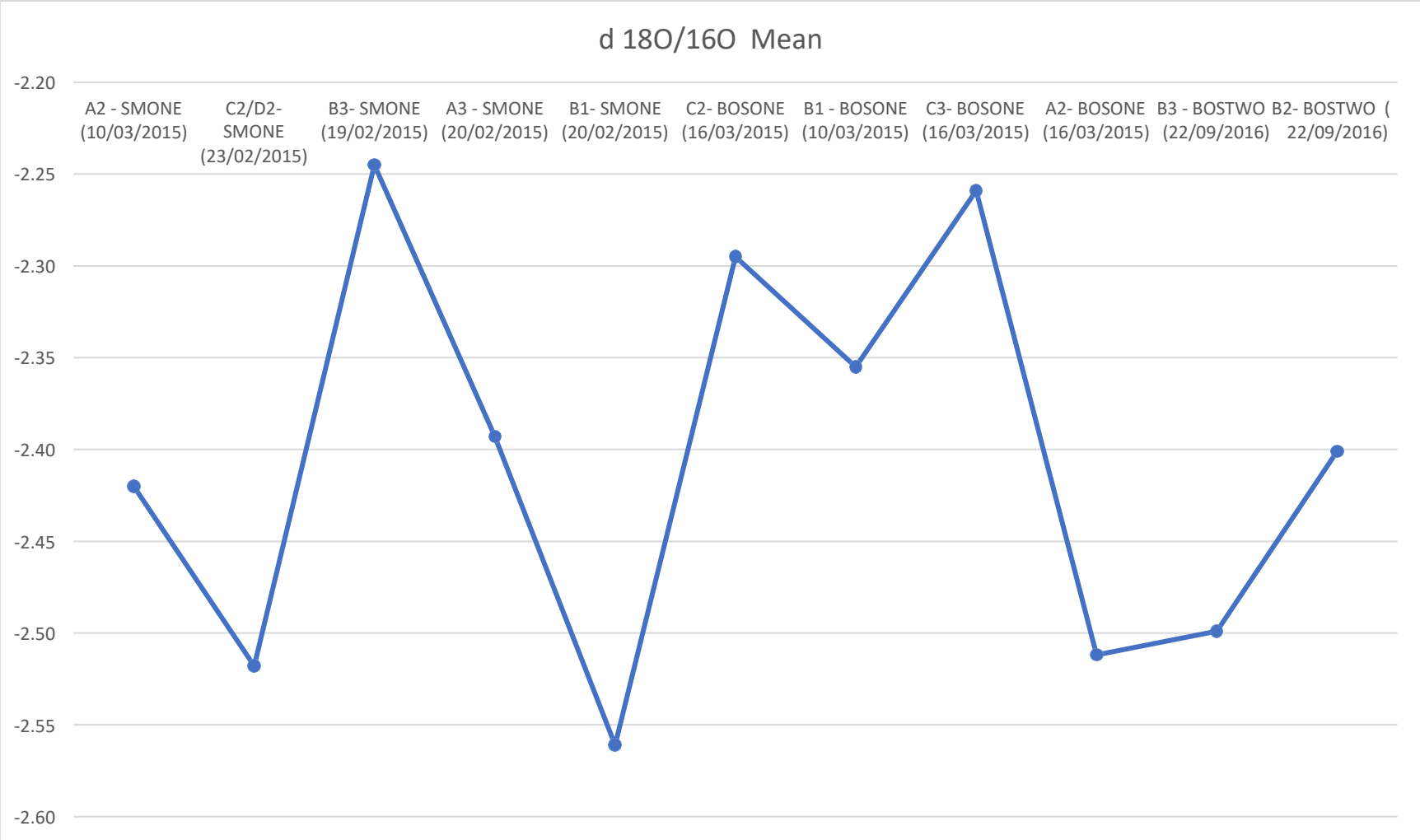


Figure 5.12 Stable oxygen isotope ($\delta^{18}O$) results from the KRM layers.

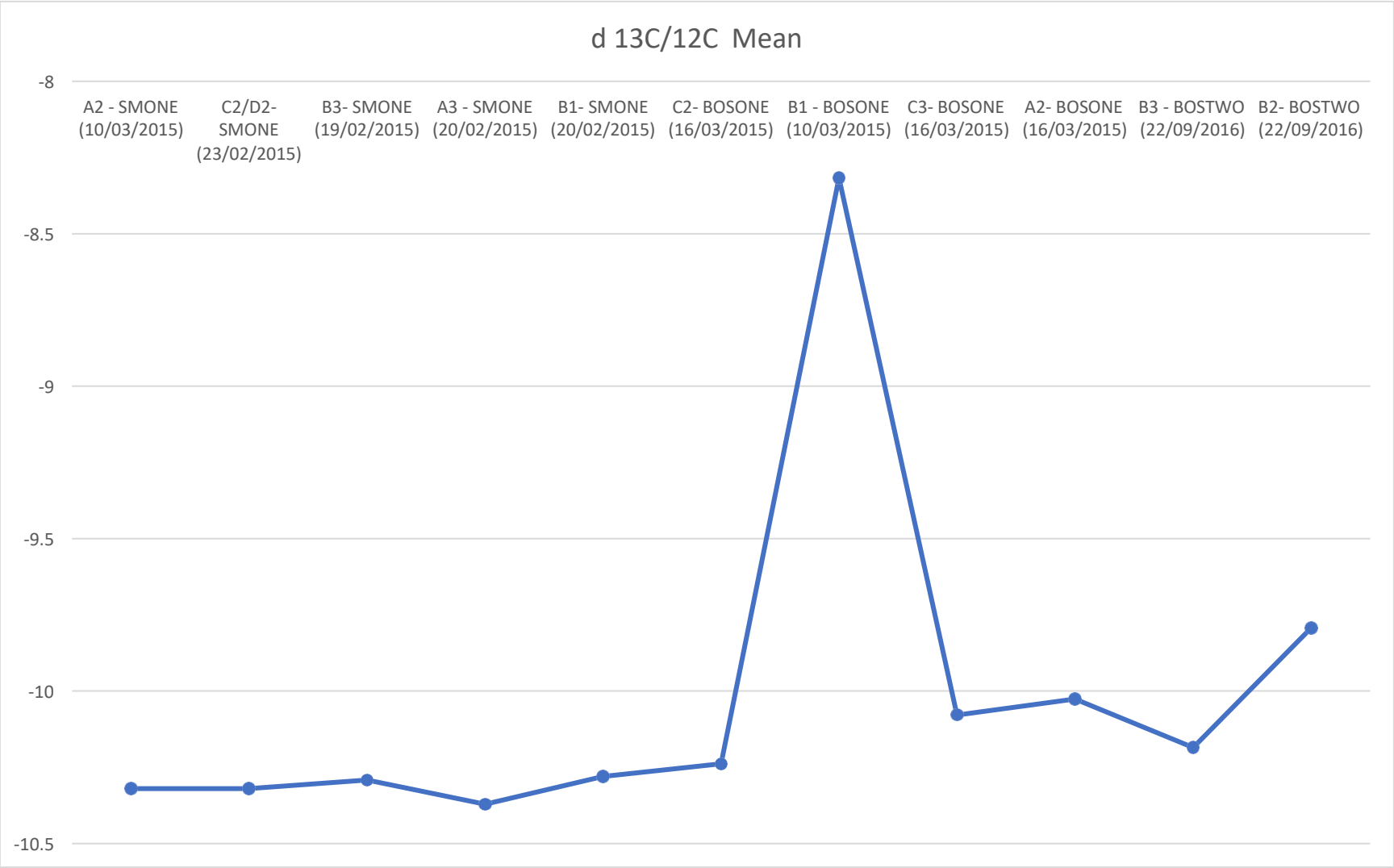


Figure 5.13 Stable carbon isotope ($\delta^{13}C$) results from the KRM layer.

5.3 Conclusion

Gomphocythere obtusata is the dominant taxa throughout the KRM samples that were analysed (Table 5.2; Table 5.3; Figure 5.8; Figure 5.9; Figure 5.10). This taxon will therefore be used as an indicator taxon for environmental conditions in the next chapter. However, this taxon co-inhabits KRM with three other taxa, whose environmental preferences will also be explored in the next chapter, as changes in the abundances of rare taxa can also infer environmental changes (Danielopol *et al*. 2002). Juvenile ostracods are the second most abundant type of ostracod in the samples (Table 5.2; Table 5.3; Figure 5.8; Figure 5.9; Figure 5.10). The adult: juvenile ratios indicate a low energy thanatocoenosis for the KRM samples. Absolute abundance data suggests that the layer with the lowest abundance is SMONE, whereas the layer with the highest abundance is BOS-Three. Certain taxa do differ significantly in their absolute and relative abundance values. Possible explanations for this occurrence will be explored in chapter 6. The Confidence intervals from the abundance data suggest that samples with smaller sizes have a larger CI width compared to larger samples (Figure 5.11).

5.4 Foraminifera

5.4.1 Foraminifera: Taxonomy

Foraminiferal specimens are infrequent in the KRM sediments; however, 10 different taxa were identified (see Systematics in Appendix C; Section C.3). Some of these taxa have also been identified in other areas of South Africa. Furthermore, foraminifera tests show signs of abnormalities and damage due to transport, erosion, and recalcification. Thus, the specimens that were classified as juvenile or highly eroded were placed into the "unidentifiable" category (see Appendix C; Figure C.11). Unidentified tests were still quantified in order to acknowledge their presence in the samples. The main emphasis of this project was the analysis of the ostracods, as their environmental interpretations are likely more reliable due to the fact that the ostracods are believed to be *in situ*, while the foraminifera ambiguous have origins. Therefore, samples were split to achieve a count of 300 ostracods (minimum) per sample. The foraminifera found in these splits were also counted, as they can still provide some information that can contribute to the ostracod data, but the samples were not enlarged to count more foraminifera. The foraminifera are presented in the results even though they will not provide much palaeoenvironmental information due to their low abundance and ambiguous origin. Limited environmental interpretations will be made from foraminiferal data. See Appendix C, Section C1, Table C.3 for the exact context of the 29 sediment samples that were analysed for foraminifera.

The 10 identified taxa include *Ammonia beccarii* (Appendix C, section C.2; Figure C.1), *Ammonia japonica* (Appendix C, section C.2; Figure C.2), *Ammonia* sp. (Appendix C, section C.2; Figure C.3), *Cassidulina* cf. *laevigata* (Appendix C, section C.2; Figure C.4), *Elphidium* sp. (Appendix C, section C.2; Figure C.6), *Cribroelphidium articulatum* (Appendix C, section C.2; Figure C.5), *Globigerinoides* sp. (Appendix C, section C.2; Figure C.7), *Lagena* sp. (Appendix C, section C.2; Figure C.8), *Nonion boueanum* (Appendix C, section C.2; Figure C.9), and *Spirillina vivipara* (Appendix C, section C.2; Figure C.10). The test composition of all the foraminiferal taxa found in the KRM sediments are calcareous. The lack of agglutinated foraminifera may be due to the fact that agglutinated foraminifera easily disaggregate (Smith 1987). The foraminiferal tests at KRM are poorly preserved and were likely subjected to erosion prior to being deposited inside Cave 1. All of the foraminiferal taxa are benthic, with the exception of

Globigerinoides sp. that is a planktic taxon. All of the foraminiferal taxa identified in the samples can be found in marine environments.

The census counts of the foraminifera suggest a relatively high number of taxa present (10 taxa), but low abundance of specimens (a total of 201 specimens counted from all the KRM samples analysed, as shown in Table 5.6). The split that was analysed for each sample is given in Appendix C; Section C.1; Table C.1 and Table C.3.

Table 5.6 Foraminifera census count per layer from KRM.

Census count													
Layer	Total weight (g) of washed >150µm sample (before splitting)	*A. beccarii*	*A. japonica*	*Ammonia* sp.	*Cassidulina* cf. *laevigata*	*Elphidium* sp.	*C. articulatum*	*Globigerinoides* sp.	*Lagena* sp.	*N. boueanum*	*S. vivipara*	Unidentifiable	Total
SMONE	89.35	4	11	14	0	17	20	7	0	19	0	11	103
BOS-ONE	73.6	0	3	0	5	7	2	2	1	1	0	10	31
BOS-TWO	80.5	0	1	0	0	2	7	1	0	0	10	6	27
BOS-THREE	146.99	2	3	4	3	2	2	2	0	3	15	5	40

5.4.2 Foraminiferal abundances

i) Absolute abundance (number specimens/gram sediment >150µm) of foraminifera

Layers BOS-One and SMONE have the lowest absolute abundance values, while BOS-Two and BOS-Three have the highest (Table 5.7). In SMONE, *Ammonia* sp. has the greatest absolute abundance, followed by *Cribroelphidium articulatum* and *N. boueanum* (Table 5.7; Figure 5.14). The abundances of all three these taxa decrease from SMONE to BOS-One and the unidentifiable specimens become the most abundant in BOS-One (Table 5.7; Figure 5.14).

Elphidium sp. has the second greatest abundance after the unidentifiable specimens in BOS-One (Table 5.7; Figure 5.14). There is a significant shift in abundances from BOS-One to BOS-Two, as taxon not identified in the previous two layers (*S. vivipara*) becomes the taxon with the highest absolute abundance in BOS-Two (Table 5.7; Figure 5.14).

There is also an increase in *Cribroelphidium articulatum* from BOS-One towards BOS-Two (Table 5.7; Figure 5.14). *Spirillina vivipara* followed by unidentifiable foraminifera have the highest absolute abundance in BOS-Three (Table 5.7; Figure 5.14). Spirillina vivipara increases from 13 specimens per gram of sediment in BOS-Two to 20 specimens per gram of sediment in BOS-Three (Table 5.7; Figure 5.14). The BOS-Three sample contains the highest absolute abundance of foraminiferal specimens out of all the layers (n=57) as illustrated in Table 5.7. The planktic foraminiferal taxon *Globigerinoides* sp. occurs in low abundances in all four samples, with the highest abundance observed in BOS-Three (Table 5.7; Figure 5.14).

Table 5.7 Foraminiferal absolute abundances per layer from KRM (decimals are rounded up).

Absolute abundance (#spec/g sed >150µm)												
Layer	*A. beccarii*	*A. japonica*	*Ammonia* sp.	*Cassidulina* cf. *laevigata*	*Elphidium* sp.	*C. articulatum*	*Globigerinoides* sp.	*Lagena* sp.	*N. boueanum*	*S. vivipara*	Unidentifiable	Total absolute abundance
SMON E	1	3	8	0	5	7	2	0	6	0	3	34
BOS-ONE	0	1	2	4	6	1	1	3	0	0	11	29
BOS-TWO	0	2	0	0	5	12	1	0	0	13	10	43
BOS-THRE E	4	5	4	5	1	4	3	0	4	20	6	57

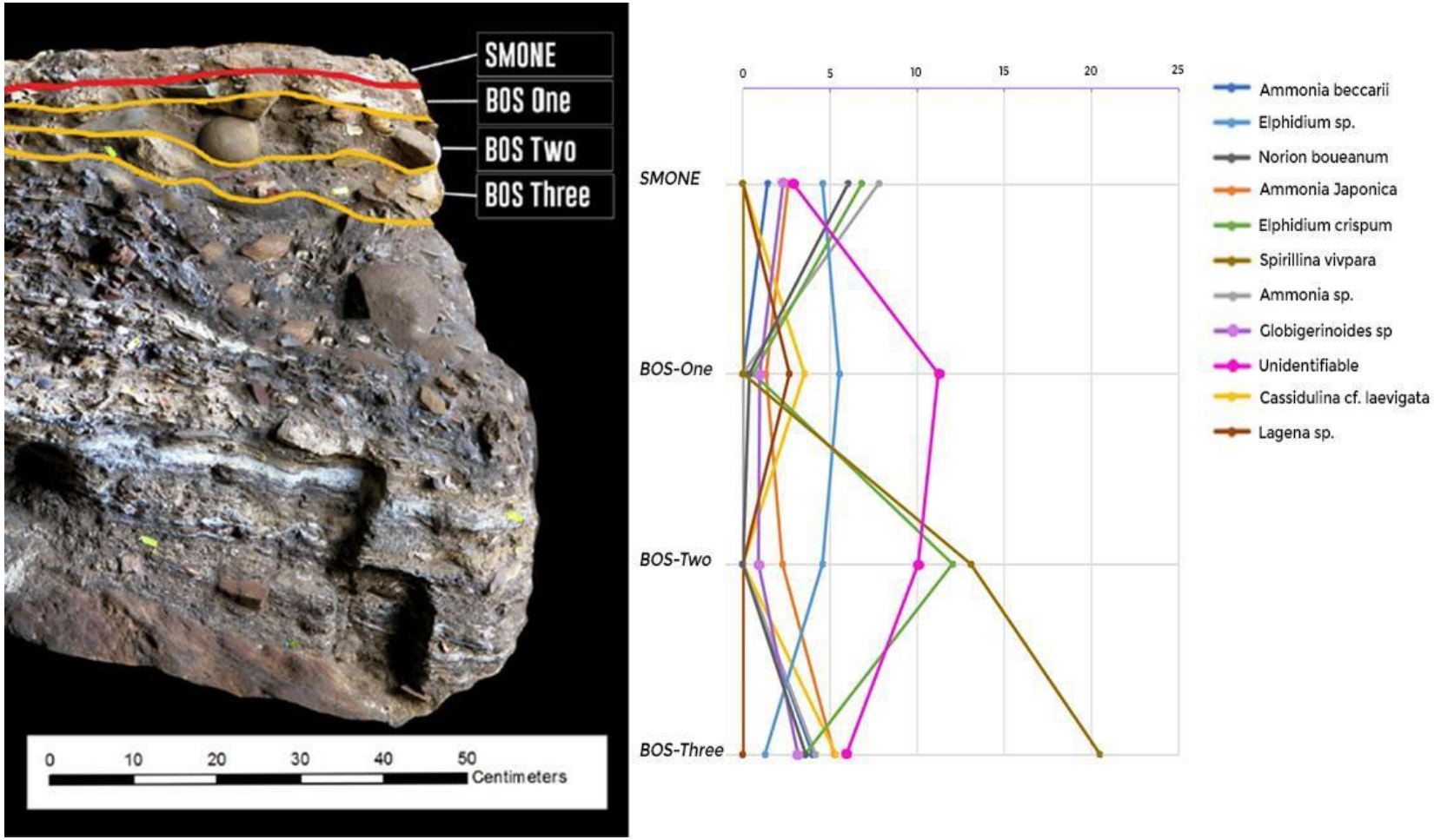


Figure 5.14 Absolute abundance of foraminifera with indication of stratigraphic zones.

ii) Relative abundance (% of total number of foraminifera within the sample)

Unlike the ostracods, there is no taxon that completely dominates the foraminiferal assemblage and the dominant taxa change from layer to layer (Table 5.8; Figure 5.15). The taxon with greatest relative abundance in SMONE is *Cribroelphidium articulatum*, followed by *N. boueanum* and *Elphidium* sp. (Table 5.8; Figure 5.15). All three of these taxa decrease in relative abundance in BOS-One (Table 5.8; Figure 5.15). In comparison to the other layers, SMONE has the lowest relative abundance of unidentifiable foraminifera followed by BOS-Three (Table 5.8; Figure 5.15).

The abundance of *Elphidium* sp. increases in BOS-One, but unidentifiable foraminifera have the greatest relative abundance in this layer (Table 5.8; Figure 5.15). *Cassidulina* cf. *laevigata* have the third highest abundance in BOS-One (Table 5.8; Figure 5.15). There is a large shift in abundances from BOS-One to BOS-Two, as a taxon (*S. vivipara*) that was not identified in the previous two layers becomes the dominant taxon in BOS-Two (Table 5.8; Figure 5.15). Unidentifiable foraminifera and *Elphidium* sp. decrease in BOS-Two (Table 5.8; Figure 5.15). *Spirillina vivipara* remains the dominant taxon in BOS-Three (Table 5.8; Figure 5.15). Unidentifiable foraminifera have the second highest absolute abundance in BOS-Three, and foraminifera such as *Ammonia* sp., *N. boueanum*, and *Cassidulina* cf. *laevigata* also increases in abundance (Table 5.8; Figure 5.15).

Table 5.8 Foraminiferal relative abundances per layer from KRM (decimals are rounded up).

Relative abundance (%)											
Layer	*A. beccarii*	*A. japonica*	*Ammonia* sp.	*Cassidulina* cf. *laevigata*	*Elphidium* sp.	*C. articulatum*	*Globigerinoides* sp.	*Lagena* sp.	*N. boueanum*	*S. vivipara*	Unidentifiable
SMONE	4	11	14	0	17	19	7	0	18	0	11
BOS-ONE	0	10	0	16	23	7	7	3	3	0	32
BOS-TWO	0	4	0	0	7	26	4	0	0	37	22
BOS-THREE	5	7	10	7	5	5	5	0	7	37	12

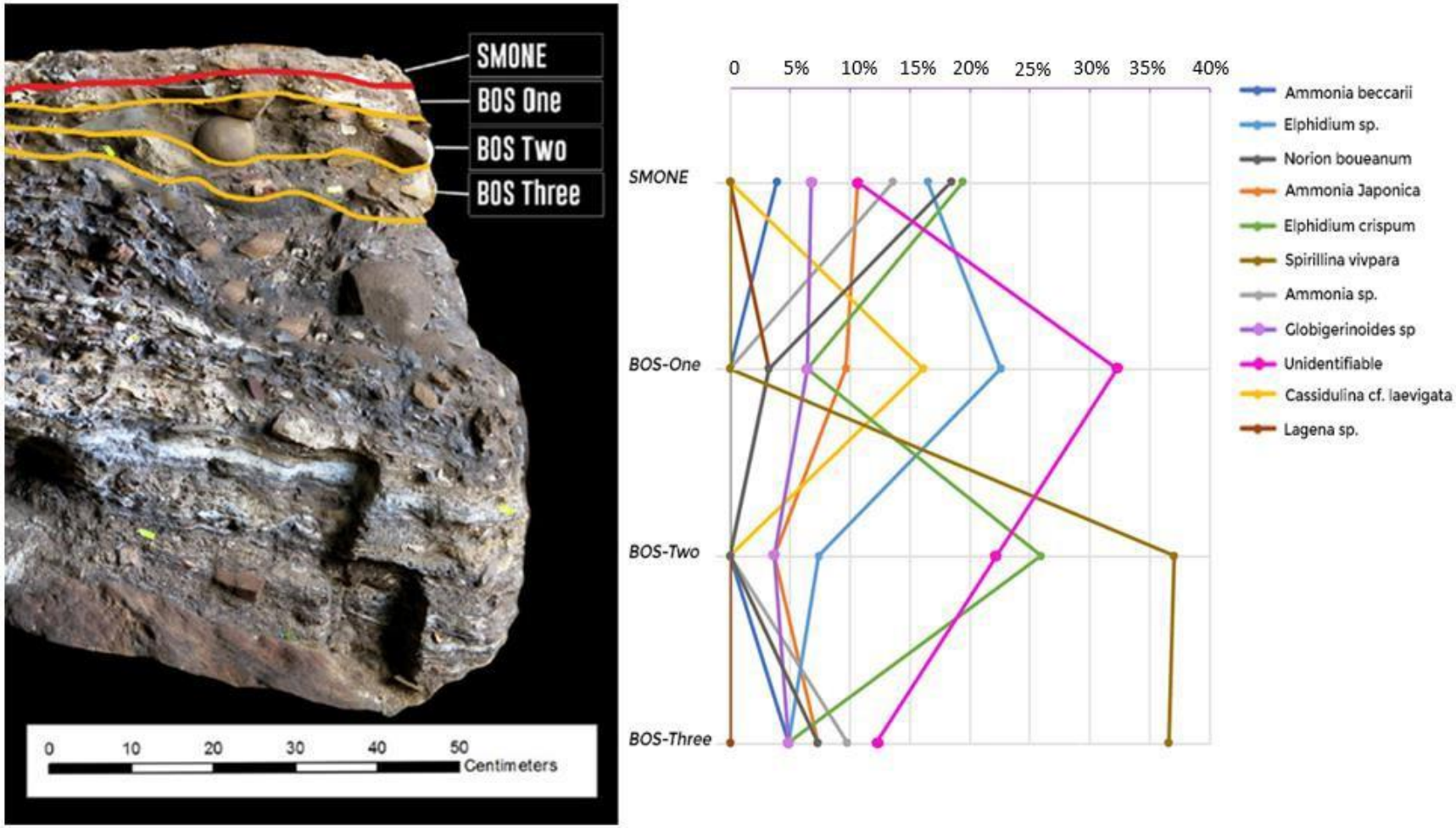


Figure 5.15 Relative abundance of foraminifera with indication of stratigraphic zones.

iii) Comparing the relative abundance and absolute abundance data of foraminifera

In SMONE, the absolute abundance of *Ammonia* sp. suggests that this taxon has the highest absolute abundance out of all the foraminifera taxa. However, relative abundance suggests that *Ammonia* sp. has the fourth greatest relative abundance in SMONE. The relative abundances and absolute abundances in BOS-One remain consistent, with unidentifiable specimens being the dominant type of foraminiferal specimen in the layer in both instances. In BOS-Two and BOS-Three, *S. vivipara* have the same relative abundance (n= 37%) despite having different absolute abundances. This can likely be due to the fact that BOS-Two has a smaller sample size compared to BOS-Three, thus causing the *S. vivipara* specimens to appear to have a greater relative abundance.

iv) Confidence Intervals

The foraminifera have higher error margins than the ostracods in the KRM samples, as the sample sizes for the foraminifera are smaller (Figure 5.16). The taxon with the highest relative abundance SMONE is *E. crispum*, and this taxon has a CI width of between 0.12 (95% CI lower) and 0.28 (95% CI upper) (Figure 5.16 D). In BOS-One, unidentifiable foraminifera have the greatest relative abundance, and the CIs indicate a range between 0.17 (95% CI lower) and 0.51 (95% CI upper) (Figure 5.16 K). *Spirillina vivipara*, the most abundant foraminifera taxon in BOS-Two and BOS-Three has CIs of between 0.19 (95% CI lower) to 0.58 (95% CI upper), and 0.22 (95% CI lower) and 0.53 (95% CI upper) respectively (Figure 5.16 A). It is important to note that despite having the same relative abundance value (n = 37%), BOS-Three does have a bigger sample size than BOS-Two, and BOS-Three also contains more *S. vivipara* specimens than BOS-Two, thus resulting in a smaller CI width in BOS-Three (Figure 5.16 A). Overall, SMONE does seem to have a smaller CI width than the BOS-layers (Figure 5.16).

5.4.3 Geochemical analysis of foraminiferal tests

The foraminifera tests in the KRM samples are not *in situ* (as suggested by evidence of erosion and transport on tests) and some have also been recalcified. Post-depositional diagenesis does alter foraminiferal δ 18O values, as δ 18O values decreases in deep-

burial diagenesis (Katz *et al*. 2010). This is attributed to the fact that fossil foraminiferal tests may recalcify in equilibrium with sediment temperatures that are higher than at the seafloor, due to the geothermal gradient (Katz *et al*. 2010).

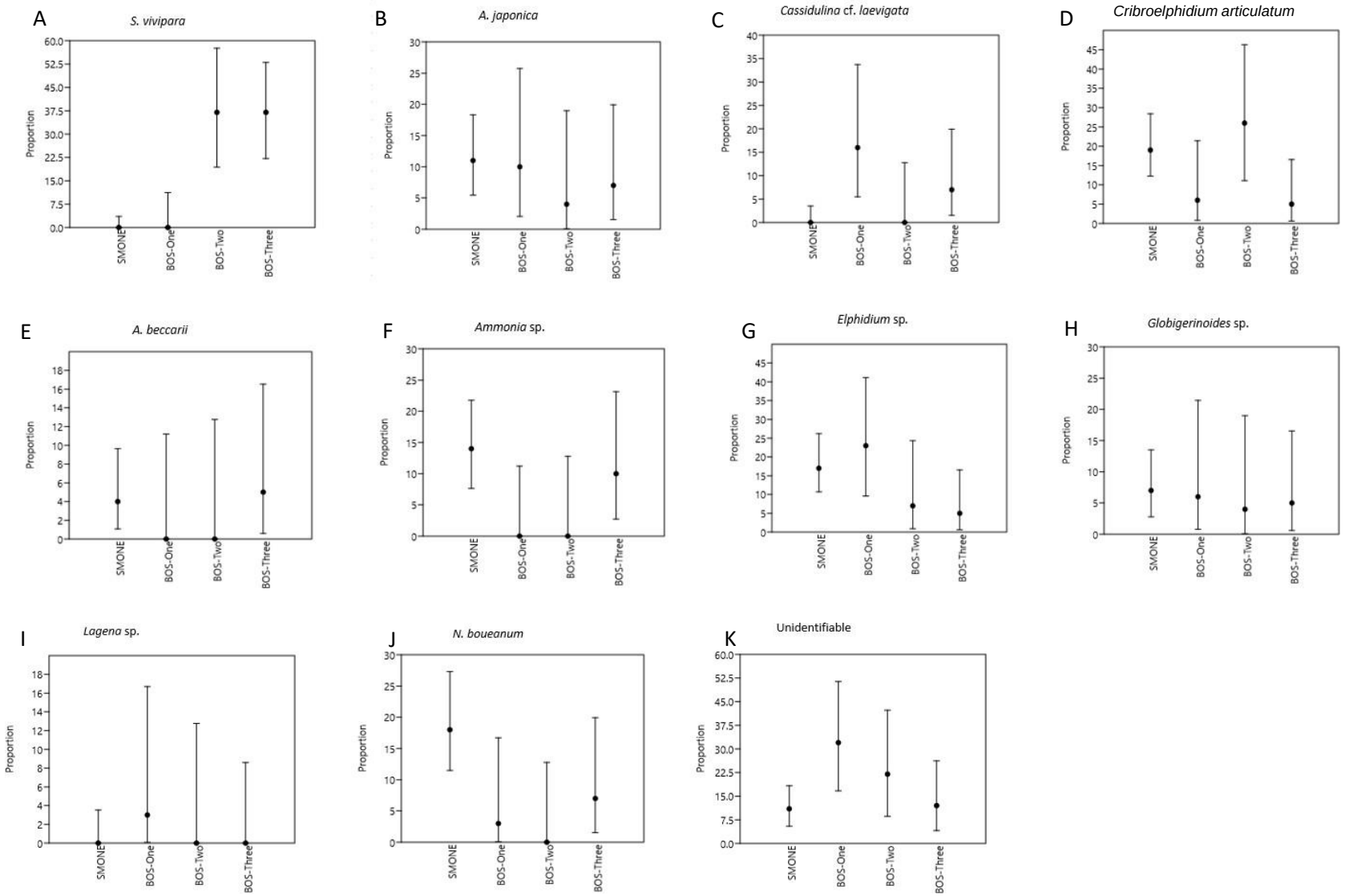


Figure 5.16 Confidence Intervals for foraminifera relative abundance.

Chapter 6: Discussion and conclusion

6.1 Introduction

This chapter discusses and interprets the results presented in Chapter 5 in relation to the research question, regarding the site formation processes and palaeoenvironment during MIS 5c-d at Klasies River through the analyses of microfossils such as ostracods and foraminifera. First, the ecological significance of taxa will be discussed and suggestions will be made with regard to their palaeoenvironmental conditions during MIS 5c-d at KRM. Secondly, the data gathered from the microfossils and their subsequent inferences regarding site formation processes will be considered. The data will be placed into context with other archaeologically significant information to increase the understanding of the environmental milieu in which modern humans evolved at KRM. The preliminary stable isotope analysis of the ostracod valves is explored in section 6.6.

6.2 Ostracods from KRM: Taxonomy and ecology in wider context

All the ostracod taxa present at KRM were also identified by Martens *et al*. (1996) at Verlorenvlei during the dry and wet season, with the exception of the taxon *Ilyodromus* only reported during the dry season at Verlorenvlei. The majority of the ostracod taxa from KRM were also reported by Fürstenberg *et al*. (2017). However, Fürstenberg *et al*. (2017) did not report any *Ilyodromus* specimens. The systematics of the ostracods are provided in Appendix C, Section C.3. The KRM ostracods have a low number of taxa present in the KRM assemblage, but a high abundance of specimens. This indicates that conditions might have been unstable and stressed for some of the ostracod taxa (Frenzel & Boomer 2005). As discussed in the previous chapter, *G. obtusata* is dominant in all the samples. The second most abundant identifiable ostracod taxon, *S. aculeata*, also appears in moderate numbers, but seems to be more stressed. Weakly calcified ostracod shells can also suggest that a certain ostracod taxon (*Ilyodromus* sp. in the KRM case) was operating at the tipping point, or “survival range” of their environmental parameters, as the valves were fragile, transparent, and broke easily (Frenzel & Boomer 2005; Lord *et al*. 2012). However, taphonomic biases should also be acknowledged, as the *Ilyodromus* sp. valves are weakly calcified and could therefore have been subjected to dissolution and other taphonomic processes that caused the taxon to be less prevalent in

the KRM assemblage. It is likely that *Physocypria* cf. *castanea* was also operating within a “survival range” (Lord *et al.* 2012). This deduction was made by analysing both the absolute abundance and relative abundance data, where *Physocypria* cf. *castanea* and *Ilyodromus* sp. appear rare in the KRM samples.

Gomphocythere obtusata is an extant species of ostracod that cannot swim (Martens *et al*. 1996). *Gomphocythere* is a brooding genus, which makes it unlikely that the eggs are desiccation-resistant (Park 1995). Due to the fact that this genus consists of mostly brooders, durable eggs are probably not essential for survival (Park 1995). Brooding does, however, limit the dispersal ability of these ostracods (Park 1995). This suggests that the ostracods in adult instars were perhaps brought into the cave by other animals or perhaps humans from a nearby water source, such as the Klasies River (freshwater) or from the estuary that was reported by Langejans *et al*. (2017) between 100-80 ka ago. This hypothesis is further discussed in section 6.3. *Gomphocythere obtusata* can usually be found in freshwater conditions but was reported in a slightly saline environment at Verlorenvlei (Martens *et al.* 1996; Fürstenberg *et al*. 2017). It does not seem as though Fürstenberg *et al*. (2017) found live specimens of *G. obtusata* in their study, but the study did report empty valves at salinities above 40 ppt.

The taxon *S. aculeata,* has previously been reported in freshwater to more saline conditions at Verlorenvlei (Martens *et al*. 1996). This taxon was one of the most widely distributed taxa at Verlorenvlei and was reported at almost all of the sampling stations set up by Martens *et al.* (1996) during the wet and dry season, with the exception of station 1 (at the mouth of the vlei) during the dry season. According to Martens *et al*. (1996) *S. aculeata* is usually an indicator of slightly saline conditions and can be found worldwide (Martens *et al*. 1996; Fürstenberg *et al.* 2017). Martens *et al*. (1996) mention that some authors classify *S. gregaria* as the spineless and sexually reproducing variant of *S. aculeata* (see Appendix B, Section B.2). Despite the proximity to the ocean, none of the ostracod specimens from KRM are normally indicative of hypersaline or marine conditions. However, living specimens of *S. aculeata* and *P. capensis* were reported in the limnetic to mesohaline conditions by Fürstenberg *et al.* (2017) as discussed in Chapter 3 (see Figure 3.3), which infers the tolerance of more saline conditions.

Fürstenberg *et al.* (2017) further notes that in their study, *S. aculeata* usually preferred areas of lower salinity than another species from the same genus, such as *S. glabrata.* Martens *et al*. (1996) describes *P*. *castanea* as an ambiguous species from the Free State and Natal and suggests that it is likely a synonym of *P*. *capensis*. Specimens from the taxon *P. capensis* were identified by Martens *et al*. (1996) at Verlorenvlei in freshwater to slightly saline (brackish) conditions. In Fürstenberg *et al.* (2017)'s study of Verlorenvlei, *P. capensis* valves were partly deformed and poorly represented. Empty *P. capensis* valves were reported in hypersaline conditions (Fürstenberg *et al.* 2017).

The Martens *et al*. (1996) study was one of the first to note *Ilyodromus viridulus* in a slightly saline environment (during the dry season), as this taxon can usually be found in freshwater pools and dams. Specimens from the genus *Ilyodromus* have also been found in granite rock pools as well as fresh-and turbid water sources in Australia (de Deckker 1981). *Ilyodromus* is usually not found in South Africa and is considered an invasive taxon from Australia (Martens *et al*. 1996). The specimens found in the KRM assemblage were too difficult to identify to species level due to the fragile nature of the valves and also the lack of some distinctive morphological characteristics. It is therefore difficult to ascertain the exact ecological preferences of this specimen. However, it is possible that the KRM specimens can also be *Ilyodromus viridulus,* as this is the only species of *Ilyodromus* that has been identified in South Africa. As discussed in the previous chapter, an *Ilyodromus* sp. specimen from BOS-One has small black stains visible on the inside of the valve (Figure 5.7). One explanation for the black stains can be manganese staining, as manganese is present in calcareous rocks, but can also occur as a result of decomposed organic substances (López-González *et al.* 2006; Lap 2020). Bones analysed in a master's project by Lap (2020) did show signs of manganese staining in the same layers that were examined for ostracods. Only a few of the other ostracod and foraminifera samples showed similar black stains (see Appendix C, section C.1, Figure C.4; Figure C.8; Figure C.12).

The specimens from *G. obtusata* are similar to the male sizes of the taxon recorded by Martens *et al*. (1996) at Verlorenvlei. This can be indicative of multiple conditions, such as temperatures that cause variations in calcification rates. For example, lower

temperatures can cause ostracods to calcify their shells at a slower rate, thus leading to slightly larger carapace sizes (Boomer *et al*. 2003). However, changes in carapace sizes can also be part of a normal genetic controls (Boomer *et al.* 2003). There is also a possibility that the *G. obtusata* assemblage contained more male specimens. Future analysis will attempt to determine the male: female ratio of the assemblage to gain information on reproduction strategies and seasonality (Boomer *et al.* 2003).

6.3 Ostracods and site formation at KRM

Freshwater to slightly brackish water sources were likely present around the caves during the deposition of the SMONE and the BOS-layers (suggested by the presence of the freshwater to slightly saline ostracod taxa). This is supported by the proximity of the Klasies River Mouth (0.5 km east of the main site) to the cave (Singer & Wymer 1982; von den Driesch 2004), and by evidence of an estuary at the river mouth during MSA II (von den Driesch 2004). The ostracods were likely able to survive in the cave due to the calcite formations (stalagmites and stalactites) that dripped water into the cave (Singer & Wymer 1982; Deacon & Geleijnse 1988). The best developed stalagmites and stalactites are in Cave 1 (where the ostracod assemblage is from). The source of the lime-rich waters in the cave is the calcarenite dune above the caves (Singer & Wymer 1982; Deacon & Geleijnse 1988; Brenner & Wurz 2019).

Gomphocythere obtusata is more abundant than *S. aculeata* in the MIS 5 assemblages from KRM. However, unlike *S. aculeata, G*. *obtusata* is usually indicative of more freshwater conditions, despite being reported in a slightly saline environment by Martens *et al*. (1996). Due to *S. aculeata* usually being indicative of a slightly saline environment and *G. obtusata* being reported in a slightly saline environment at Verlorenvlei, it is possible that low levels of salinity could have been present inside the cave. Especially in BOS-One where there is an increase in both absolute and relative abundances of *S. aculeata* (Figure 5.8; Figure 5.9). If the environment in which the ostracods lived was mildly saline, it is unlikely that the saline water would have come from the speleothems above, as salt is often associated with the decay of porous limestone (Ruiz-Agudo *et al*. 2007). The salinity inside the cave could possibly have occurred as a result of windblown salt from the ocean. Sea salt particles can be picked up by winds and transported

elsewhere in coastal environments (Yaalon & Lomas 1970). The main components of aerosols in a coastal atmosphere are sea salt particles and spray droplets and are most intensive in the nearshore breaker zone of waves (Yaalon & Lomas 1970). If the salinity levels of a waterbody surpass the preferred salinity of an ostracod taxon, the specimens may appear smaller than when they are in their ideal environment (Karanovic 2012). As noted in Chapter 5, the sizes of the ostracods found at KRM are very similar to those reported by Martens *et al.* (1996) at Verlorenvlei. This can suggest that there was no environmental variable present that caused drastic changes in the size of the ostracod valves and that conditions were likely more indicative of freshwater to brackish water conditions.

Certain ostracod taxa can become more abundant than others due to competition with other organisms or food supply (Karanovic 2012). Freshwater ostracods are often viewed as “generalists” and will eat algae, dead and living plant material, organic detritus, bodies of the dead animals, and invertebrate faeces, as mentioned in Chapter 3 (Karanovic 2012). It has been theorised that some ostracod taxa prefer certain types of sustenance, but there is little information regarding this (Karanovic 2012). At KRM there is enough archaeological evidence to support the presence of material such as dead plants (Larbey *et al.* 2019) and organic detritus from, for example shellfish (Thackeray 1988; Langejans *et al.* 2012, 2017) for the ostracods to live off of.

There are three plausible scenarios in which the ostracods could have been deposited in the KRM sediments. The first possible scenario involves the ostracods attaching themselves to an animal such as a waterfowl or any other bird that frequent water bodies before entering the cave and depositing the ostracods (Boomer *et al*. 2003). In this case, there is evidence in the form of avian remains to support the presence of certain birds (such as penguins and seagulls) in the cave during the MIS 5 sequence (von den Driesch 2004). The second possible method of ostracod transport is through a storm or flooding event that moved the ostracods from one area to another (Boomer *et al*. 2003; Frenzel & Boomer, 2005). The final scenario involves fish foraging by early inhabitants of the cave, as some ostracods can survive passing through fish intestines by closing their shells tightly (Vinyard 1979; Karanovic 2012). Fish often consume ostracods in large quantities

(Karanovic 2012). The early modern humans could have caught the fish outside of the cave and carried them inside for cooking and consumption, thus depositing the ostracods into the cave sediments. Von den Driesch (2004) does report an increase in estuarine fish during the Mossel Bay phase (MSA II), relevant to the ostracod assemblage discussed here, which could explain the presence of freshwater and slightly saline ostracod taxa. The estuary was likely closer to the main site during the MSA II phase than in the present day (von den Driesch 2004). The ostracods likely did not enter the cave attached to foraged shellfish, as the majority of shellfish that were foraged by humans were marine taxa such as *Perna perna*, and not from freshwater to brackish water origins (see Langejans *et al*. 2012, 2017; Brenner *et al*. 2020). One of the only freshwater shells to occur in the MSA sequence is *Nassarius kraussianus* (Thackeray 1988), but these shells do not occur as frequently as the estuarine fish remains.

Von den Driesch (2004) did identify fish taxa in the MSA II deposits at KRM, such as *Tilapia*, that inhabit fresh-to slightly saline water and were likely brought into the cave by humans and other animals. The *Tilapia* specimens were likely caught at the mouth of the Klasies River (von den Driesch 2004). Although there are likely multiple accumulators of the fish assemblage (such as penguins, cormorants, seagulls and other mammals), some fish remains (such as sharks) are too large to be brought into the cave by most animals, thus making humans the likely accumulator. Estuarine systems are important habitats for sharks, such as the genus *Carcharhinus* (McCord & Lamberth 2009). Von den Driesch (2004) did identify *Carcharhinus* remains in the KRM MSA II assemblage. Although there is little research available on whether ostracods will survive inside the intestines of sharks, the possibility that the ostracods could have been carried into the cave in this manner cannot be overlooked.

6.4 Change through time in the ostracod assemblage at KRM

i) Absolute abundances

The absolute abundances of the ostracods are lowest in layer SMONE. The highest total absolute abundance of ostracods occurs in BOS-Three, and findings from Lap (2020) and Brenner *et al*. (2020) suggest a higher rate of site occupation during SMONE (MIS 5c) than in the BOS-layers (MIS 5d). The low absolute abundances of SMONE supports the

hypothesis that there were less ostracods inside the cave during this time, likely due to drier conditions outside the cave (less drip water from the calcite formations) and higher levels of human occupation inside the cave. In general, environments during the deposition of SMONE (MIS 5c) were likely less moist than the BOS-layers (MIS 5d). Some studies, such as Maringa (2020) and Lap (2020) suggest that water was present inside the cave during the BOS phase. The occurrence of wetter conditions during MIS 5d can begin to suggest why more ostracods are present in the BOS-layers than in SMONE. The absolute abundance of ostracods possibly infers a relationship between site occupation and ostracod abundance.

ii) Relative abundances

SMONE is the layer with the smallest sample size, followed by BOS-Two. Due to these smaller sample sizes, some statistical error margins need to be taken into account when interpreting the abundance data. In layer SMONE, there is a decrease in the relative abundance of *G. obtusata* compared to the BOS-layers and an increase in juvenile instars. The relative abundance of *G. obtusata* and *S. aculeata* increases from SMONE to BOS-One, while juveniles decrease from SMONE to BOS-One. This perhaps infers that there were changes in environmental factors, such as waters that have a low pH, that caused the juvenile valves to dissolve and adult instars to appear more abundant. The samples were all dominated by adult instars. Layer BOS-Two has the highest relative abundance of *G. obtusata* (Figure 5.9; Figure 5.10), while *S. aculeata* and juvenile ostracods decrease in abundance from BOS-One to BOS-Two (Figure 5.9). This can perhaps suggest that environments that were more favourable to *G. obtusata* and less favourable to *S. aculeata* were present. This could subsequently infer an environment more indicative of more freshwater conditions inside the cave (Martens *et al*. 1996). However, it is important to note that although BOS-Two has the highest relative abundance of *G. obtusata*, it has a smaller sample size than BOS-One and BOS-Three and thus has a larger Confidence Interval width (Figure 5.11).

6.5 Adult: juvenile ratios and assemblage composition

As discussed in the previous chapter, the ostracod assemblage consists of a mixture of adult and juvenile ostracods, but the adults are more abundant than the juveniles. The assemblage also consists of mainly disarticulated valves. The adult: juvenile ratio from the KRM samples thus reflect an autochthonous low energy thanatocoenosis (see Boomer *et al*. 2003: 157). An autochthonous low energy thanatocoenosis indicates that there was little *post-mortem* disturbance and the assemblage is considered to be an effective indicator of the conditions in which the ostracods lived (Boomer *et al.* 2003). There is not much difference between the adult: juvenile ratio of the various layers, however, BOS-Two has the highest difference between the adults and juveniles (Table 5.5), but does not consist of only juvenile or only adult valves (Boomer *et al*. 2003). Juvenile ostracods did make up a large portion of the assemblage (usually has the second highest abundance after *G*. *obtusata*), which suggests that the environment at KRM was probably environmentally favourable for one or two of the taxa, and also that preservation within the cave is good. However, one must note that a slight bias might have been introduced while cleaning the samples in the lab, as juveniles in the first four stages are oftentimes washed away (Danielopol *et al*. 2002).

6.6 An isotopic perspective on ostracod calcification and the environment

The stable isotope results for the ostracods were interpreted with the assistance of Prof. Jonathan Holmes from the University College London. Calcite is precipitated in oxygen-isotope equilibrium with water (Kim & O'Neil 1997) and ostracods tend to show positive offsets from this equilibrium (Caporaletti 2011 and references therein). As discussed in Chapter 4, different taxa have different offsets. At present, the nearest estimate for *Gomphocythere obtusata* is from the related genus *Cytheridella* (+1‰) (Bristow *et al*. 2018). The equivalent values for calcite in isotopic equilibrium with water in the KRM samples are thus between -3.4‰ to - 3.6‰ (personal communication, Prof. J Holmes, March 2021). Figure 6.1 shows the results for the isotopes next to their corresponding stratigraphic profiles.

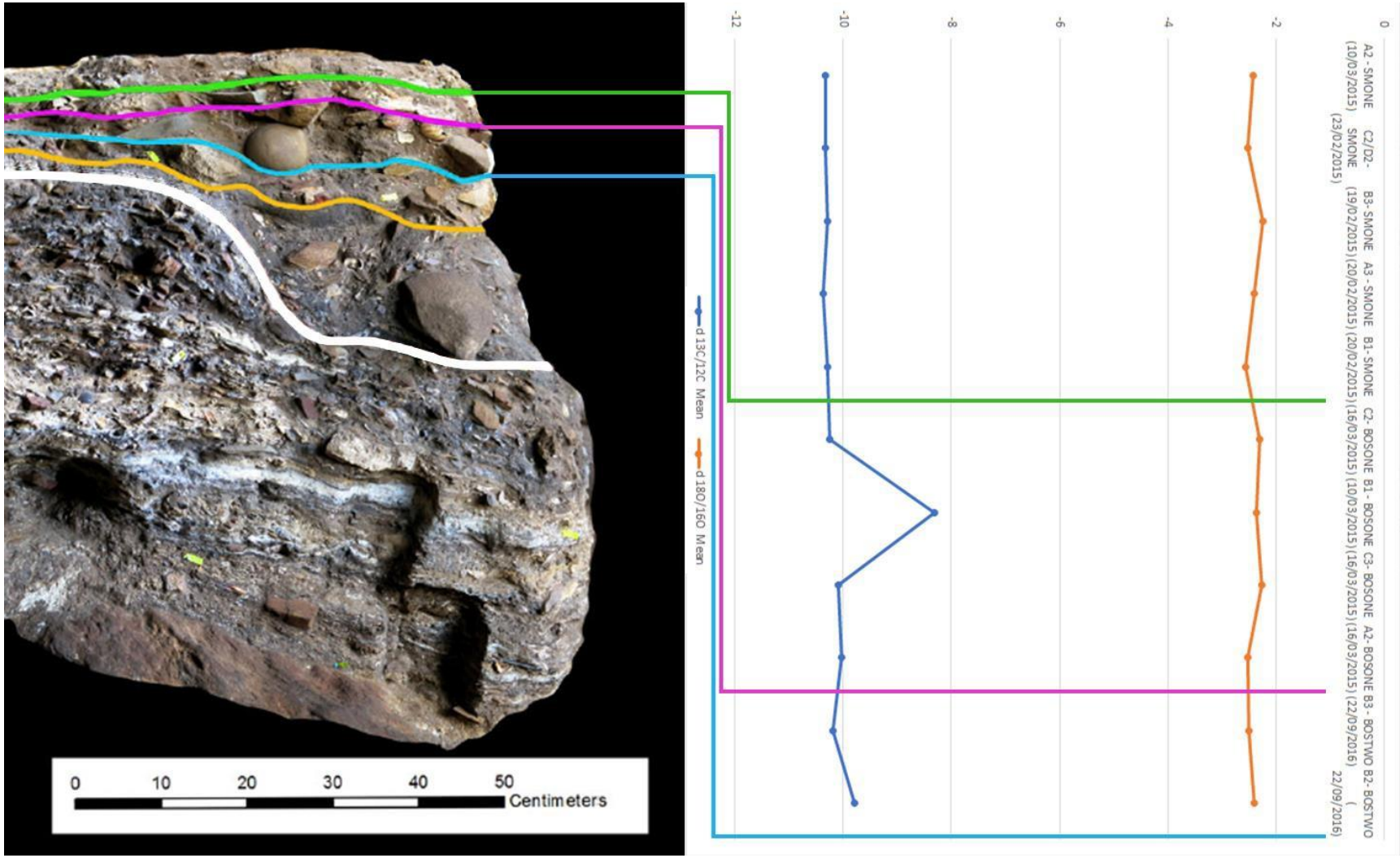


Figure 6.1 Stable isotope values with indication of stratigraphic zones.

When these vital effects are taken into consideration for all samples, then values for SMONE ranges from -3.2 ‰ to -3.6 ‰, BOS-One ranges from -3.3‰ to -3.5‰, and the two samples from BOS-Two range from -3.4‰ to -3.5‰. The values between the samples are similar and sample sizes will need to be increased in future to create a higher resolution analysis.

The Global Network of Isotopes in Precipitation (GNIP) is an isotope monitoring network of oxygen isotopes in precipitation. Information from this database was used to compare the KRM ostracod oxygen isotope values. The closest GNIP record to KRM is from the Cape Town station (roughly 700 km west of KRM). The Cape Town GNIP record (http://www-naweb.iaea.org/napc/ih/IHS_resources_isohis.html) suggests that the weighted annual mean value of isotopes in precipitation is -3.3 ‰ (Personal communication, Prof J Holmes, March 2021). Modelled values (https://wateriso.utah.edu/waterisotopes/pages/data_access/form.html) for KRM are thus broadly similar, but seasonality might cause differences (Personal communication, Prof J Holmes, March 2021). As mentioned in Chapter 2, temperatures on the southern Cape coast today have a mean annual temperature of ~18 ºC (Esteban *et al*. 2020). However, $\delta^{18}O$ data for MIS 5 from *T. sarmaticus* suggests that MIS 5 SST's were lower than ~18 ºC (Loftus *et al.* 2017). Modern day precipitation values are likely different from MIS 5 values, as cooler temperatures during MIS 5 may have resulted in lower values (personal communication, Prof. J Holmes, March 2021). Unfortunately, temperatures could not be determined as $\delta^{18}O$ values for water (inside or in close proximity to the cave) are unavailable at present.

According to data from PP, C3 vegetation was dominant during the majority of MIS 5 (Braun *et al*. 2019), although similar data are not available for KRM. "If the dissolved inorganic carbon (DIC) from the water in which the ostracods calcified was provided by a 50:50 mixture of CO_2 from C3 plants ($\delta^{13}C$ = -30 to -20 ‰) and dissolution of limestone ($\delta^{13}C$ = 0 to +2 ‰) then the $\delta^{13}C$ should be in the range -15 to -9 ‰, with ostracod calcite values of -14 to -8 ‰" (Personal communication, Prof J Holmes, March 2021). Water on the ground surface would be able to exchange with atmospheric CO_2 (also see Holmes 1996), which would elevate the $\delta^{13}C$ of the DIC and also the ostracods calcifying from it,

which likely happened to the KRM samples (Personal communication, Prof. J Holmes, March 2021). In general terms, negative values of the $\delta^{13}C$ isotopes can suggest that there was a tendency towards oligotrophic conditions and low water turbidity, whereas high (positive) values of $\delta^{13}C$ infer a tendency towards eutrophism and higher water turbidity (see Caporaletti 2011). Turbidity occurs when particles become suspended in water causing a reduction in clarity (Grobbelaar 2009). Oligotrophic environments refer to environments with low concentrations of mixed substrates where there are little resources to sustain the most types of organisms (Hammes *et al.* 2011). Examples of oligotrophic environments include deep ocean sediments or caves. The negative values of $\delta^{13}C$ possibly suggest that the environment inside the cave 1 at KRM was unfavourable for most organisms to live in.

6.7 Foraminifera from KRM: taxonomy and ecology in wider context

The occurrence of foraminifera is rare in the KRM sediments; however, 10 taxa of foraminifera were identified (see Appendix C; Section C.2). The foraminifera have lower abundances than the ostracods, but a higher number of taxa. The foraminifera also have smaller sample sizes compared to the ostracods. The condition of the foraminiferal tests suggests that many specimens were likely subjected to heavy erosion and transport prior to being buried inside Cave 1 at KRM (see Appendix C; Section C.2; Figure C.11). This suggests that the foraminiferal specimens are not *in situ* and were likely outside of their host waters and died before reaching the caves. The foraminifera are therefore only used in more conservative paleoenvironmental interpretations.

Spirillina vivipara (the identifiable taxon that occurs in highest numbers, absolute abundance and relative abundance) is usually found on hard and stable substrates and can tolerate a wide salinity range (Murray 1991). Specimens from *S. vivipara* were only present in two layers at KRM, namely BOS-Two and BOS-Three. Strachan *et al.* (2016, 2017) did identify *Spirillina vivipara* at Keiskamma and Knysna Estuaries, but did specifically note the absence of the taxon at –0.02 m to 1.05 m above mean sea level at Keiskamma. At Knysna, *S. vivipara* only occurred in low numbers (Strachan *et al.* 2016, 2017). Specimens from the *Lagena* taxon (*Lagena* spp.) were found together with *S. vivipara* by Strachan *et al*. (2016, 2017) at an elevation that was deeper and characterised

by more saline waters at Keiskamma and Knysna estuaries. The occurrence of *S. vivipara* in BOS-Two and BOS-Three can therefore infer the presence of hard and stable substrate with saline conditions in close proximity to the cave.

Some of the foraminifera that were identified in the KRM samples (*Ammonia beccari;, Elphidium* sp.) are indicative of marginal marine environments and shallow waters, but prefer living in tidal estuaries with reduced salinity (Murray 1991). The highest relative abundance of *Cribroelphidium articulatum* occurs in SMONE and BOS-Two. *Ammonia beccarii* also occurs in SMONE. The highest relative abundance of *Elphidium* sp. is seen in BOS-One. This perhaps indicates the presence of an environment where a tidal estuary with low levels of salinity was nearby the cave between MIS 5c-d. *Ammonia* spp. was identified by Fürstenberg *et al*. (2017) in polyhaline to hyperhaline salinity ranges. *Ammonia japonica* is not widely documented in South Africa, but has previously been documented in the sandflats of the Knysna estuary by Simpson (2003) and in vibracores recovered from the western continental shelf of southern Africa by Bergh & Compton (2020). Strachan (2016) reports that the identification of specimens from the *Ammonia* taxon is problematic and the literature is inconsistent in South Africa, thus causing uncertainties when classifying this taxon. *Cassidulina laevigata* has been reported by Bergh & Compton (2020) at inner shelf depths. *Globigerinoides* sp. is a surface-dwelling planktic foraminifera (Bé *et al.* 1982). No planktic foraminifera were found in the salt-marshes investigated by Strachan (2013) or Strachan *et al.* (2014, 2015, 2016, 2017) or in the Mort Creek cultural deposits investigated by Rosendahl *et al*. (2007). Due to the varying depths at which the foraminifera occur (and the occurrence of planktic foraminifera), the notion that the foraminifera were likely either blown into the cave or carried in along with foraged shellfish (or fish) is the most plausible explanation for their presence in the cave. This is further explored in section 6.8. Foraminifera that are indicative of hard, and stable substrates as well as foraminifera that can be indicative of tidal estuaries with low levels of salinity are present (and at times, dominant) in the MIS 5 c-d assemblage at KRM.

6.8 Foraminifera and site formation at KRM

Natural foraminifera deposits of foraminifera can be introduced to archaeological sites by processes such as tidal action and storm surges (Rosendahl *et al.* 2007). As mentioned in Chapter 3, foraminifera can also be introduced into the cave by cultural activities (such as foraging shellfish) but will occur in lower abundances than in natural deposits (Rosendahl *et al*. 2007). At KRM it is unlikely that the ocean reached cave 1 on a regular basis, as sea levels were not high enough to reach the inside of the cave (as discussed in Chapter 2), but storm events that carry foraminiferal samples further inland (and possibly into the cave) are possible, as well as human and animals that carry marine life into the cave.

Some foraminiferal tests could have entered the cave while adhering to the shells of shellfish, such as *Perna perna,* that were exploited for food throughout MIS 5 by early modern humans (for example, in Brenner *et al.* 2020). Other tests could have been wind-blown into the cave by coastal winds that also transported some saline aerosols from the ocean. Planktic foraminifera are present in all the layers that were analysed, but in low numbers. Similar to the ostracods, foraminifera could also have been brought into the cave by cave occupants that foraged fish or other marine wildlife, but unlike the ostracods, likely died before reaching the cave. For example, fish and sea turtles are known to consume foraminifera that adhere themselves to algae, seagrass and other types of plants consumed by marine animals (for example, Lipps 1988; Rosendahl *et al*. 2007). Foraminiferal tests can be damaged when they are consumed by fish (Lipps 1988). Due to the extensive damage seen on the tests from KRM, it is not impossible that they passed through the digestive tracts of fish. All of the foraminifera that were identified inside Cave 1 (layers SMONE, BOS-Three, BOS-Two, BOS-One) can be associated with saline conditions. The majority of foraminiferal samples from KRM likely occur as a result of cultural activities (for example, see Rosendahl *et al.* 2007), as the abundances for all the foraminifera specimens remains low. Evidence from SMONE and the BOS-layers suggests a significant level of occupation by early modern humans inside the cave (Brenner & Wurz 2019). When SMONE was deposited, during MIS 5c, KRM was used as a long-term residential site and high densities of shellfish indicate intensive foraging of

rocky shores. In BOS-Three, shellfish densities are lower, and lithic densities higher, suggesting higher mobility and shorter-term visits to the cave. During this period the increased diversity in shellfish and species occurring in sandy environments, indicates that the environment changed (Brenner *et al*. 2020).

BOS-Three has the highest absolute abundance (Figure 5.14) of all the layers (n= 57 spec/g sed >150µm) and also contains a higher number of taxa than the other layers (nine out of ten taxa are present). *Spirillina vivipara*, the identifiable foraminifera taxon with the most individuals counted in the KRM sequence (in BOS-Two and BOS-Three), did not occur in BOS-One or SMONE. BOS-Three has a greater variety of taxa present compared to the other layers, as every foraminifera taxon, other than *Lagena* sp. was identified in this layer. This likely indicates a less intensive occupation of the site, as the abundances of foraminiferal specimens are higher.

In BOS-One, the unidentifiable foraminifera have the highest relative abundance and absolute abundance (Figure 5.14; Figure 5.15), possibly suggesting that these specimens were more subjected to erosion or dissolution. The other taxonomic identifications for the foraminifera are uncertain in BOS-One, with only two taxa having certain identifications (*Cribroelphidium articulatum* and *Ammonia japonica*). This is likely due to extensive transport by wind, or due to damage caused by the digestive tracts of fish that were hunted and brought into the cave. There have been reports from elsewhere in the world where foraminiferal tests have been transported by the wind (for example, Goudie & Sperling 1977).

The foraminiferal assemblage at KRM therefore likely primarily accumulated as a result of the cultural activities (shellfish foraging or fish hunting) of early inhabitants of the cave. It is possible that humans activities were not the only contributors to the foraminiferal assemblage, as animal remains (such as seagulls, discussed by von den Driesch 2004) were also found in the cave and are known to consume various types of marine life that the foraminifera could have adhered themselves to.

6.9 The palaeoenvironment during MIS 5c-d at KRM

At present, it is not possible to relate the changing conditions discussed in Chapter 2 straightforwardly to KRM, as KRM is too far away from BBC, Vankervelsvlei and PP (approximately 300 km), and KRM was likely subjected to different environmental conditions. The majority of the information available on MIS 5c-d in South Africa are for the period as a whole, making it difficult to interpret the various changes that could have influenced the site choices and subsistence strategies of early anatomically modern humans on the southern Cape coast during this period.

This is the first study in context of the South African Pleistocene to analyse ostracods and foraminifera in archaeological deposits. This study is in broad agreement with the data from the micromammal study conducted by Nel *et al*. (2018) discussed in Chapter 2. Nel *et al*. (2018) suggest that conditions during MSA II were likely moist and indicative of freshwater to slightly brackish water conditions, since both *Gomphocythere obtusata* and juvenile instars are present in high abundances in SMONE and the BOS-layers from Cave 1, albeit the abundances of the ostracods were generally lower in SMONE than in the other layers. SMONE has the lowest absolute abundance (n=1033) of ostracods and BOS-Three has the highest absolute abundance (n= 6595), thus suggesting that SMONE was possibly deposited during drier conditions than the BOS-layers. There is a slight decrease in the absolute abundance of ostracods from BOS-Three to BOS-Two (n=4473), likely suggesting that there was a brief period in which conditions were less moist. Another increase in the absolute abundances is noted from BOS-Two to BOS-One (n=6528). The MSA II Lower period as a whole contained more evidence of micromammals that are linked to moist grasses or waterlogged environments, likely indicative of small lakes, reed-beds and wetlands (also see Avery 1987; Nel *et al*. 2018). At PP the period between 102 ka –91 ka also likely had moist conditions and relatively open habitats (Rector & Reed 2010; Carr *et al*. 2016). As mentioned above, these trends cannot be straightforwardly related to the KRM conditions due to the differences in resolution.

During MIS 5c, Langejans *et al.* (2017) suggest that a rocky shore was present as well as a high degree of occupation at KRM, whereas MIS 5d was noted as having a sandy

shore and less occupation (also see Brenner *et al.* 2020). Due to decreased occupation of KRM by early modern humans during MIS 5d, it is possible that there were less anthropogenic disturbances that enabled the ostracods to become more abundant in the cave, or, that conditions were moist and thus made the cave more favourable for the ostracods to live in due to drip water. The lowest concentration of ostracods did occur in SMONE (MIS 5c), which would be consistent with the site being used for more residential purposes by early modern humans (see Brenner *et al*. 2020).

As discussed in Chapter 2, low stable carbon isotope values from speleothem material (less than -7.5‰) were recorded for MIS 5 at PP, which indicates that C3 plants were the dominant type of vegetation (Braun *et al*. 2019). The low stable carbon isotope values reported at PP are broadly consistent to the stable carbon isotope data from KRM.

6.10 Limitations to study and future analysis

Initially, the purpose of the study was to analyse the foraminifera that were previously identified in the KRM sediments micromorphological slides by Susan Mentzer (Mentzer *et al*. 2015). Ostracods were only later identified in the washed sediment by Prof. Carin Andersson. The initial study was therefore aimed at extracting the foraminifera from the KRM sediment, not the ostracods, and sieve sizes that are standard in foraminiferal analysis were therefore used. Although the sieve sizes did end up being a good compromise for both microfossil groups, future studies will aim at improving this resolution by washing samples of foraminifera and ostracods separately. In future studies an attempt will be made to count a minimum of 300 foraminiferal specimens, as splits in this study were counted until reaching a minimum of 300 ostracods, as the ostracods were more abundant and also *in situ,* thus making it easier to gather environmental data from them. The foraminifera will still not be used in stable isotope analysis, as they are not *in situ* in the KRM sediments. However, if the sample sizes are increased, then more information can perhaps be obtained on the origin of the foraminifera in the sediment. Furthermore, sample sizes used for stable isotope analysis were too small, so future studies will include more samples for stable isotope analysis. In order to use the palaeotemperature equation suggested by Kim & O'Neil (1997) future studies should aim to determine the $\delta\,^{18}O$ of

water sources inside and around the caves. In context of the ostracod analysis, future studies will benefit from a modern analogue method from the KRM area.

6.11 Conclusion

Absolute abundance data from the ostracods at KRM suggests that ostracods were more abundant per gram of sediment in BOS-Three than in the other layers from KRM. Layer SMONE has the lowest absolute abundance, perhaps indicating conditions that were less moist or favourable for the ostracods to live in than during the deposition of the BOS-layers. This trend also corresponds with occupational intensity at the site, as SMONE had a higher rate of occupation than the BOS-layers. Relative abundance data show that *Gomphocythere obtusata* and juvenile instars are the most dominant in all the layers, with little variation between layers. *Gomphocythere obtusata* is the dominant taxon in the KRM assemblage and is usually indicative of freshwater to slightly saline (brackish water) conditions, supporting the notion of an estuary near the caves, especially in relation to BOS-Three (von den Driesch 2004).

The foraminiferal specimens from KRM are not *in situ* and have likely been recalcified. Their limited interpretation suggests that they were likely introduced to the cave by strong coastal winds or by being attached to shellfish (or inside of the digestive tract of fish) that were brought into the cave by foraging humans and animals. Foraminiferal specimens such as *Ammonia beccarii,* and *Elphidium* sp. that were identified in the KRM samples usually are indicative of marginal marine environments and shallow waters, but prefer living in tidal estuaries with reduced salinity (Murray 1991). The taxon with the highest absolute abundance, *Spirillina vivipara,* has been reported on stable substrates and can tolerate a wide salinity range (Murray 1991).

The hypothesis in Chapter 1 stated that “There are differences in the ostracod and foraminifera fauna in the sediment of layers SMONE (MIS 5c) and BOS One, Two and Three (MIS 5d) from Cave 1 at KRM, indicating fluctuations in the environment and depositional processes”. This hypothesis is largely proven to be true, as there are differences in ostracod and foraminifera fauna in the sediment, albeit smaller for the ostracods than the foraminifera. However, although the ostracods have less taxa present, the interactions between various taxa as suggested by abundance data do provide

important environmental information. SMONE is related to intensive human occupation during a period when rocky shores occurred close to the cave. BOS-One has the highest relative abundance of unidentifiable foraminifera compared to the other layers, likely indicating an environment that was more conductive of foraminiferal test erosion, perhaps indicating a period of abandonment, exposure and erosion. BOS-Three has the largest sample size and also contains the highest absolute abundances of *G. obtusata*. The greatest total absolute abundance of foraminiferal taxa is also present in BOS-Three. The high abundance of ostracods that can withstand fresh- and brackish waters likely supports the presence of an estuarine environment and exploitation of estuarine fish. The data presented here confirms the hypothesis presented in Chapter 1 and indicates that paleoenvironments in MIS 5c and 5d at KRM were different.

References

Alve, E. 1999. Colonization of new habitats by benthic foraminifera: a review. *Earth-Science Reviews* 46 (1-4): 167-185.

Avery, D.M. 1987. Late Pleistocene coastal environment of the southern Cape Province of South Africa: micromammals from Klasies River Mouth. *Journal of Archaeological Science* 14 (4): 405 - 421.

Badenhorst, S., Van Niekerk, K.L. & Henshilwood, C.S. 2016. Large mammal remains from the 100 ka middle stone age layers of Blombos cave, South Africa. *The South African Archaeological Bulletin* 71 (203): 46-52.

Bar-Matthews, M., Marean, C.W., Jacobs, Z., Karkanas, P., Fisher, E.C., Herries, A.I., Brown, K., Williams, H.M., Bernatchez, J., Ayalon, A., & Nilssen, P.J. 2010. A high resolution and continuous isotopic speleothem record of paleoclimate and paleoenvironment from 90 to 53 ka from Pinnacle Point on the south coast of South Africa. *Quaternary Science Reviews* 29 (17-18): 2131-2145.

Bate, R.H. & East, B.A. 1972. The structure of the ostracode carapace. *Lethaia* 5(2) 177-194.

Bé, A.W. 1959. A method for rapid sorting of foraminifera from marine plankton samples. *Journal of Paleontology* 33 (5): 846-848.

Bé, A.W.H., Spero, H.J. & Anderson, O.R. 1982. Effects of symbiont elimination and reinfection on the life processes of the planktonic foraminifer Globigerinoides sacculifer. *Marine Biology* 70 (1): 73-86.

Bergh, E.W. & Compton, J.S. 2020. Quaternary foraminifera and mollusc assemblages on the southwestern African shelf. *Palaeontologia Electronica* 23 (2): 1-28.

Boomer, I., Horne, D.J. & Slipper, I.J. 2003. The use of ostracods in palaeoenvironmental studies, or what can you do with an ostracod shell? *The Paleontological Society Papers* 9: 153-180.

BouDagher-Fadel, M.K. 2015. *Biostratigraphic and Geological Significance of Planktonic Foraminifera.* London: UCL Press.

BouDagher-Fadel, M.K. 2018. *Evolution and geological significance of larger benthic foraminifera*. London: UCL Press.

Bowen, G. 2019. Waterisotopes.org. University of Utah. Accessible at: https://wateriso.utah.edu/waterisotopes/pages/data_access/form.html Accessed on: “17/03/2021”.

Braun, K., Bar-Matthews, M., Matthews, A., Ayalon, A., Cowling, R.M., Karkanas, P., Fisher, E.C., Dyez, K., Zilberman, T. & Marean, C.W. 2019. Late Pleistocene records of speleothem stable isotopic compositions from Pinnacle Point on the South African south coast. *Quaternary Research* 91 (1): 265-288.

Brenner, M.J., Ryano, K.P. & Wurz, S. 2020. Coastal adaptation at Klasies River main site during MIS 5c-d (93,000–110,000 years ago) from a southern Cape perspective. *The Journal of Island and Coastal Archaeology:* 1-28.

Brenner, M.J., & Wurz, S. 2019. A high-resolution perspective on MIS 5c-d lithic assemblages from Klasies River main site Cave 1. *Journal of Archaeological Science*: *Reports* 26: 1-33.

Bristow, C.S., Holmes, J.A., Mattey, D., Salzmann, U. & Sloane, H.J. 2018. A late Holocene palaeoenvironmental ‘snapshot’of the Angamma Delta, Lake Megachad at the end of the African Humid Period. *Quaternary Science Reviews* 202: 182-196.

Börner, N., De Baere, B., Yang, Q., Jochum, K.P., Frenzel, P., Andreae, M.O. & Schwalb, A. 2013. Ostracod shell chemistry as proxy for paleoenvironmental change. *Quaternary International* 313: 17-37.

Caporaletti, M. 2011. Ostracods and stable isotopes: proxies for palaeoenvironmental reconstructions. *Joannea--Geologie und Palaontologie* 11 :345-359.

Carr, A.S., Chase, B.M. & Mackay, A. 2016. Mid to Late Quaternary landscape and environmental dynamics in the Middle Stone Age of southern South Africa. In: Jones, S.C. & Stewart, B.A. (eds) *Africa from MIS 6-2*: 23-47. Dordrecht: Springer.

Cawthra, H.C., Jacobs, Z., Compton, J.S., Fisher, E.C., Karkanas, P. & Marean, C.W. 2018. Depositional and sea-level history from MIS 6 (Termination II) to MIS 3 on the southern continental shelf of South Africa. *Quaternary Science Reviews* 181: 156-172.

Clopper, C.J. and Pearson, E.S., 1934. The use of confidence or fiducial limits illustrated in the case of the binomial. *Biometrika* 26 (4) : 404-413.

Compton, J.S. 2011. Pleistocene sea-level fluctuations and human evolution on the southern coastal plain of South Africa. *Quaternary Science Reviews* 30 (5-6): 506-527.

Compton, J.S. 2016. *Human Origins: How Diet, Climate and Landscape Shaped Us*. Cape Town: Earthspun Books.

Coplen, T.B. 1994. Reporting of stable hydrogen, carbon, and oxygen isotopic abundances (technical report). *Pure and applied chemistry* 66(2): 273-276.

Creative Commons Attribution 3.0 (link is external) Australia license OzCoasts (Geoscience Australia) .2012. Available at: https://www.e-education.psu.edu/earth107/node/1026 Accessed: 01/03/2020.

Danielopol, D.L. & Vespremeanu, E.E. 1964. The presence of ostracods on floating fen soil in Romania. *Fragm Balc* 5: 29–36.

Danielopol, D.L., Ito, E., Wansard, G., Kamiya, T., Cronin, T.M. & Baltanás, A. 2002. Techniques for collection and study of Ostracoda. *Geophysical Monograph-American Geophysical Union* 131: 65-98.

de Deckker, P. 1981. Ostracoda from Australian inland waters–notes on taxonomy and ecology. *Proceedings of the Royal Society of Victoria* 93(1): 43-85.

Deacon, H.J. & Geleijnse, V.B. 1988. The stratigraphy and sedimentology of the main site sequence, Klasies River, South Africa. *The South African Archaeological Bulletin* 43: 5-14.

Deacon, H.J. & Wurz, S. 2005. A Late Pleistocene archive of life at the coast, Klasies River. In: Stahl, A.B. (ed) *African Archaeology: A Critical Introduction:* 130-149. Oxford: Blackwell Publishing.

d'Errico, F. & Henshilwood, C.S. 2007. Additional evidence for bone technology in the

southern African Middle Stone Age. *Journal of Human Evolution* 52(2): 142-163.

Dingle, R.V. & Rogers, J. 1972. Pleistocene palaeogeography of the Agulhas Bank. *Transactions of the Royal Society of South Africa* 40(3): 155-165.

Dodd, J.R. & Stanton, R.J. 1990. *Paleoecology: Concepts and Applications*. New York: John Wiley & Sons.

Dor, G. 2017. Using GIS to model the changing land-ocean interface for the southern coast of South Africa associated with the fluctuations in sea level through an important period of human occupation between 190-40ka. Unpublished honours research project. University of the Witwatersrand, Johannesburg.

Dreher, C.A. & Flocks, J.G. 2011. *Methods for Processing and Imaging Marsh Foraminifera* (No. 2011-3098). US Geological Survey.

Dryden Jr, A.L. 1931. Accuracy in percentage representation of heavy mineral frequencies. *Proceedings of the National Academy of Sciences of the United States of America* 17(5): 233-238.

Eggins, S. M., Grün, R., McCulloch, M.T., Pike, A.W.G., Chappell, J., Kinsley, L., Mortimer, G., Shelley, M., Murray-Wallace, C.V., Spötl, C. & Taylor, L. 2005. In situ U-series dating by laser-ablation multi-collector ICPMS: new prospects for Quaternary geochronology. *Quaternary Science Reviews* 24(23): 2523–2538.

Esteban, I., Marean, C.W., Cowling, R.M., Fisher, E.C., Cabanes, D. & Albert, R.M. 2020. Palaeoenvironments and plant availability during MIS 6 to MIS 3 on the edge of the Palaeo-Agulhas Plain (south coast, South Africa) as indicated by phytolith analysis at Pinnacle Point. *Quaternary Science Reviews* (235): 1-15.

Finnegan, S. & Droser, M.L. 2005. Relative and absolute abundance of trilobites and rhynchonelliform brachiopods across the Lower/Middle Ordovician boundary, eastern Basin and Range. *Paleobiology* 31(3): 480-502.

Fisher, E.C., Bar-Matthews, M., Jerardino, A. & Marean, C.W. 2010. Middle and Late Pleistocene paleoscape modeling along the southern coast of South Africa. *Quaternary Science Reviews* 29(11-12): 1382-1398.

Franceschini, G., Mc Millan, I.K. & Compton, J.S. 2005. Foraminifera of Langebaan Lagoon salt marsh and their application to the interpretation of late Pleistocene depositional environments at Monwabisi, False Bay coast, South Africa. *South African Journal of Geology* 108(2): 285-296.

Frenzel, P. & Boomer, I. 2005. The use of ostracods from marginal marine, brackish waters as bioindicators of modern and Quaternary environmental change. *Palaeogeography, Palaeoclimatology, Palaeoecology* 225(1-4): 68-92.

Fürstenberg, S., Gründler, N., Meschner, S. & Frenzel, P. 2017. Microfossils in surface sediments of brackish waters on the west coast of South Africa and their palaeoecological implications. *African Journal of Aquatic Science* 42(4): 329-339.

Goudie, A.S. & Sperling, C.H.B. 1977. Long distance transport of foraminiferal tests by wind in the Thar Desert, northwest India. *Journal of Sedimentary Research* 47(2): 630-633.

Griffiths, H.I. & Holmes, J.A. 2000. Non-marine ostracods and Quaternary palaeoenvironments. *Technical Guide 8* London: Quaternary Research Association.

Grine, F.E., Henshilwood, C.S. & Sealy, J.C. 2000. Human remains from Blombos Cave, South Africa:(1997–1998 excavations). *Journal of Human Evolution* 38(6): 755-765.

Grine, F.E., Wurz, S. & Marean, C.W. 2017. The middle stone age human fossil record from Klasies River Main site. *Journal of Human Evolution* 103: 53-78.

Grobbelaar, J.U. 2009. Turbidity. In: Likens, G.E (ed) *Encyclopedia of Inland Waters:* 699-704. Oxford: Academic Press.

Hammer, Ø., Harper, D.A.T., & Ryan, P.D. 2001. PAST: paleontological statistics software package for education and data analysis. *Palaeontol. Electron* (4) 1–9.

Hammes, F., Velten, S., Egli, T. & Juhna, T. 2011. Biotreatment of drinking water. In: Moo-Young, M. (ed) *Comprehensive Biotechnology*: 517-530. Amsterdam: Elsevier.

Hanai, T., Ikeya, N. & Ishizaki, K. 1988. Evolutionary biology of Ostracoda: its fundamentals and applications: proceedings of the Ninth International Symposium on Ostracoda, held in Shizuoka, Japan, 29 July-2 August 1985. Elsevier Science &

Technology.

Haunold, T.G., Baal, C. & Piller, W.E. 1997. Benthic foraminiferal associations in the northern Bay of Safaga, Red Sea, Egypt. *Marine Micropaleontology* 29(3-4): 185-210.

Hemleben, C. & Kaminski, M.A. 1990. Agglutinated foraminifera: an introduction. In: Hemleben, C., Kaminski, M.A., Kuhnt, W., & Scott, DB. (eds) *Paleoecology, biostratigraphy, paleoceanography and taxonomy of agglutinated foraminifera*. Dordrecht: Springer.

Henshilwood, C.S., d'Errico, F., van Niekerk, K.L., Coquinot, Y., Jacobs, Z., Lauritzen, S.E., Menu, M. & García-Moreno, R. 2011. A 100,000-year-old ochre-processing workshop at Blombos Cave, South Africa. *Science* 334(6053): 219-222.

Henshilwood, C.S., d'Errico, F. & Watts, I. 2009. Engraved ochres from the middle stone age levels at Blombos Cave, South Africa. *Journal of Human Evolution* 57(1): 27-47.

Holmes, J.A. 1992. Nonmarine ostracods as Quaternary palaeoenvironmental indicators. *Progress in Physical Geography* 16(4): 405-431.

Holmes, J.A. 1996. Trace-element and stable-isotope geochemistry of non-marine ostracod shells in Quaternary palaeoenvironmental reconstruction. *Journal of Paleolimnology* 15(3) 223-235.

Holmes, J.A. & de Deckker, P. 2012. The chemical composition of ostracod shells: applications in Quaternary palaeoclimatology. In: Horne, D.J., Holmes, J., Rodriguez-Lazaro, J. & Viehberg, F. (eds) *Ostracoda as Proxies for Quaternary Climate Change, Developments in Quaternary Sciences* 17: 131-144. Amsterdam: Elsevier.

Hong, Y., Kummerow, C.D. & Olson, W.S. 1999. Separation of convective and stratiform precipitation using microwave brightness temperature. *Journal of Applied Meteorology* 38(8): 1195-1213.

Horne, D.J. & Siveter, D.J. 2016. Collecting and processing fossil ostracods. *Journal of Crustacean Biology* 36(6): 841-848.

Hutton, J. 1795. *Theory of the Earth: With Proofs and Illustrations (1).* Library of Alexandria.

IAEA/WMO. 2021. Global Network of Isotopes in Precipitation. The GNIP Database. Accessible at: http://www.iaea.org/water Accessed on: “17/03/2021”.

Jacobs, Z., Jones, B.G., Cawthra, H.C., Henshilwood, C.S. & Roberts, R.G. 2020. The chronological, sedimentary and environmental context for the archaeological deposits at Blombos Cave, South Africa. *Quaternary Science Reviews* 235: 1-22.

Jerardino, A. & Marean, C.W. 2010. Shellfish gathering, marine paleoecology and modern human behavior: perspectives from cave PP13B, Pinnacle Point, South Africa. *Journal of Human Evolution* 59(3-4): 412-424.

Jin, Z., Bickle, M., Chapman, H., Yu, J., Greaves, M., Wang, S. & Chen, S. 2006. An experimental evaluation of cleaning methods for fossil ostracod Mg/Ca and Sr/Ca determination. *Journal of Paleolimnology* 36(2) 211-218.

Jocque, M., Martens, K., Riddoch, B. & Brendonck, L. 2006. Faunistics of ephemeral rock pools in southeastern Botswana. *Archiv für Hydrobiologie* 165: 415–431.

Jones, R.W. 2013. *Foraminifera and their Applications*. Cambridge: Cambridge University Press.

Karanovic, I. 2011. On the recent Cyclocypridinae (Podocopida, Candonidae) with description of two new genera and one new species. *Zootaxa* 2820(1): 1-61.

Karanovic, I. 2012. *Recent Freshwater Ostracods of the World: Crustacea, Ostracoda, Podocopida.* Heidelberg: Springer.

Katz, M.E., Cramer, B.S., Franzese, A., Hönisch, B., Miller, K.G., Rosenthal, Y. & Wright, J.D. 2010. Traditional and emerging geochemical proxies in foraminifera. *The Journal of Foraminiferal Research* 40(2): 165-192.

Kesling, R.V. 1951. *The Morphology of Ostracod Molt Stages (Vol. 21, No. 1-3)*. Urbana: University of Illinois Press.

Kim, S.T. & O'Neil, J.R. 1997. Equilibrium and nonequilibrium oxygen isotope effects in synthetic carbonates. *Geochimica et Cosmochimica Acta* 61(16): 3461-3475.

Klein, R.G. 1976. The mammalian fauna of the Klasies River mouth sites, southern Cape Province, South Africa. *South African Archaeological Bulletin* 31(123): 75-98.

Langejans, G.H., Dusseldorp, G.L. & Thackeray, J.F. 2017. Pleistocene molluscs from Klasies River (South Africa): Reconstructing the local coastal environment. *Quaternary International* 427: 59-84.

Langejans, G.H., van Niekerk, K.L., Dusseldorp, G.L. & Thackeray, J.F. 2012. Middle Stone Age shellfish exploitation: Potential indications for mass collecting and resource intensification at Blombos Cave and Klasies River, South Africa. *Quaternary International* 270: 80-94.

Lap, A. 2020. Bones for thought: a taphonomic study of the faunal remains from the BOS layers at Klasies River main site. Unpublished MSc study. Johannesburg: University of the Witwatersrand.

Larbey, C., Mentzer, S.M., Ligouis, B., Wurz, S. & Jones, M.K. 2019. Cooked starchy food in hearths ca. 120 kya and 65 kya (MIS 5e and MIS 4) from Klasies River Cave, South Africa. *Journal of Human Evolution* 131: 210-227.

Lawrence, J.R., Scharf, B., Packroff, G. & Neu, T.R. 2002. Microscale evaluation of the effects of grazing by invertebrates with contrasting feeding modes on river biofilm architecture and composition. *Microbial Ecology 44*(3): 199-207.

Leng, M.J. & Marshall, J.D. 2004. Palaeoclimate interpretation of stable isotope data from lake sediment archives. *Quaternary Science Reviews* 23(7-8): 811-831.

Lipps, J.H. 1988. Predation on foraminifera by coral reef fish; taphonomic and evolutionary implications. *Palaios* 3(3): 315-326.

Loftus, E., Sealy, J.C., Leng, M.J. & Lee-Thorp, J.A. 2017. A late Quaternary record of seasonal sea surface temperatures off southern Africa. *Quaternary Science Reviews* 171: 73-84.

Lopez, L.C.S., Filizola, B., Deiss, I. & Rios, R.I. 2005. Phoretic behaviour of bromeliad annelids (Dero) and ostracods (Elpidium) using frogs and lizards as dispersal vectors. *Hydrobiologia* 549(1): 15-22.

López-González, F., Grandal-d'Anglade, A. & Vidal-Romaní, J.R. 2006. Deciphering bone depositional sequences in caves through the study of manganese coatings. *Journal of Archaeological Science* 33(5): 707–717.

Lord, A.R., Boomer, I., Brouwers, E. & Whittaker, J.E. 2012. Ostracod taxa as palaeoclimate indicators in the Quaternary. In: Horne, D.J., Holmes, J.A., Rodriguez Lazaro, J. & Viehberg, F. (eds), *Ostracoda as Proxies for Quaternary Climate Change, Developments in Quaternary Science* 17: 37-45. Amsterdam: Elsevier.

Lutjeharms, J.R.E., Monteiro, P.M., Tyson, P.D. and Obura, D., 2001. The oceans around southern Africa and regional effects of global change: START Regional Syntheses. *South African Journal of Science* 97(3): 119-130.

Marean, C.W. 2010. Pinnacle Point Cave 13B (Western Cape Province, South Africa) in context: the Cape floral kingdom, shellfish, and modern human origins. *Journal of Human Evolution* 59(3-4): 425-443.

Maringa, M. 2020. A palaeoecological and taphonomic analysis of the micromammals from a Marine Isotope Stage 5 layer at Klasies River, southern Cape, South Africa. Unpublished MSc study. Johannesburg: University of the Witwatersrand.

Martens, K. 1994. Ostracod speciation in ancient lakes: a review. *Ergebnisse der Limnologie* (44)203-203.

Martens, K. 1998. General morphology of non-marine ostracods. Sex and Parthenogenesis. In: Martens, K. (ed) *Evolutionary Ecology of Reproductive Modes in Non-marine Ostracods*: 57-75. Leiden: Blackhuys Publishers.

Martens, K., Davies, B.R., Baxter, A.J. & Meadows, M.E. 1996. A contribution to the taxonomy and ecology of the Ostracoda (Crustacea) from Verlorenvlei (Western Cape, South Africa). *African Zoology* 31(1): 22-36.

Martens, K. & Savatenalinton, S., 2011. A subjective checklist of the Recent, free-living, non-marine Ostracoda (Crustacea). *Zootaxa* 2855 (1) 1-79.

Martinez, A., Hernández-Terrones, L., Rebolledo-Vieyra, M. & Paytan, A. 2018. Impact of carbonate saturation on large Caribbean benthic foraminifera assemblages. *Biogeosciences* 15(22): 6819-6832.

Matthews, T., Marean, C. & Nilssen, P. 2009. Micromammals from the Middle Stone Age (92–167 ka) at Cave PP13B, Pinnacle Point, south coast, South Africa. *Palaeontologia Africana* 44: 112-20.

Matthews, T., Rector, A., Jacobs, Z., Herries, A.I. & Marean, C.W. 2011. Environmental implications of micromammals accumulated close to the MIS 6 to MIS 5 transition at pinnacle Point cave 9 (Mossel Bay, Western Cape Province, South Africa). *Palaeogeography, Palaeoclimatology, Palaeoecology* 302 (3-4): 213-229.

Mazzini, I., Goiran, J.P. & Carbonel, P. 2015. Ostracodological studies in archaeological settings: a review. *Journal of Archaeological Science* 54: 325-328.

McCord, M.E. & Lamberth, S.J. 2009. Catching and tracking the world's largest Zambezi (bull) shark Carcharhinus leucas in the Breede Estuary, South Africa: the first 43 hours. *African Journal of Marine Science* 31(1): 107-111.

Meadows, M.E., Baxter, A.J. & Parkington, J. 1996. Late Holocene environments at Verlorenvlei, Western Cape Province, South Africa. *Quaternary International* 33: 81-95.

Mentzer, S.M., Miller, C.E. & Wurz, S. 2015. 'Middle Stone Age combustion features at Klasies River Main Site, South Africa.' (PowerPoint Presentation). European Society for the Study of Human Evolution Conference. Available at: https://www.researchgate.net/profile/Susan-Mentzer/publication/282731135_Middle_Stone_Age_combustion_features_at_Klasies_River_Main_Site_South_Africa/links/561a3eb108ae78721f9f61b1/Middle-Stone-Age-combustion-features-at-Klasies-River-Main-Site-South-Africa.pdf. Accessed: "15/03/2021".

Mesquita-Joanes, F., Smith, A.J. & Viehberg, F.A. 2012. The ecology of Ostracoda across levels of biological organisation from individual to ecosystem: a review of recent developments and future potential. In: Horne, D.J., Holmes, J., Rodriguez-Lazaro, J. &

Viehberg, F. A. (eds) *Ostracoda as Proxies for Quaternary Climate Change* 15–35. Amsterdam: Elsevier.

Mezquita, F., Roca, J.R. & Wansard, G. 1999. Moulting, survival and calcification: the effects of temperature and water chemistry on an ostracod crustacean (*Herpetocypris intermedia*) under experimental conditions. *Archiv für Hydrobiologie* 146(2): 219.

Mills, H., Kirby, J., Holgate, S. & Plater, A. 2013. The distribution of contemporary saltmarsh foraminifera in a macrotidal estuary: an assessment of their viability for sea-level studies. *Journal of Ecosystem and Ecography* (3) 1-16.

Morley, M.S. & Hayward, B.W. 2012. Ostracoda of the Hauraki Gulf, New Zealand. *Records of the Auckland Museum*: 51-75.

Mucina, L. & Rutherford, M.C. 2006. *The Vegetation of South Africa, Lesotho and Swaziland*. Pretoria: South African National Biodiversity Institute.

Murray, J.W. 1979: *British near shore Foraminiferids: Key and Notes for the identification of the Species*. London: Academic press.

Murray, J.W. 1991. *Ecology and Palaeoecology of Benthic Foraminifera*. London: Longman Scientific and Technical.

Murray, J.W. 2006. *Ecology and applications of benthic foraminifera*. Cambridge: Cambridge University Press.

Murray, J.W. 2013. Living benthic foraminifera: biogeographical distributions and the significance of rare morphospecies. *Journal of Micropalaeontology* 32(1): 1-58.

Neale, J.W. 1983. The Ostracoda and uniformitarianism. The later record: Recent, Pleistocene and Tertiary. *Proceedings of the Yorkshire Geological Society* 44(3) 305-326.

Nel, T.H., Wurz, S. & Henshilwood, C.S. 2018. Small mammals from marine isotope stage 5 at Klasies River, South Africa–reconstructing the local palaeoenvironment. *Quaternary International* 471:6-20.

Ohrel, R.L. & Register, K.M. 2006. *Volunteer estuary monitoring: a methods manual.* Ocean Conservancy.

Olempska, E., Horne, D.J. & Szaniawski, H. 2012. First record of preserved soft parts in a Palaeozoic podocopid (Metacopina) ostracod, Cytherellina submagna: phylogenetic implications. *Proceedings of the Royal Society B: Biological Sciences*, *279* (1728) 564-570.

Park, L.E. 1995. Assessing diversification patterns in an ancient tropical lake: Gomphocythere (Ostracoda) in Lake Tanganyika. PhD dissertation. Arizona: University of Arizona.

Patterson, R.T. & Fishbein, E. 1989. Re-examination of the statistical methods used to determine the number of point counts needed for micropaleontological quantitative research. *Journal of Paleontology* 63 (2): 245-248.

Peypouquet, J.P., Carbonel, P., Ducasse, O., Töulderer-Farmer, M. & Lété, C. 1988. Environmentally Cued Polymorphism of Ostracods A Theoretical and Practical Approach. A Contribution to Geology and to the Understanding of Ostracod Evolution. *Developments in Palaeontology and Stratigraphy* (11): 1003-1019.

Quick, L.J., Meadows, M.E., Bateman, M.D., Kirsten, K.L., Mäusbacher, R., Haberzettl, T. & Chase, B.M. 2016. Vegetation and climate dynamics during the last glacial period in the fynbos-afrotemperate forest ecotone, southern Cape, South Africa. *Quaternary International* 404: 136-149.

Rector, A.L., & Reed, K.E. 2010. Middle and Late Pleistocene fauna of Pinnacle Point and their paleoecological implications. *Journal of Human Evolution* 59: 340–357.

Resig, J. M. 1974. Recent foraminifera from a landlocked Hawaiian lake. *Journal of Foraminiferal Research* 4: 69–76.

Reynard, J.P. & Wurz, S. 2020. The palaeoecology of Klasies River, South Africa: An analysis of the large mammal remains from the 1984–1995 excavations of Cave 1 and 1A. *Quaternary Science Reviews* 237: 1-17.

Roberts, D.L., Bateman, M.D., Murray-Wallace, C.V., Carr, A.S. & Holmes, P.J. 2008. Last interglacial fossil elephant trackways dated by OSL/AAR in coastal aeolianites, Still Bay, South Africa*. Palaeogeography, Palaeoclimatology, Palaeoecology*, 257 (3): 261-279.

Roberts, P., Henshilwood, C.S., van Niekerk, K.L., Keene, P., Gledhill, A., Reynard, J., Badenhorst, S. & Lee-Thorp, J. 2016. Climate, environment and early human innovation: stable isotope and faunal proxy evidence from archaeological sites (98-59ka) in the southern Cape, South Africa. *PLoS One* 11(7): 1-20.

Rosendahl, D., Ulm, S. & Weisler, M.I. 2007. Using foraminifera to distinguish between natural and cultural shell deposits in coastal eastern Australia. *Journal of Archaeological Science* 34(10): 1584-1593.

Ruiz, F., Abad, M., Bodergat, A.M., Carbonel, P., Rodríguez-Lázaro, J., González-Regalado, M.L., Toscano, A., García, E.X. & Prenda, J. 2013. Freshwater ostracods as environmental tracers. *International Journal of Environmental Science and Technology* 10(5): 1115-1128.

Ruiz-Agudo, E., Mees, F., Jacobs, P. & Rodriguez-Navarro, C. 2007. The role of saline solution properties on porous limestone salt weathering by magnesium and sodium sulfates. *Environmental Geology* 52(2): 269-281.

Schönfeld, J. 2012. History and development of methods in recent benthic foraminiferal studies. *Journal of Micropalaeontology* 31(1): 53–72.

Scott, G.H. 1963. Uniformitarianism, the uniformity of nature, and paleoecology. *New Zealand Journal of Geology and Geophysics* 6(4): 510-527.

Sen Gupta, B.K. 1999. Foraminifera in marginal marine environments. In: Sen Gupta, B.K. (ed) *Modern Foraminifera:* 141-160. London: Kluwer Academic Publishers.

Shearn, R., Halse, S., Koenders, A., Schön, I. & Martens, K. 2014. Redescriptions of six species of Ilyodromus Sars, 1894 (Crustacea, Ostracoda, Cyprididae) from New Zealand and Eastern Australia. *Zootaxa* 3878 (2): 101-145.

Simpson, G.L. 2012. Analogue methods in palaeolimnology. In: Last, W.M. & Smol, J.P. (eds)*Tracking Environmental Change using Lake Sediments:* 495-522. Dordrecht: Springer.

Simpson, K. 2003. Foraminiferal species distributions and sedimentological dynamics of the Knysna estuary, South Africa. Master's thesis. Cape Town: University of Cape Town.

Sinclair, S.A., Lane, S.B. & Grindley, J.R. 1986. Estuaries of the Cape: Part II: Synopses of available information on individual systems Rep. no. 32 Verlorenvlei (CW 13). In: Heydorn, A.E.F. & Morant, P.D. (eds) Stellenbosch: *CSIR Research Report:* 431.

Singer, R. & Wymer, J. 1982. *The Middle Stone Age at Klasies River Mouth in South Africa*. Chicago: University of Chicago Press.

Smith, R.K. 1987. Fossilization potential in modern shallow-water benthic foraminiferal assemblages. *The Journal of Foraminiferal Research* 17(2): 117-122.

Strachan, K.L. 2013. Application of intertidal salt-marsh foraminifera to reconstruct late Holocene sea-level change at Kariega Estuary, South Africa. Master's thesis. KwaZulu Natal: University of KwaZulu Natal.

Strachan, K.L. 2016. Intertidal salt-marsh foraminifera as sea-level indicators: lessons from the South African coastline. Doctoral dissertation. KwaZulu Natal: University of KwaZulu Natal.

Strachan, K.L., Finch, J.M., Hill, T. & Barnett, R.L. 2014. A late Holocene sea-level curve for the east coast of South Africa. *South African Journal of Science* 110(1-2): 1-9.

Strachan, K.L., Finch, J.M., Hill, T.R., Barnett, R.L., Morris, C.D. & Frenzel, P. 2016. Environmental controls on the distribution of salt-marsh foraminifera from the southern coastline of South Africa. *Journal of Biogeography* 43(5): 887-898.

Strachan, K.L., Hill, T.R., Finch, J.M. & Barnett, R.L. 2015. Vertical zonation of foraminifera assemblages in Galpins salt marsh, South Africa. *Journal of Foraminiferal Research* 45(1): 29-41.

Strachan, K.L., Hill, T.R., Finch, J.M., Barnett, R.L. & Frenzel, P. 2017. Distribution of salt-marsh foraminifera in two South African estuaries and the application as sea-level indicators. *Journal of Coastal Research* 33(3): 619-631.

Suchéras-Marx, B., Escarguel, G., Ferreira, J. & Hammer, Ø. 2019. Statistical confidence intervals for relative abundances and abundance-based ratios: Simple practical solutions for an old overlooked question. *Marine Micropaleontology* 151: 101751.

Tetard, M. & Marchant, R. 2020. Two new free-access dry splitter designs (1/2 to 1/32 aliquots) for sediment fractionation. *Marine Micropaleontology* 154: 101800.

Thackeray, J.F. 1988. Molluscan fauna from Klasies River, South Africa. *The South African Archaeological Bulletin* 43(147) 27-32.

Turpen, J.B. & Angell, R.W. 1971. Aspects of molting and calcification in the ostracod Heterocypris. *Biological Bulletin* 140(2): 331-338.

van Andel, T.H. 1989. Late Pleistocene sea levels and the human exploitation of the shore and shelf of southern South Africa. *Journal of Field Archaeology* 16: 133-155.

van Dijk, D.E. 2006. Anura from the late Pleistocene at Klasies River main site. *South Africa African Natural History* 2: 167-171.

van Pletzen, L. 2000. The large mammal fauna from Klasies River. Doctoral dissertation. Stellenbosch: Stellenbosch University.

van Pletzen-Vos, L., Brink, J., Reynard, J.P. & Wurz, S. 2019. Revisiting Klasies River. *The South African Archaeological Bulletin* 74(211): 127-137.

van Wijk, Y., Tusenius, M.L., Rust, R., Cowling, R.M. & Wurz, S. 2017. Modern vegetation at the Klasies River archaeological sites, Tsitsikamma coast, south-eastern Cape, South Africa: a reference collection. *Plant Ecology and Evolution* 150(1): 13-34.

Vermeij, G.J. & Herbert, G.S. 2004. Measuring relative abundance in fossil and living assemblages. *Paleobiology* 30(1): 1-4.

van Wijk, Y., Tusenius, M.L., Rust, R., Cowling, R.M. & Wurz, S. 2017. Modern vegetation at the Klasies River archaeological sites, Tsitsikamma coast, south-eastern Cape, South Africa: a reference collection. *Plant Ecology and Evolution* 150(1): 13-34.

Vinyard, G.1979. An ostracod (*Cypridopsis vidua*) can reduce predation from fish by resisting digestion. *The American Midland Naturalist Journal* 102:108-190.

von den Driesch, A. 2004. Middle Stone Age fish fauna from the Klasies River main site, South Africa. *Anthropozoologica* 39(2): 33–59.

Von Grafenstein, U., Erlernkeuser, H. & Trimborn, P. 1999. Oxygen and carbon isotopes in modern fresh-water ostracod valves: assessing vital offsets and autecological effects of interest for palaeoclimate studies. *Palaeogeography, Palaeoclimatology, Palaeoecology* 148(1-3): 133-152.

Wadley, L. 2015. Those marvellous millennia: The Middle Stone Age of southern Africa. Azania: *Archaeological Research in Africa* 50(2): 155-226.

Whatley, R.C. 1983. The application of Ostracoda to paleoenvironmental analysis. *Applications of Ostracoda*: 51-77.

White, T.S., Preece, R.C. & Whittaker, J.E. 2013. Molluscan and ostracod successions from Dierden's Pit, Swanscombe: insights into the fluvial history, sea-level record and human occupation of the Hoxnian Thames. *Quaternary Science Reviews* 70: 73-90.

Wurz, S. 2019. Human Evolution, archaeology and the South African stone age landscape during the last 100,000 years. In: Knight, J. & Rogerson, C.M. (eds) *The Geography of South Africa*: 125-132. Cham: Springer.

Wurz, S., Bentsen, S.E., Reynard, J., van Pletzen-Vos, L., Brenner, M., Mentzer, S., Pickering, R. & Green, H. 2018. Connections, culture and environments around 100 000 years ago at Klasies River main site. *Quaternary International* 495: 102-115.

Wurz, S.S.J.D. 2000. The Middle Stone Age at Klasies River, South Africa. Doctoral dissertation. Stellenbosch: Stellenbosch University.

Wurz, S. 2012. The significance of MIS 5 shell middens on the Cape coast: A lithic perspective from Klasies River and Ysterfontein 1. *Quaternary International* 270: 61-69.

Yasuhara, M., Tittensor, D.P., Hillebrand, H. & Worm, B. 2017. Combining marine macroecology and palaeoecology in understanding biodiversity: microfossils as a model. *Biological Reviews* 92(1): 199-215.

Yaalon, D.H. & Lomas, J. 1970. Factors controlling the supply and the chemical composition of aerosols in a near-shore and coastal environment. *Agricultural Meteorology* 7: 443-454.

Appendices

Appendix A

Section A.1

General description of ostracods

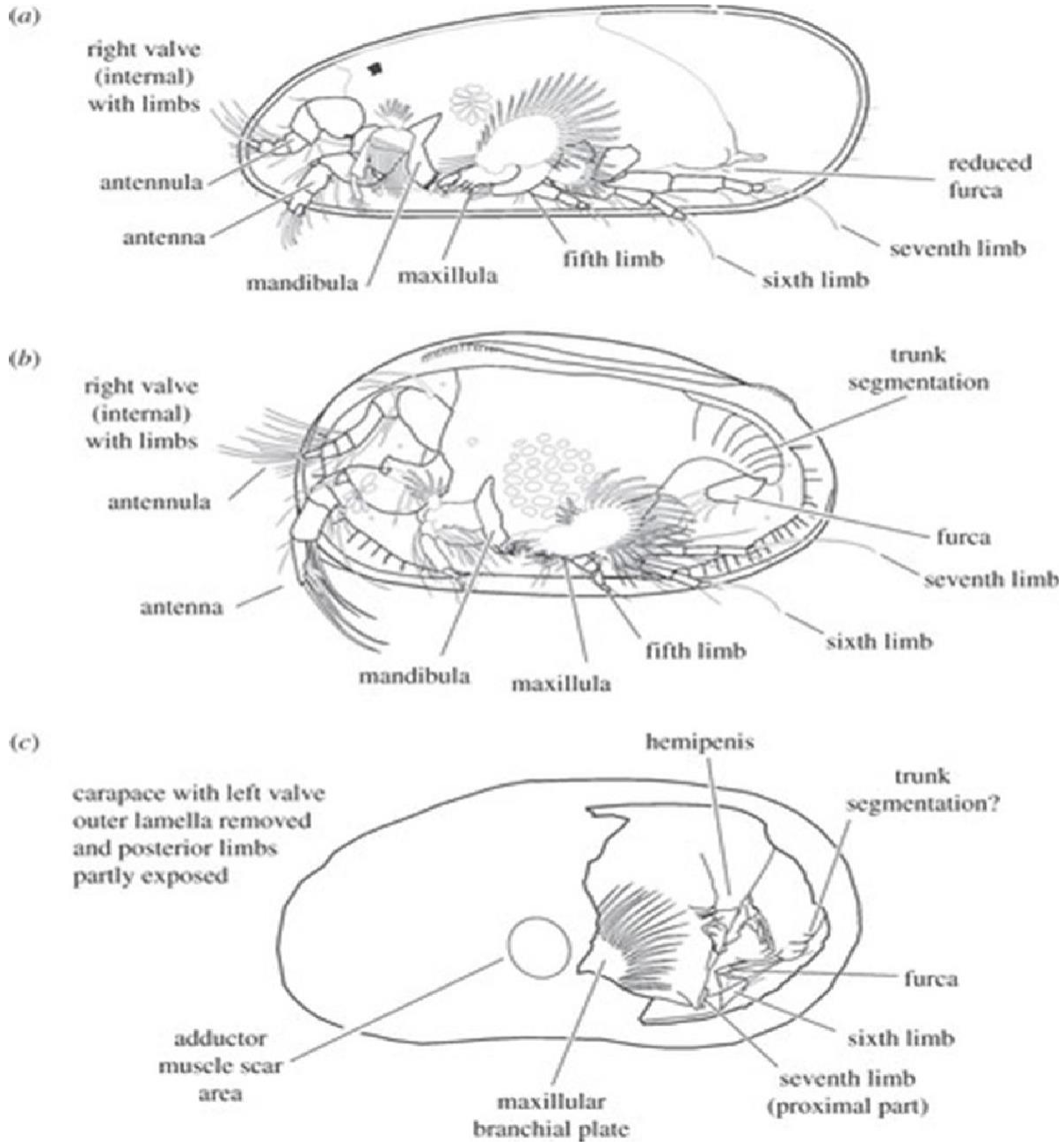


Figure A.1 Diagram of the comparative anatomy of ostracod specimens (Olempska *et al*. 2012: 568; Figure 3).

General description of foraminifera

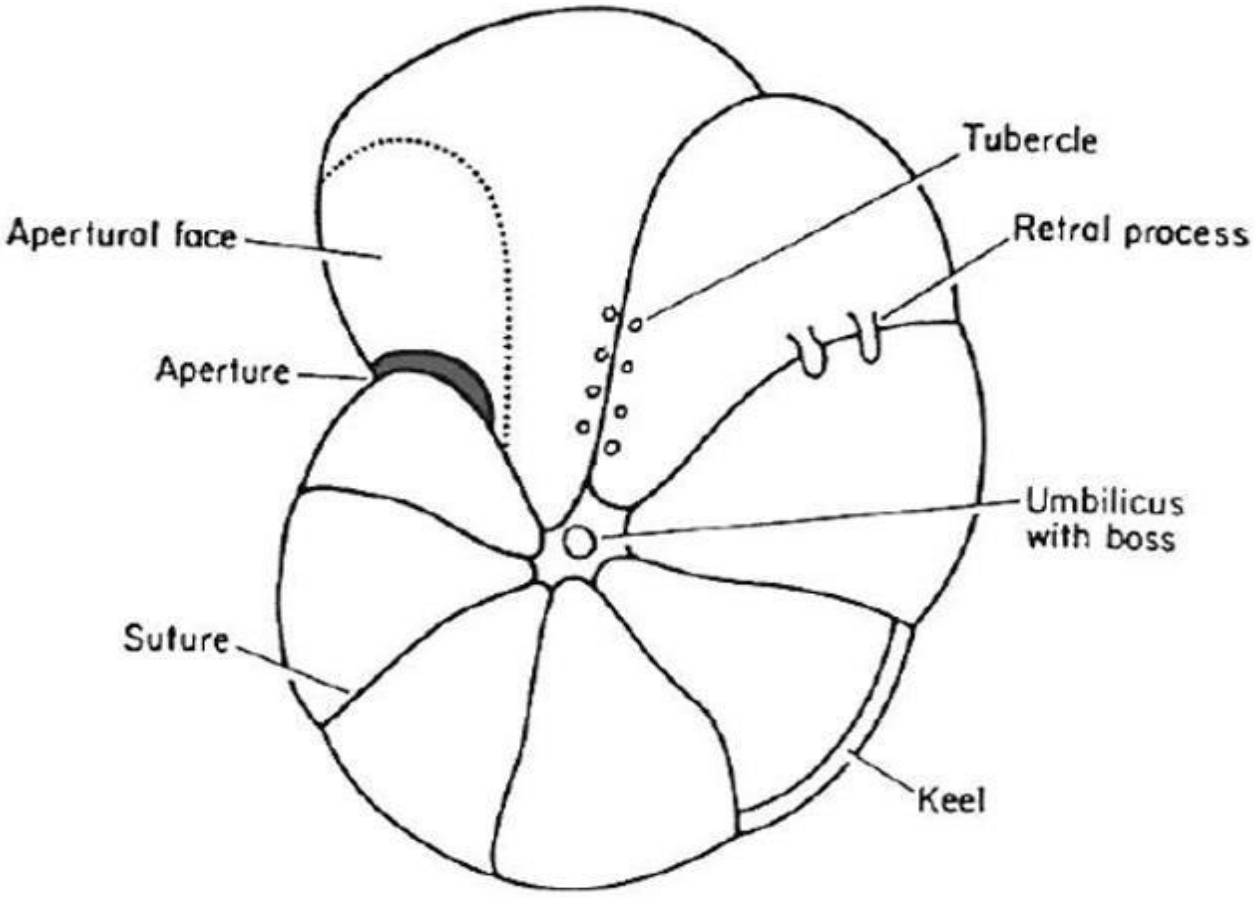


Figure A.2 The basic morphological features of a benthic foraminifera (after Murray 1979) (from Strachan 2013: 7).

Appendix B

Section B.1

Table B.1 MIS ages with their approximate start ages relevant to this study as defined by Wadley (2015:168).

Marine Isotope Stage	Approximate start date	Climate
MIS 4	73 ka	Cool
MIS 5a	84 ka	Warm
MIS 5b	93 ka	Cool
MIS 5c	106 ka	Warm
MIS 5d	115 ka	Cool
MIS 5e	130 ka	Warm (last interglacial period; Eemian).
MIS 6	188 ka	Cool with warm oscillations

Table B.2 Characteristics of ostracod growth stages (instars) as proposed by Kesling (1951:94-100).

Instar (Stage)	Characteristic features of live specimens:
1	• *Shell is well-rounded (weakly calcified). • Three pairs of appendages (antennules, antennae, mandibles). • Five setae, three are terminal.
2	• Occurs at first moulting of the valves. • *Shell is larger and thicker. • *Shell rim is simplistic. • Antennule is composed of four podomeres. • Antenna consists of three distinct podomeres.
3	• Antennules have the same number of podomeres; length of the natatory setae is increased. • Antenna has the same form.
4	• Antennule has five podomeres. • Antenna has a similar form to previous instar.
5	• *Shell has a more complex rim and a thicker structure. • Antennule has five podomeres; length of natatory setae is increased.
6	• All appendages are present. • There are six podomeres with well-developed natatory setae on the antennule. • Antenna has same number of podomeres as the previous instar.
7	• All appendages are well defined antenna are approaching definitive form, with the exception of the protopodite.
8	• Instar takes the likeness of the adult stage, with the exception of the specimen size. • Genital lobe is developed.
9 (Adult)	• Strong chitinous development of appendages. • Enlarged dorsal posterior portion of the valves. • *Greater valve thickness. • Complex rim structures.

*Visible in valves from “fossil” assemblages.

Appendix C

Section C.1 Raw data

Table C.1 Sediment sample context from KRM

SAMPLE	Weight of washed 150 µm fraction (g)	Split counted	Location processed:
C2/D2 SMONE (23/02/2015)	14	1/8	Norway
B1/B0 SMONE (20/02/2015)	10.1	1/8	Norway
A3 SMONE (20/02/2015)	23.15	1/ 2	Norway
B3 SMONE (19/02/2015)	7	1/ 4	Norway
B2 SMONE (19/02/2015)	6	1/ 4	Norway
B1 SMONE (20/02/2015)	7.1	1 (entire sample)	Norway
A2 SMONE (10/03/2015)	8	1/ 2	Norway
C1/C0; D1; D0 SMONE (19/02/2015)	14	1/ 2	Norway
TOTAL WEIGHT FOR LAYER	**89.35**		
C2 BOSONE (16/03/2015)	12	1/32	Norway
A2 BOSONE (16/03/2015)	11	1/ 4	Norway
A3 BOSONE (05/03/2015)	8.2	1/ 4	Norway
A1/A0 BOSONE (06/03/2015)	9.1	1 (entire sample)	Norway
B1 BOSONE (10/03/2015)	11	1/16	Norway
C3 BOSONE (16/03/2015)	11.3	8	Norway
C1 BOSONE (16/03/2015)	11	1/32	Norway
TOTAL FOR LAYER	**73.6**		
A3 BOSTWO (23/09/2016)	7	1/16	South Africa
C2 BOSTWO (21/09/2016)	10	1/16	South Africa
C1 BOSTWO (21/09/2016)	7	1/16	South Africa
B2 BOSTWO (22/09/2016)	7	1/16	Norway
B3 BOSTWO (22/09/2016)	7.5	1/8	Norway
A2 BOSTWO (23/09/2016)	18	1/16	South Africa
A1 BOSTWO (23/09/2016)	24	1/32	South Africa
TOTAL FOR LAYER	**80.5**		
A1 BOSTHREE (18/08/2017)	8	1/16	South Africa
A2 BOSTHREE (22/08/2017)	20	1/16	South Africa
C3 BOSTHREE (8/8/2017)	18	1/32	South Africa
B2 BOSTHREE (08/08/2017)	6	1/16	Norway
A2 BOSTHREE (14/08/2017; 16/08/2017; 18/08/2017)	43.5	1/32	South Africa
B1 BOSTHREE (20/08/2017)	33.33	1/16	South Africa
C3 BOSTHREE (21/02/2017)	18.16	1/32	South Africa
TOTAL FOR LAYER	**146.99**		

Table C.2 The census data from the 29 sediment samples (Ostracods).

SAMPLE	Weight of entire washed >150 µm fraction (g)	1/x (split)	*G. obtusata*	*Physocpria* cf. *castanea*	*S. aculeata*	*Ilyodromus* sp.	Juveniles	Total ostracods counted
C2/D2 SMONE (23/02/2015)	14	8	180	0	6	0	116	302
B1/B0 SMONE (20/02/2015)	10.1	8	116	0	10	0	176	302
A3 SMONE (20/02/2015)	23.15	2	156	2	11	0	131	300
B3 SMONE (19/02/2015)	7	4	130	0	102	0	98	330
B2 SMONE (19/02/2015)	6	4	171	0	8	0	153	332
B1 SMONE (20/02/2015)	7.1	1	138	2	17	0	143	300
A2 SMONE (10/03/2015)	8	2	217	0	29	0	147	393
C1/C0; D1;D0 SMONE(19/02/2015)	14	2	133	1	9	1	170	314
Total			1241	5	192	1	1134	2573
C2 BOSONE (16/03/2015)	12	32	375	17	265	3	255	915
A2 BOSONE (16/03/2015)	11	4	156	0	3	0	142	301
A3 BOSONE (05/03/2015)	8.2	4	140	1	29	0	143	313
A1/A0 BOSONE (06/03/2015)	9.1	1	43	2	23	0	78	146
B1 BOSONE (10/03/2015)	11	16	200	2	15	0	261	478
C3 BOSONE (16/03/2015)	11.3	8	263	0	12	0	134	409
C1 BOSONE (16/03/2015)	11	32	597	10	25	1	338	971
Total			1774	32	372	4	1351	3533
A3 BOSTWO (23/09/2016)	7	16	242	6	38	6	118	410
C2 BOSTWO (21/09/2016)	10	16	202	0	15	3	176	396
C1 BOSTWO (21/09/2016)	7	16	269	7	34	3	105	418

B2 BOSTWO (22/09/2016)	**7**	**16**	**198**	**4**	**27**	**0**	**90**	**319**
B3 BOSTWO (22/09/2016)	**7.5**	**8**	**230**	**0**	**15**	**2**	**122**	**369**
A2 BOSTWO (23/09/2016)	**18**	**16**	**244**	**2**	**6**	**0**	**138**	**390**
A1 BOSTWO (23/09/2016)	**24**	**32**	**293**	**5**	**29**	**1**	**255**	**583**
Total			**1678**	**24**	**164**	**15**	**1004**	**2885**
A1 BOSTHREE (18/08/2017)	**8**	**16**	**180**	**9**	**31**	**0**	**80**	**300**
A2 BOSTHREE (22/08/2017)	**20**	**16**	**132**	**29**	**58**	**0**	**116**	**335**
C3 BOSTHREE (8/8/2017)	**18**	**32**	**596**	**3**	**29**	**0**	**283**	**911**
B2 BOSTHREE (08/08/2017)	**6**	**16**	**345**	**1**	**25**	**0**	**300**	**671**
A2 BOSTHREE (14/08/2017; 16/08/2017; 18/08/2017)	**43.5**	**32**	**452**	**23**	**87**	**3**	**290**	**855**
B1 BOSTHREE (20/08/2017)	**33.33**	**16**	**391**	**10**	**70**	**2**	**326**	**799**
C3 BOSTHREE (21/02/2017)	**18.16**	**32**	**384**	**19**	**56**	**2**	**280**	**741**
Total			**2480**	**94**	**356**	**7**	**1675**	**4612**

Table C.3 The census data from the 29 sediment samples (Foraminifera).

	WEIGHT 150 µm fraction (g)	1/x	*A. beccarii*	*A. japonica*	*Ammonia sp.*	*Cassidulina* cf. *laevigata*	*Elphidium* sp.	*E. crispum*	*Globigerinoides* sp	*Lagena sp.*	*N. boueanum*	*S. vivipara*	Unidentifiable	Total foraminifera counted
C2/D2 SMONE (23/02/2015)	14	8	2	0	0	0	2	5	0	0	2	0	0	11
B1/B0 SMONE (20/02/2015)	10.1	8	0	0	7	0	2	2	2	0	4	0	2	19
A3 SMONE (20/02/2015)	23.15	2	0	2	0	0	2	2	0	0	4	0	0	10
B3 SMONE (19/02/2015)	7	4	0	0	0	0	0	1	0	0	0	0	0	1
B2 SMONE (19/02/2015)	6	4	0	2	2	0	0	0	0	0	0	0	0	4
B1 SMONE (20/02/2015)	7.1	1	0	0	0	0	4	0	3	0	0	0	5	12
A2 SMONE (10/03/2015)	8	2	0	1	2	0	1	2	0	0	1	0	0	7
C1/C0; D1;D0 SMONE(19/02/201)	14	2	2	6	3	0	6	8	2	0	8	0	4	39
Total			4	11	14	0	17	20	7	0	19	0	11	103
C2 BOSONE (16/03/2015)	12.0	32	0	0	0	0	0	0	0	1	0	0	3	4
A2 BOSONE (16/03/2015)	11.0	4	0	1	0	0	1	0	0	0	1	0	5	8
A3 BOSONE (05/03/2015)	8.2	4	0	2	0	0	1	1	2	0	0	0	0	6
A1/A0 BOSONE (06/03/2015)	9.1	1	0	0	0	0	3	1	0	0	0	0	0	4
B1 BOSONE (10/03/2015)	11.0	16	0	0	0	0	1	0	0	0	0	0	0	1
C3 BOSONE (16/03/2015)	11.3	8	0	0	0	5	0	0	0	0	0	0	2	7
C1 BOSONE (16/03/2015)	11.0	32	0	0	0	0	1	0	0	0	0	0	0	1
Total			0	3	0	5	7	2	2	1	1	0	10	31
A3 BOSTWO (23/09/2016)	7	16	0	1	0	0	1	0	0	0	0	3	3	8
C2 BOSTWO (21/09/2016)	10	16	0	0	0	0	0	4	0	0	0	0	0	4
C1 BOSTWO (21/09/2016)	7	16	0	0	0	0	0	2	0	0	0	0	0	2
B2 BOSTWO (22/09/2016)	7	16	0	0	0	0	1	0	0	0	0	0	0	1

B3 BOSTWO (22/09/2016)	**7.5**	**8**	**0**	**0**	**0**	**0**	**0**	**1**	**0**	**0**	**0**	**0**	**3**	**4**
A2 BOSTWO (23/09/2016)	**18**	**16**	**0**	**0**	**0**	**0**	**0**	**0**	**1**	**0**	**0**	**7**	**0**	**8**
A1 BOSTWO (23/09/2016)	**24**	**32**	**0**	**0**	**0**	**0**	**0**	**0**	**0**	**0**	**0**	**0**	**0**	**0**
Total			**0**	**1**	**0**	**0**	**2**	**7**	**1**	**0**	**0**	**10**	**6**	**27**
A1 BOSTHREE (18/08/2017)	**8**	**16**	**2**	**0**	**0**	**0**	**0**	**0**	**0**	**0**	**1**	**2**	**0**	**5**
A2 BOSTHREE (22/08/2017)	**20**	**16**	**0**	**1**	**3**	**0**	**1**	**0**	**0**	**0**	**2**	**0**	**3**	**10**
C3 BOSTHREE (8/8/2017)	**18**	**32**	**0**	**1**	**1**	**3**	**0**	**2**	**0**	**0**	**0**	**0**	**2**	**9**
B2 BOSTHREE (08/08/2017)	**6**	**16**	**0**	**1**	**0**	**0**	**0**	**0**	**1**	**0**	**0**	**0**	**0**	**2**
A2 BOSTHREE (14/08/2017; 16/08/2017; 18/08/2017)	**43.5**	**32**	**0**	**0**	**0**	**0**	**0**	**0**	**0**	**0**	**0**	**5**	**0**	**5**
B1 BOSTHREE (20/08/2017)	**33.33**	**16**	**0**	**0**	**0**	**0**	**1**	**0**	**1**	**0**	**0**	**1**	**0**	**3**
C3 BOSTHREE (21/02/2017)	**18.16**	**32**	**0**	**0**	**0**	**0**	**0**	**0**	**0**	**0**	**0**	**7**	**0**	**7**
Total			**2**	**3**	**4**	**3**	**2**	**2**	**2**	**0**	**3**	**15**	**5**	**41**

Section C.2 SEM images



Figure C.1 SEM image of *Ammonia beccarii.*



Figure C.2 SEM image of *Ammonia japonica.*

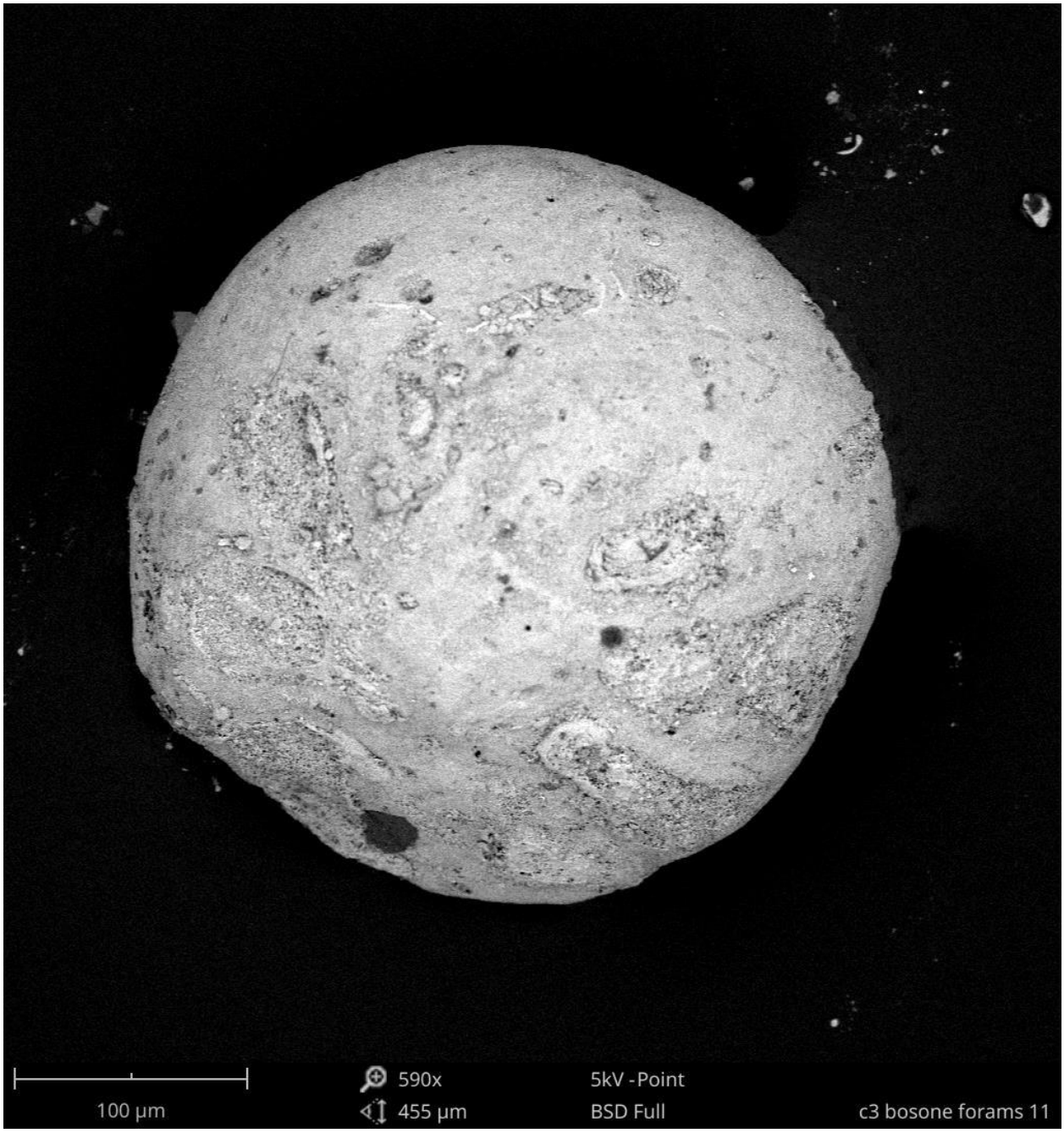


Figure C.3 SEM image of *Ammonia* sp.



Figure C.4 SEM image of *Cassidulina* cf. *laevigata.*

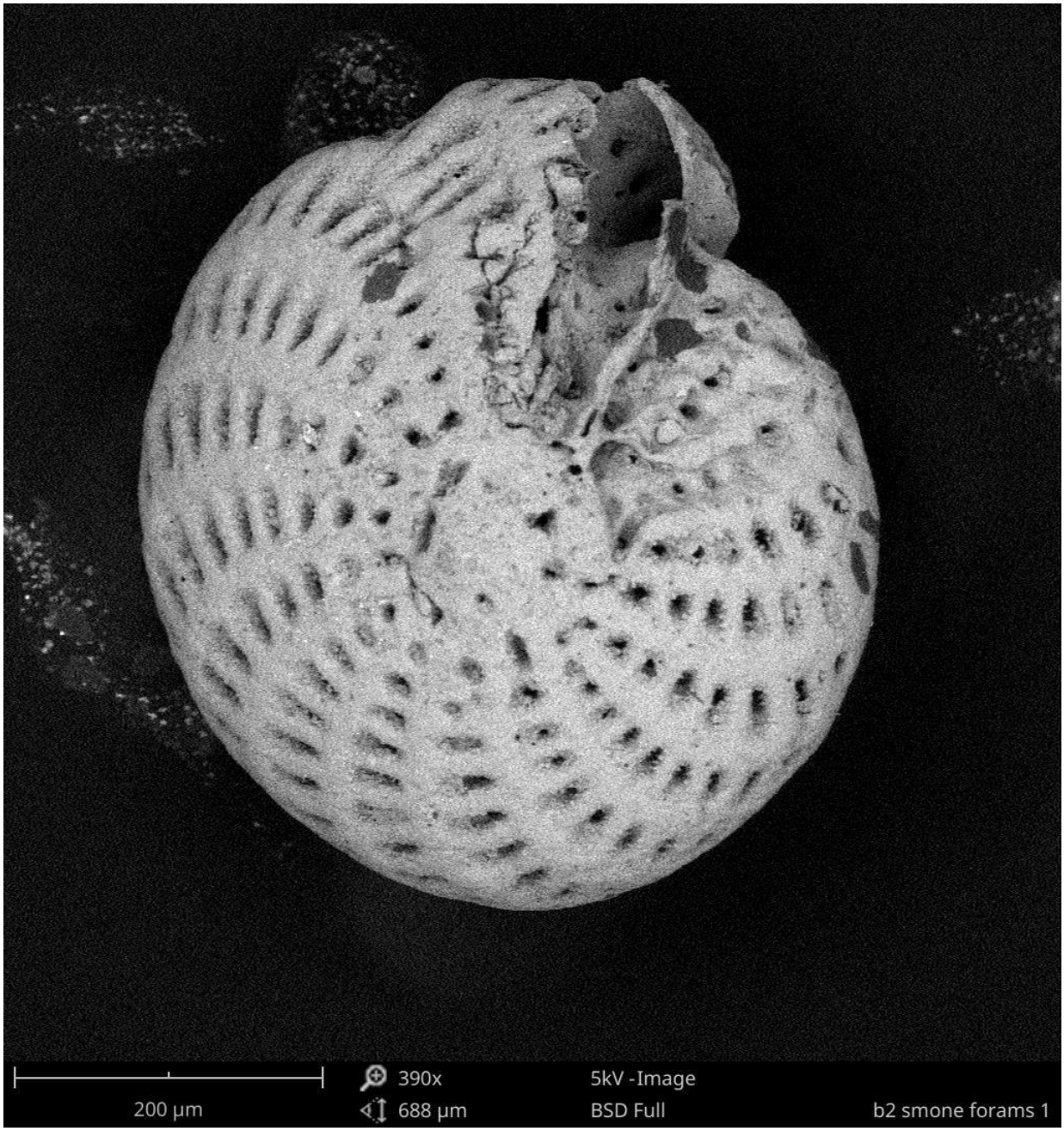


Figure C.5 SEM image of *Cribroelphidium articulatum.*

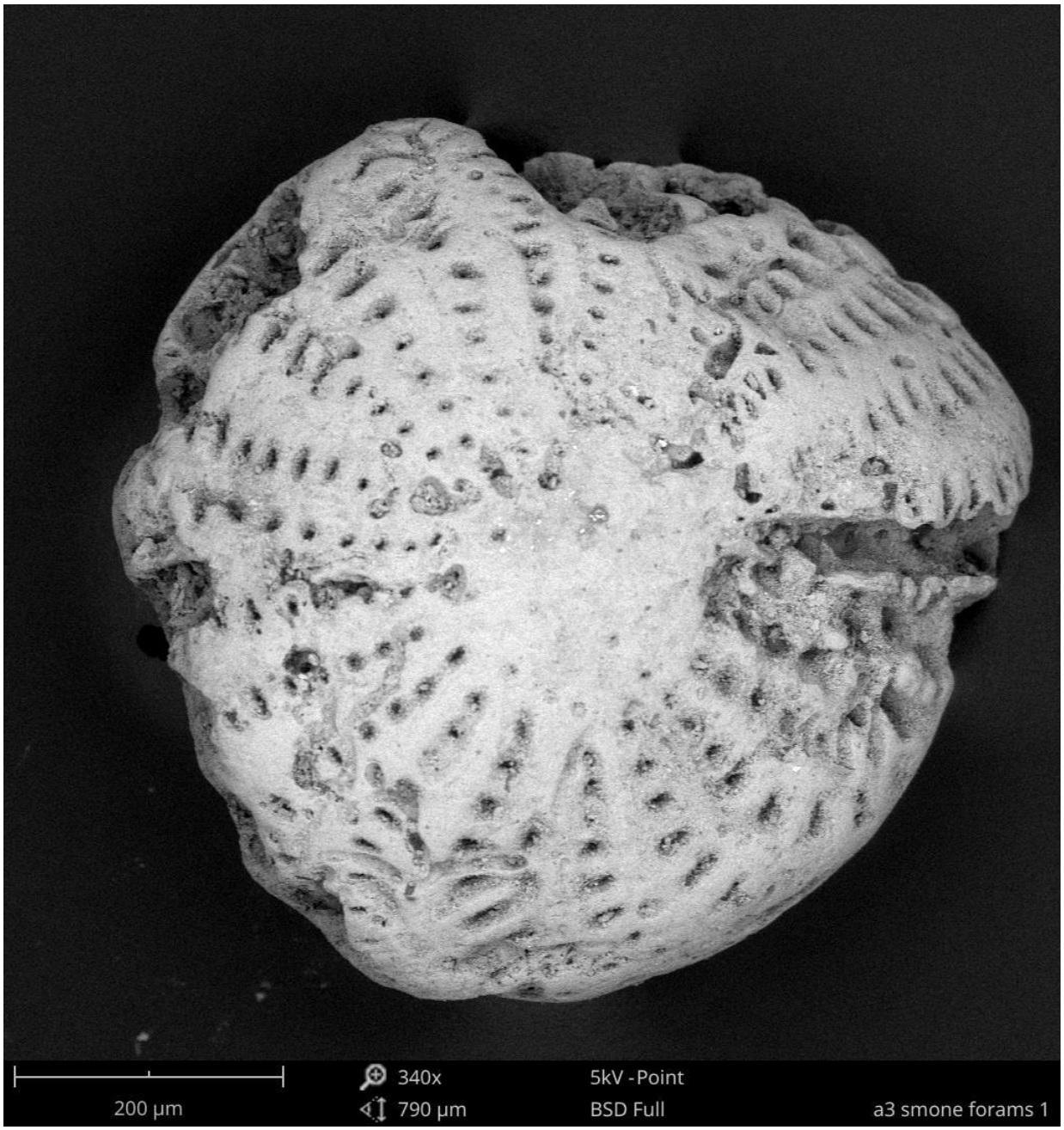


Figure C.6 SEM image of *Elphidium* sp.

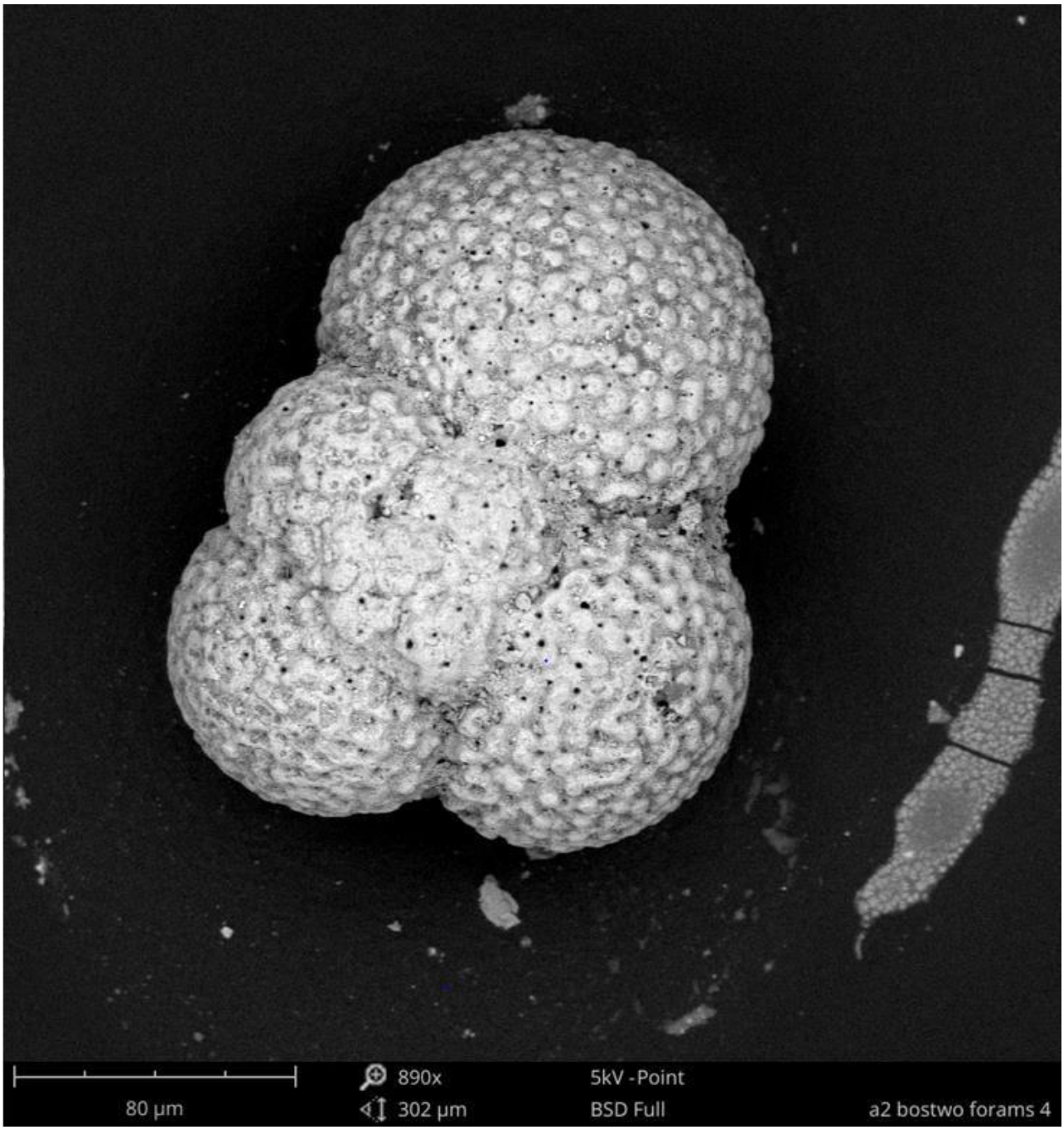


Figure C.7 SEM image of *Globigerinoides* sp.



Figure C.8 SEM image of *Lagena* sp.

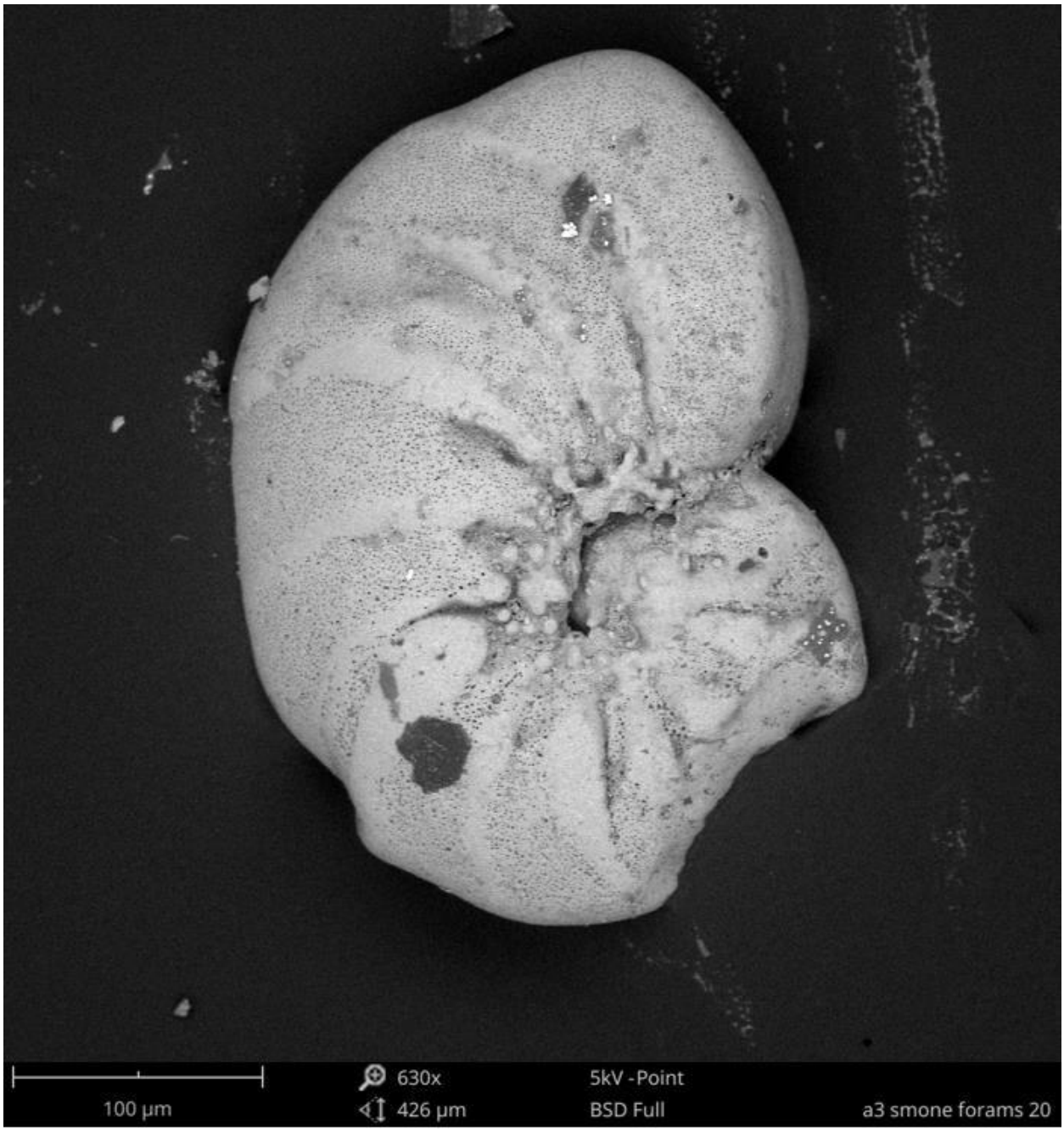


Figure C.9 SEM image of *Nonion boueanum.*

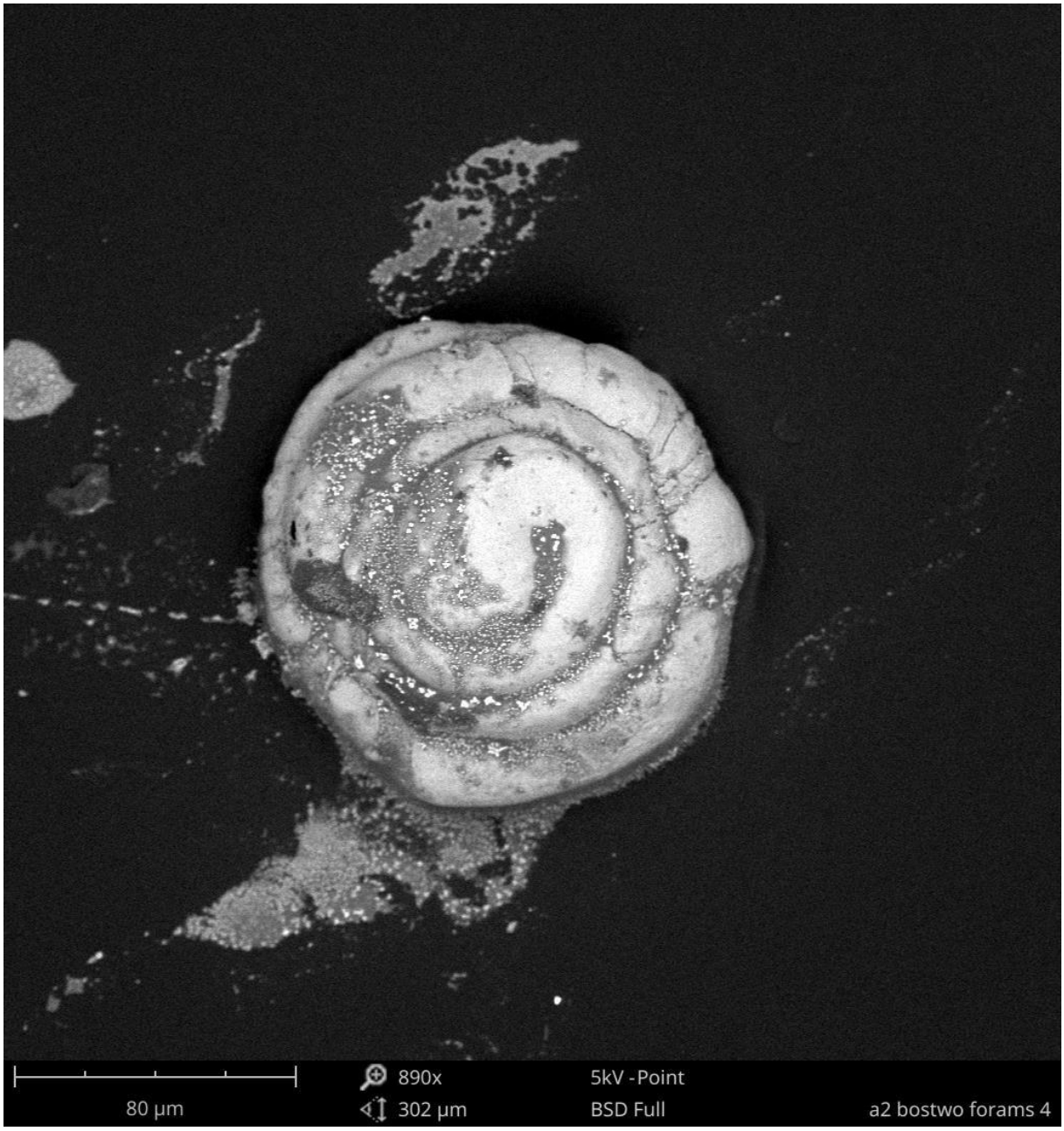


Figure C.10 SEM image of *Spirillina vivipara.*



Figure C.11 SEM image of unidentifiable foraminifera specimen.



Figure C.12 *G. obtusata* with dark stains on the valve exterior.

Section C.3 Systematics

In this section the systematics of the ostracod and foraminifera taxa are provided. The information regarding the systematics of the microfossils were found on the “World Foraminifera Database” and the “World Ostracoda Database”. Martens *et al*. (1996) and Martens & Savatenalinton (2011), and Fürstenberg et al. (2017) were also used for the ostracod systematics. Fürstenberg *et al*. (2017) and Strachan (2013; 2016) were used for the foraminifera systematics.

Ostracod systematics (bauplan)

Phylum **Arthropoda** von Siebold 1848
Class **Ostracoda** Latreille 1806
Subclass **Podocopa** G.W. Müller 1894
Order **Podocopida** Sars 1866

Superfamily **Cytheroidea** Baird 1850
Family **Limnocytheridae** Klie 1938
Genus *Gomphocythere* Sars 1924
Species *Gomphocythere obtusata* Sars 1910

Superfamily **Cypridoidea** Baird 1845
Family **Candonidae** Kaufmann 1900
Genus *Physocypria* Vávra 1897
Species *Physocypria castanea* Brady 1904
Family **Cyprididae** Baird 1845
Genus *Sarscypridopsis* McKenzie 1977
Species *Sarscypridopsis aculeata* Costa 1847
Genus *Ilyodromus* Sars 1894

Foraminifera systematics (bauplan)

Phylum **Foraminifera** d'Orbigny 1826

Class **Globothalamea** Pawlowski, Holzmann & Tyszka 2013

Subclass **Rotaliana** Mikhalevich 1980

Order **Rotaliida** Delage & Hérouard 1896

Superfamily **Rotalioidea** Ehrenberg 1839

Family **Ammoniidae** Saidova 1981

Genus *Ammonia* Brünnich 1771

Species *Ammonia beccarii* Linnaeus 1758

Species *Ammonia japonica* Hada 1931

Family **Elphidiidae** Galloway 1933

Genus *Elphidium* Montfort 1808

Genus *Cribroelphidium* Cushman & Brönnimann 1948

Species *articulatum* d'Orbigny 1839

Superfamily **Cassidulinoidea** d'Orbigny 1839

Family **Cassidulinidae** d'Orbigny 1839

Genus *Cassidulina* d'Orbigny 1826

Species *Cassidulina laevigata* d'Orbigny 1826

Superfamily **Globigerinoidea** Carpenter *et al*. 1862

Family **Globigerinidae** Carpenter *et al.* 1862

Genus *Globigerina* d'Orbigny 1826

Species *Globigerina bulloides* d'Orbigny 1826

Superfamily **Nonionoidea** Schultze 1854

Family **Nonionidae** Schultze 1854

Genus *Nonion* Montfort 1808

Species *Nonion boueanum* d'Orbigny 1846

Class **Nodosariata** Mikhalevich, 1992 emend. Rigaud *et al*. 2015

Subclass **Nodosariana** Mikhalevich 1992

Order **Nodosariida** Calkins 1926

Superfamily **Nodosarioidea** Ehrenberg 1838

Family **Lagenidae** Reuss 1862

Genus *Lagena* Walker & Jacob 1798

Class **Tubothalamea** Pawlowski, Holzman & Tyszka 2013

Order **Spirillinida** Hohenegger & Piller 1975

Family **Spirillinidae** Reuss & Fritsch 1861

Genus *Spirillina* Ehrenberg 1843

Appendix D

Section D.1 Isotope data

Table D.1 Summary of stable carbon (δ ^{13}C) and oxygen (δ ^{18}O) isotope results.

Stratigraphic layer	Excavation square and date excavated	Weight [µg]	δ13C/12C Mean (‰)	δ18O/16O Mean (‰)	Taxon used	Age of stratigraphic layer	MIS Stage associated with the sample
SMONE	Square A2 Date: 10/03/2015	35	-10.32	-2.42	*G. obtusata*	101 ± 12 ka (Eggins *et al*. 2005)	MIS 5c
SMONE	Square C2/D2 Date: 23/02/2015	32	-10.32	-2.52	*G. obtusata*	101 ± 12 ka (Eggins *et al.* 2005)	MIS 5c
SMONE	Square A3 Date: 20/02/2015	41	-10.37	-2.39	*G. obtusata*	101 ± 12 ka (Eggins *et al*. 2005)	MIS 5c
SMONE	Square B3 Date: 19/02/2015	39	-10.29	-2.25	*G. obtusata*	101 ± 12 ka (Eggins *et al*. 2005)	MIS 5c
SMONE	Square B1 Date: 20/02/2015	34	-10.28	-2.56	*G. obtusata*	101 ± 12 ka (Eggins *et al*. 2005)	MIS 5c
BOS-ONE	Square C2 Date: 16/03/2015	40	-10.24	-2.30	*G. obtusata*	*ca.*110ka (Wurz *et al*. 2018)	MIS 5d
BOS-ONE	Square B1 Date: 10/03/2015	38	-8.32	-2.36	*G. obtusata*	*ca.*110ka (Wurz *et al*. 2018)	MIS 5d

BOS-ONE	Square C3 Date: 16/03/2015	41	-10.08	-2.26	*G. obtusata*	*ca.*110ka (Wurz *et al*. 2018)	MIS 5d
BOS-ONE	Square A2 Date: 16/03/2015	41	-10.03	-2.51	*G. obtusata*	*ca.*110ka (Wurz *et al*. 2018)	MIS 5d
BOS-TWO	Square B2 Date: 22/09/2016	38	-9.79	-2.40	*G. obtusata*	*ca.*110ka (Wurz *et al*. 2018)	MIS 5d
BOS-TWO	Square B3 Date: 22/09/2016	32	-10.19	-2.50	*G. obtusata*	*ca.*110ka (Wurz *et al*. 2018)	MIS 5d
		STANDARD DEVIATION	**0.59**	**0.11**			

Table D.2 Summary of stable carbon (δ ^{13}C) and oxygen (δ ^{18}O) isotope samples that did not weigh enough for the results to be interpreted accurately.

Stratigraphic layer	Excavation square and date excavated	Weight [µg]	δ13C/12C Mean	δ18O/16O Mean	Taxon used	Age of stratigraphic layer	MIS Stage associated with the sample
BOSONE	Square C1 Date: 16/03/2015	27	-10.668	-2.69	*G. obtusata*	*ca.*110 ka (Wurz *et al*. 2018)	MIS 5d
SMONE	Square C1/CO Date: 19/02/2015	28	-9.535	-2.344	*G. obtusata*	101 ± 12 ka (Eggins *et al*. 2005)	MIS 5c
BOSTHREE	Square B2 Date: 08/08/2017	25	-9.694	-2.519	*G. obtusata*	*ca.*110ka (Wurz *et al*. 2018)	MIS 5d
SMONE	Square B1/BO Date: 20/02/2015	19	-9.672	-2.391	*G. obtusata*	101 ± 12 ka (Eggins *et al*. 2005)	MIS 5c
BOSONE	Square A3 Date: 05/03/2015	16	-10.241	-2.31	*G. obtusata*	*ca.*110ka (Wurz *et al*. 2018)	MIS 5d